An evaluation of local and community-scale multispecies competition among corals, sponges, and macroalgae on reefs in the U.S. Virgin Islands

by
Lauren Olinger

A THESIS

submitted to the

University of the Virgin Islands

in partial fulfillment of the requirements for the degree of

Master of Science

Presented December 15th, 2017

Commencement January 2017

ACKNOWLEDGEMENTS

I would like to thank Elizabeth Brown for her relentless field support and advice throughout this research. I also thank Tanya Ramseyer, Rossie Ennis, John Cassell, Alex Gutting, Danielle Lasseigne, Kristen Ewen, Rob Brewer, and Ian Byrne for their help with field work and logistics. I also thank Dr. Amy Scott-Murray for sharing her expertise in 3D photogrammetry. Funding for this project was provided by the NOAA Coral Reef Conservation Program, VI-EPSCoR, and the Lana Vento Charitable Foundation. No funding agency participated in the design or interpretation of this research.

CONTRIBUTION OF AUTHORS

Lauren Olinger contributed to conceptualization, data curation, formal analysis, investigation, methodology, project administration, software development, validation, visualization, writing (original draft), and writing (review and editing). Dr. Marilyn Brandt contributed to conceptualization, funding acquisition, methodology, provision of resources, and writing (review and editing). Dr. Andia Chaves Fonnegra contributed to conceptualization, investigation, methodology, project administration, and writing (review and editing). Dr. Ian Enochs contributed to conceptualization, methodology, and writing (review and editing).

DEDICATION

In memory of Taco.

TABLE OF CONTENTS

LIST OF FIGURES

LIST OF TABLES

Chapter 1: Introduction

In the past several decades, anthropogenic impacts and stressors have killed corals and driven Caribbean reefs away from coral dominated states (Ginsburg 1994; Aronson et al. 2002). To persist on the benthos, corals must interact with competitively favored sponges and macroalgae, groups that are expected to proliferate as a consequence of terrestrial runoff, overfishing, diseases, thermal stress, and other environmental fluctuations (Norström et al. 2009). On heavily impacted reefs, the cumulative effect of chronic stressors and large-scale disturbances can drive cascading coral mortality and colonization by other opportunistic sponges and macroalgae (Dizon and Yap 2006; Mumby et al. 2007; Norström et al. 2009). For example, an outbreak of white band disease in the 1980s drove replacement of competitive *Acropora cervicornis* by weedy *Agaricia tenuifolia* as the dominant coral in Channel Cay reef complex in Belize; subsequent mass bleaching of *A. tenuifolia* during the 1997-1998 El Nino Southern Oscillation (ENSO) resulted in a phase shift from corals to the sponge *Chondrilla nucula* (Aronson et al. 2002; Darling et al. 2012). Similarly, mass coral bleaching in 2005 drove proliferation of fleshy macroalgae up to 50% on impacted nearshore reefs in the U.S. Virgin Islands (Smith et al. 2015). As environmental degradation and large-scale disturbances drive takeover by colonizing organisms and put reefs at risk of catastrophic phase shifts, there is a need to better understand the processes structuring benthic communities.

Mechanisms of Competition

Interspecific competition plays a considerable role in structuring benthic communities, and the structuring influence of these interactions are becoming more prominent as opportunistic taxa become more abundant (Dayton 1971; Connell 1983; Aerts and Van Soest 1997). Some corals can defend themselves from these groups. For example, *Orbicella spp.* and *Montastrea cavernosa* can use mesenterial filaments to physically damage and reduce the competitive ability of fleshy macroalgae, including the green algae *Halimeda opuntia* and *Dictyota spp.* and the brown alga *Lobophora variegata* (Womersley ex E.C.Oliveira 1977; De Ruyter van Steveninck et al. 1988; Nugues et al. 2004). Though not as well studied, *Montastrea cavernosa* and *Siderastrea siderea* utilize sweeper tentacles to defend against aggressive bioeroding sponges (Richardson et al. 1979; López-Victoria et al. 2006). Other species competing with bioeroding sponges alter their growth from plate-shaped to dome-shape, and expanding in three dimensions is believed to be a strategy to compensate for space lost to the encroaching sponge (López-Victoria et al. 2006).

Many sponges and macroalgae can outcompete corals by shading, smothering, and releasing allelopathic secondary metabolites (Loh et al. 2015; Morrow et al. 2011). Competitive mechanisms of

sponges vary among morphotypes (e.g., encrusting, rope, vase, barrel) (Luter and Duckworth 2010). For example, encrusting sponges *Chondrilla nucula* and *Desmapsamma anchorata* (Carter 1882) overgrow and degrade coral tissues through the release of allelopathic compounds. *D. anchorata* grows rapidly and is one of the most prevalent and aggressive coral competitors on Caribbean reefs (Aerts and Van Soest 1997; Pawlik et al. 2007). Another sponge commonly found overgrowing corals is the purple rope sponge *Aplysina cauliformis* (Carter 1882; Aerts and Van Soest 1997; Loh and Pawlik 2014). Unlike encrusting sponges, *A. cauliformis* grows slowly and does not appear to produce secondary metabolites for spatial competition (Easson et al. 2014), but its competitive success may result indirectly from its production of alkaloid metabolites that make it unpalatable (Pawlik et al. 2013). Macroalgae employ similar competitive mechanisms as sponges (Morrow et al. 2011). An example of an algal species that uses shading, abrasion, and allelopathy is the brown alga *L. variegata*. The leathery and tough morphology of this species allows for effective shading and abrading of live coral tissue (Jompa and McCook 2002). *L. variegata* also produces hydrophilic compounds with antimicrobial activity that can degrade the delicate coral holobiont (Morrow et al. 2011).

Multispecies Competition

Benthic communities on Caribbean reefs are structured by competition among corals, sponges, and macroalgae, yet little is known about how these groups compete in a multispecies context (Connell 1983; González-Rivero et al. 2016). Pairwise coral-sponge and coral-algae interactions are well studied, but much less is known about sponge-alga interactions and how these may affect corals. One recent report found that contact with the sponge *A. cauliformis* accelerated growth of the green alga *Microdictyon marinum*, and such facilitating associations may affect how either group competes with corals (Easson et al. 2014). Antagonistic sponge-alga associations have been previously linked to preservation of corals after a mass bleaching event in Belize. In this study, asymmetric competitive dominance of the macroalgae *L. variegata* over the sponge *Cliona tenuis* prevented an outbreak of *C. tenuis* on bleached *Orbicella spp.* corals (González-Rivero et al. 2016). In an earlier study, the same authors found that *Cliona tenuis* facilitated the growth of the brown algae *L. variegata,* and it was proposed that rapidly growing *C. tenuis* diverted herbivores from grazing on macroalgae (González-Rivero et al. 2011). Overall, better understanding of multispecies interactions among these abundant benthic groups may improve predictions of ecosystem response to disturbance and shed light on factors that reinforce or destabilize feedbacks favoring shifts to non-coral dominated states (González-Rivero et al. 2011).

Multispecies competition is characterized in terms of transitivity, or the dominance order of its component species. Perfectly transitive competition is referred to as a competitive hierarchy (A← B← C), and the inferior competitor (species C) in a competitive hierarchy can be competitively excluded when

too many resources become limited (Grace et al. 1993). Stable competitive hierarchies among scleractinean corals have been documented (Logan 1984), but interspecific competitive hierarchies can be dynamic (i.e., reverse over time) because each group uses different competitive mechanisms and thrives under different conditions (Nugues et al. 2004). For example, the use of mesenterial filaments by *Montastrea cavernosa, Diploria strigosa,* and *Colpophylla natans* make them competitively dominant over *H. opuntia*, but the competitive dominance of these corals may be compromised by sedimentation (Nugues et al. 2004). Additionally, hierarchies can be dominated by an asymmetrically dominant species whose competitive ability increases disproportionately with size. Macroalgae possess an asymmetrically superior competitive ability over most benthic reef organisms (López-Victoria et al. 2006); for example, asymmetric competitive dominance of the algae *L. variegata* over the sponge *C. tenuis* allowed the algae to prevent coral takeover by the sponge (González-Rivero et al. 2016).

Intransitive competition is referred to as a competitive network (A ← B, B ← C, and C ← A). Similar to the game of rock-paper-scissors, each species in a competitive network outcompetes and is outcompeted by another species. Networks can thus promote coexistence because there is no strictly inferior member competing for all resources; species C may be better at competing for one resource than species A or species B, even though species A and B can outcompete species C for another resource (Grace et al. 1993; Allesina and Levine 2011). A diversity of competitive strategies can promote networks; species A may overgrow species B, which overgrows species C, which chemically inhibits species A (Edwards and Schreiber 2010). However, networks can depend on pairwise dominance orders that depend, for example, on orientation of competitors. Networks can also be sensitive to competitive reversals that occur over time as a result of extrinsic factors such as seasonality, disturbance regimes, and resource availability (Buss and Jackson 1979; Karlson and Jackson 1981; Sebens 1987; Benedetti-Cecchi and Cinelli 1996).

Since the seventies, researchers have been interested in how competitive networks may maintain coexistence of benthic reef organisms engaged in spatial competition. Buss and Jackson (1979) described multiple, overlapping 3-species and 6-species competitive networks that linked ectoprocts, sponges, corals, coralline algae, ascidians, and forams on Caribbean fore-reef environments along the north coast of Jamaica. A decade later, another study described a four-species network between a scleractinean, alcyonarian, hydrocoral and a sponge *(Diplastrella gardineri*) in the Gulf of Eilat, Red Sea (Rinkevich et al. 1992). These reports used single time point surveys to evaluate competitive networks, and such studies have provided valuable insight into the mechanisms of diversity on benthic reef habitats (Chadwick and Morrow 2011).

Photogrammetry

Single time point surveys have been used to evaluate outcomes of spatial competition among benthic groups, but it has proven more challenging to measure the growth and morphological plasticity of these sessile organisms over time. The conventional method of characterizing reef communities is to measure benthic cover on a two-dimensional (2D) plane and estimate percent cover, but this fails to capture the complex three-dimensional (3D) morphology of sessile organisms (Burns et al. 2016). For example, percent cover of sponges is traditionally underestimated because of many species' vertical rope-like growth forms (Wulff 2012). Alternative methods such as foil-wrapping and wax-dipping have been used to quantify size of individuals, but these methods are laborious, destructive, and inaccurate (Veal et al. 2010).

Because of its capability to capture 3D structure, close-range photogrammetry has gained recent popularity as a technique to examine reef habitat composition and structural complexity (Ferrari et al. 2016). Photogrammetry is a stereoscopic technique that generates a 3D point cloud by cross-referencing a set of 2D photographs taken from multiple perspectives. Advanced processing of a 3D point cloud can produce a photorealistic 3D model (Burns et al. 2016). Surface area measurements of the underlying mesh can be accurate enough to detect ecologically relevant growth of benthic organisms (e.g., Scott-Murray and Schläppy 2017). Accuracy decreases with increasing structural complexity, but millimeter-scale accuracy can be achieved from photogrammetric 3D models of massive corals (Figueira et al. 2015). Photogrammetry has gained popularity among coral scientists as a reliable means to measure structural complexity and, more recently, growth (Figueira et al. 2015; Burns et al. 2016).

Modeling Approaches to Studying Competition and Life-History Tradeoffs

Tradeoffs in competitive ability and life history strategies can promote coexistence, similar to traditional competitive intransitivity (Edwards and Schreiber 2010). Competitors have diverse strategies and different relative abilities to colonize space, capturing it from other competitors, or preempt it from being captured, and these diverse strategies demonstrate the challenges inherent to predicting the outcomes of benthic competition (Karlson and Jackson 1981; Edwards and Schreiber 2010). To address the basic causes of coexistence and exclusion, mathematical models of pairwise and multispecies competition have been used. Ordinary differential equations (ODE) describing pairwise competition were used to show that inferior competitor species j can coexist with a superior competitor species i, as long as species j maintains high enough recruitment and low enough mortality to offset the competitive advantage of species i (Crowley et al. 2005). A mathematical model of multispecies competition also demonstrated that coexistence depends on species gaining an overgrowth advantage at great expense to reproductive output, or gaining a space pre-emption advantage at a medium expense to reproductive output (Edwards

and Schreiber 2010). Such models demonstrate, for example, that coexistence of corals may be possible in the absence of traditional intransitivity if the competitive ability of sponges and macroalgae is gained at the expense of reproductive output.

Mathematical models are valuable in detecting emergent properties and novel processes underscoring changes in benthic structure, but they do not capture the subtle ecological interactions that depend on spatial orientation of competitors (González-Rivero et al. 2011). For example, a theoretical aggregation of locally competing species engaged in cyclic competition for space can form heterogeneous patches and maintain a "balanced chase" with surrounding patches by overgrowing subordinate competitors in one direction and being overgrown by dominant competitors in another direction (Laird and Schamp 2008). This theoretical example demonstrates the importance of a spatial context in evaluating interactions among sessile corals, sponges, and macroalgae. Simulations of individual interactions in explicit space, using individual based models (IBMs), can be better than mathematical models in predicting community response to competitive interactions (Grimm et al. 2006).

Objectives

General Objective

The aim of this thesis was to evaluate local and community-scale multispecies competitive interactions among corals, sponges, and macroalgae on reefs in the U.S. Virgin Islands.

Specific Objectives

1. Determine if competition between one or more species of corals, sponges, and macroalgae may promote coexistence of corals.
2. Assess community-scale patterns resulting from individual interactions among corals, sponges, and macroalgae.
3. Evaluate whether tradeoffs in competitive ability and life-history dynamics may promote coral coexistence despite proliferation of sponges and macroalgae.

Chapter 1 addressed objective 1 and comprised a six-month field experiment on local competition and benthic survey on community interactions. In the experiment, multispecies and pairwise local competition were evaluated by simulating interactions among corals (*P. astreoides*), sponges (*D. anchorata*, *A. cauliformis*), and macroalgae (*L. variegata*). High resolution 3D models of experimental colonies were generated using photogrammetry, to accurately measure changes in individual morphology. In the survey, data on pairwise overgrowth and standoff interactions were collected and used to calculate transitivity indices for 18 combinations of locally abundant species. Chapter 2 was designed to address

objective 2 and 3. In this chapter, a spatially-explicit modelling framework was built in MATLAB and parameterized with growth and overgrowth rates measured during the experiment.

Chapter 2: Field Observations Exploring Multispecies Competition among Corals, Sponges, and Macroalgae.

Introduction

Although corals, sponges, and macroalgae are the three most abundant benthic taxa on Caribbean reefs, little is known about outcomes of multispecies competition among these groups (González-Rivero et al. 2016). Of particular concern is how the consideration of a third competitor in a pairwise coral-sponge or coral-macroalgae competition may influence continued coexistence of reef-building corals. During pairwise competition, corals are susceptible to overgrowth by either sponges or macroalgae, and overgrowth reduces coral fitness because reproductive output is proportional to surface area of living tissue (Tanner 1997). Persistent competitive inferiority of corals during multispecies competition may imply a risk of coral exclusion, if they are the inferior members of a competitive hierarchy. Alternatively, dominance of corals over either group may imply a competitive network and the potential for coral coexistence (Edwards and Schreiber 2010).

The gap in knowledge regarding multispecies competition among these groups was addressed using experimental and observational field research on two reef sites in St. Thomas, U.S. Virgin Islands. Research was framed to answer the following research question: how do competitive outcomes among the three groups differ when multispecies (coral-sponge-macroalgae) competition is compared to pairwise (coral-macroalgae and coral-sponge) competition? It was broadly hypothesized that a competitive network exists among the three groups, as this may partly explain coral persistence. Even though corals are increasingly threatened, none have gone extinct in recent history (Fenner 2001; Baker et al. 2008). A secondary hypothesis of both components of this research was that results would vary among species, as many previous studies demonstrate species-specificity inherent to competitive interactions (reviewed in Chadwick and Morrow 2011).

A six-month field experiment was conducted to simulate individual-scale interactions among the coral species *Porites astreoides* (Lamarck 1816), sponge species *Aplysina cauliformis* or *Desmapsamma anchorata*, and the brown macroalga *Lobophora variegata*. The experiment tested the overall hypothesis that sponge and macroalgae overgrowth of corals differs between multispecies (coral-sponge-macroalgae) and pairwise (coral-sponge and coral-macroalgae) interactions. It was specifically predicted that during local multispecies competition, corals would benefit if sponge-macroalgae interactions reciprocally inhibited each other's combative ability over corals, resulting in less overgrowth of coral. This is a mechanism of intransitively-mediated coexistence referred to as "enemy's enemy indirect facilitation" (Laird and Schamp 2008). To increase measurement accuracy of individual growth, high-resolution models of experimental colonies were generated using 3D photogrammetry.

Observational field research comprised a benthic survey of pairwise interactions designed to investigate community-scale interactions. The objective of the survey was to broadly assess the dominance order (i.e., transitivity) of pairwise interactions between target coral species *Orbicella annularis* (Ellis and Solander, 1768), *Siderastrea siderea* (Ellis & Solander, 1768), and *P. astreoides,* sponge species *Amphimedon compressa* (Duchassaing & Michelotti, 1864), *D. anchorata*, and *A. cauliformis,* and macroalgae species *Dictyota spp*. and *L. variegata.* For a competitive network to arise from these surveys, there would need to be some indication of coral dominance. Since corals are incapable of overgrowing sponges or macroalgae (Bell and Barnes 2003), it was predicted that networks would arise from coral-sponge standoffs that, when monitored over time, would reveal coral competitive superiority. Similar, traditional single time point surveys (e.g., Buss and Jackson 1979; Rinkevich et al. 1992) did not monitor standoffs, but the present research follows an adapted survey technique that incorporates standoff monitoring and considers standoffs to be of equal importance to overgrowth interactions (Tanaka and Nandakumar 1994).

Methods

Study Sites

All research activities were conducted at two reef sites located to the south of St. Thomas, U.S. Virgin Islands (Figure 1). The first site is a 10-17 m deep reef located northwest of Flat Key (18° 19’06” N 64° 59’27” W). This site has been monitored since 2003 as part of the Territorial Coral Reef Monitoring Program (TCRMP). It maintains a high abundance of *Orbicella spp*. corals, sponges, and the macroalgae *L. variegata*. It is threatened locally by industrial port activities, diving tourism, fishing pressure, and sedimentation due to residential development (Smith et al. 2015). The second site is a 7-8 m deep reef located in Perseverance Bay (18° 20’ 45” N, 64° 59’58” W). It is a fringing reef notable for its high water motion and nearshore location (Henderson 2012). It is also an *Orbicella spp*. dominated reef with abundant sponges and *L. variegata*, and its coral cover is similar to that of Flat Key (Sabine et al. 2015).

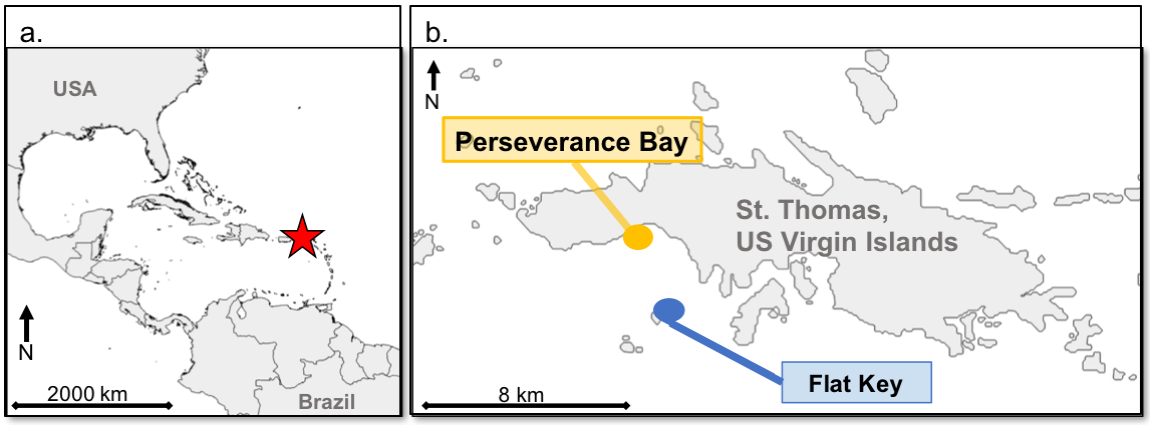

Figure 1: Location of a) St. Thomas, U.S. Virgin Islands in the Caribbean, denoted by red star and b) study sites Perseverance Bay and Flat Key with respect to St. Thomas

All research activities occurred between August 2016 and April 2017. Between April and November, prevailing winds are out of the southeast and expose southeast-facing Perseverance Bay to high winds and wave action. The small key south of the reef at Flat Key buffers some of the wind and wave action, but the reef can still be subjected to considerable wind swell. The calmest conditions for Perseverance Bay and Flat Key typically occur during winter months (December to March); their leeward location with respect to mountainous St. Thomas protects them from seasonal northeasterly winds (Olinger et al. 2017).

Manipulative Experiment: Local Multispecies Competition

Experimental Setup

To evaluate the effect of three-way and two-way competitive interactions on benthic organisms, 20 colonies of the coral *P. astreoides* (mean diameter of 18 ± 8cm) were identified and mapped at each site in August 2016 (Figure 2). One fragment of the sponge *D. anchorata* was attached with nails to each of ten coral colonies, and fragments of the sponge *A. cauliformis* were attached to the remaining ten coral colonies. Sponge fragments were trimmed to a length roughly equal to half of the perimeter of the coral colony. Fronds of macroalgae (*L. variegata*) were attached with monofilament to all coral colonies, and *L. variegata* were placed so that the macroalgae was in contact with half of the perimeter of the coral colony. Sponge fragments and macroalgae were oriented on each colony to create four treatment quadrants; a portion of living coral tissue in each quadrant competed with either sponge and macroalgae (sponge-algae treatment), sponge-only (sponge treatment), algae-only (algae treatment), or neither (coral treatment) (Figure 3).

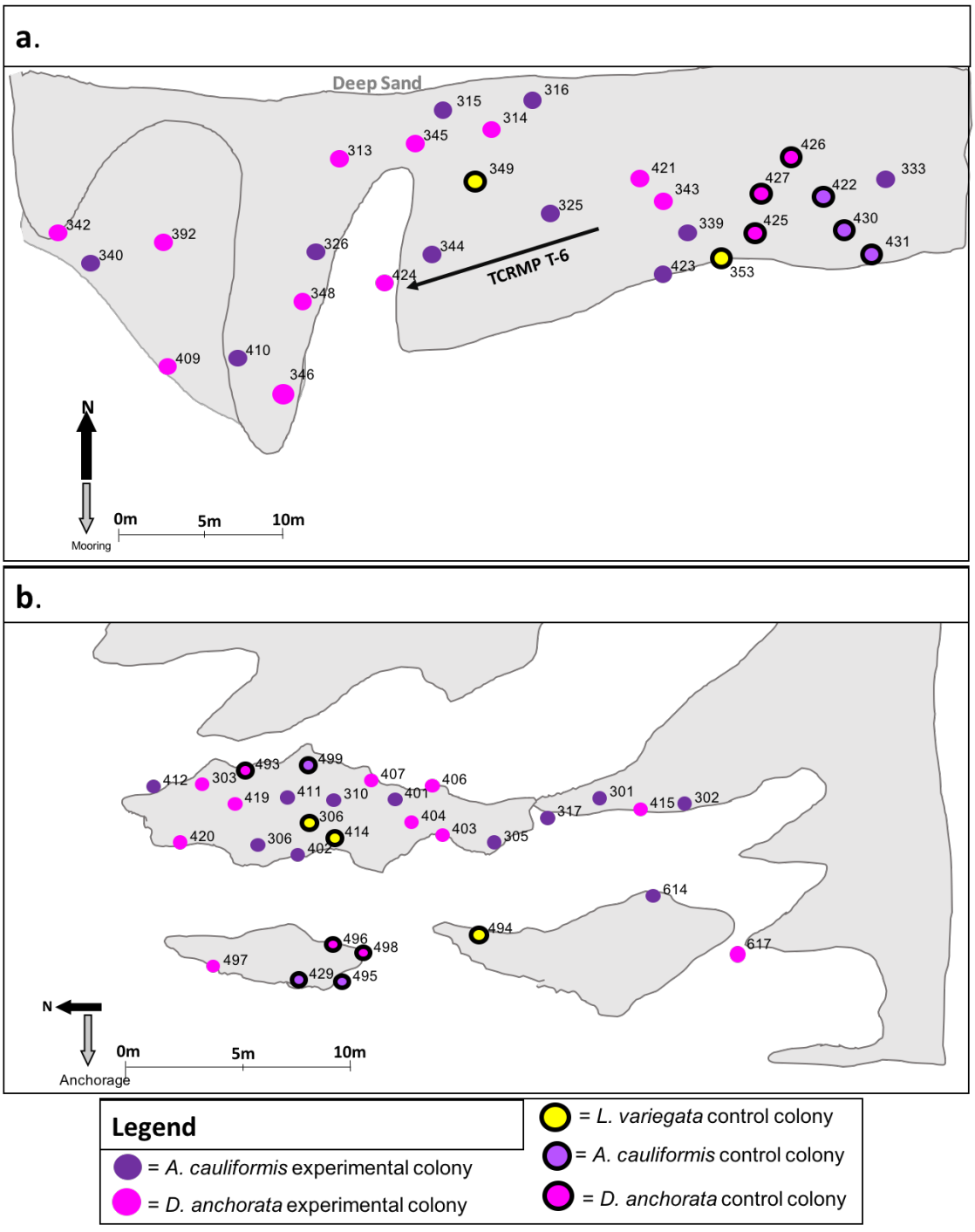

Figure 2: Map of experimental colonies at a) Flat Key and b) Perseverance Bay.

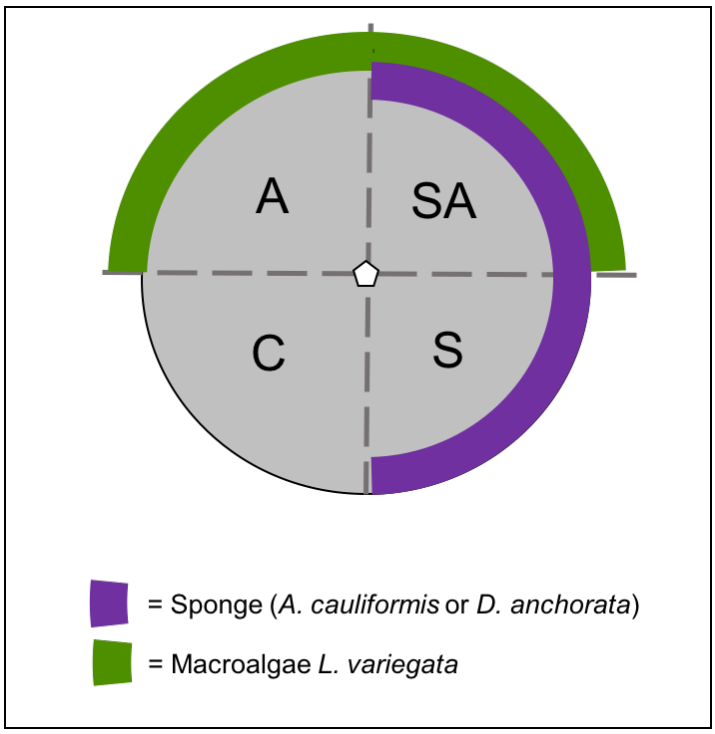

Figure 3: Schematic top-down view of experimental colony, split into treatments. SA = Sponge-Algae, S = Sponge, A = Algae, C = Coral only (no competitors)

Each month, an area within a 15-20 cm radius of experimental and control colonies was cleared of all algae, predominately *Dictyota spp*., and other recently settled organisms. This was done to isolate the experimental competitors from the effect of other sessile competitors. Once maintenance was complete, the colony was photographed.

In November, procedural control colonies were added to test for the effect of having multiple treatments on one colony. Nine control colonies were identified and mapped at each site (Figure 2), and *L. variegata*, *A. cauliformis*, and *D. anchorata* were each attached to three colonies. No third competitor was added to the colonies. The overgrowth of each competitor and growth of the coral colony was monitored along with experimental colonies for the remainder of the experiment.

Though sponges and macroalgae were attached in August, the analyses don't include any data collected before November. Regularly scheduled maintenance was still conducted August-November. During this period, additional measures had to be taken to resolve unforeseen complications as a result of storms and imperfect experimental design.

In October, many colonies had very little macroalgae (*L. variegata*) treatment remaining, likely as a result of storm swells from storms such as Hurricane Matthew that affected St. Thomas in September. Macroalgae was therefore reapplied to all experimental treatment colonies at both sites in November. Macroalgae was reapplied evenly around the same half perimeter that it had previously covered,

regardless of the amount left over from the previous application. Macroalgae was also reapplied in January, following wind swells caused by strong easterly winds in December.

Of the original 10 colonies competing with each sponge species at each site, some colonies were lost prior to beginning the analyses. The process of nailing the sponges into the colonies sometimes resulted in separation of the corals from the substrate. The issue of colony fragmentation was exacerbated because preferred colonies were those that protruded from the substrate; these "lollipop" shapes could be photographed from more angles and result in better photogrammetric scans. An attempt was made reattach the colonies to the substrate using wire or epoxy, but this was ineffective. Four of the 20 colonies at Perseverance Bay were lost, and the analyses were conducted on the remaining seven colonies competing with *A. cauliformis* and nine colonies competing with *D. anchorata* at Perseverance Bay. Three of the 20 original colonies at Flat Key were lost, and the analyses were conducted on the remaining eight colonies competing with *A. cauliformis* and nine colonies competing with *D. anchorata.*

Photogrammetry

To evaluate changes in the 3D growth of benthic competitors, photogrammetric models of each colony were generated. Photographs used for the models were taken at Flat Key between December 2016 and March 2017, and in Perseverance Bay between January 2017 and April 2017 for both treatments and control colonies. The amount of time that passed between 3D scans of all colonies at both sites was consistent (91 ± 3 d), but Perseverance 3D reconstructions were generated from photographs taken one month later than Flat Key colonies due to storms in December that prevented safe access to Perseverance Bay.

Before photographs of each colony were taken, a circular washer (diameter = 1.25 cm) was placed next to each colony. This was the scale bar used to reference the 3D models. Next, all flagging tape from tags was secured, and any loose algae within 20 cm of the colony was removed. This was done because items that move (such as those that wave with the water) can prevent proper alignment of photographs in the initial steps of the 3D reconstruction.

Between 50-60 photographs were captured of the colony and scale bar with point and shoot Canon digital cameras (Model: Canon G12 and G1X) in Ikelite underwater housings. Flash was disabled, and the underwater photography mode was used. For maximum model accuracy and precision, photographs were captured from 360° angle around the colony, with a minimum rotation of ~20° around the base of the colony (Supplementary Figure 1). Most importantly, care was taken to photograph the object so that photographs of the colony had considerable overlap; this is important for alignment of photos during processing.

Post-Processing of Photogrammetric Scans

Agisoft Photoscan (Agisoft L.L.C., 2013) was used to generate high-definition textured 3D models from photographs of each experimental colony. The workflow that was used to process scans from photograph sets to a textured mesh was adapted from Mallison and Wings (2014). Initially, the 50 – 60 photographs taken of each colony were batch-uploaded into Photoscan and then aligned (High accuracy, pair preselection disabled, key point limit 40000, tie point limit 10000) to create a sparse point cloud (Supplementary Figure 2a). The point cloud was optimized using built-in gradual selection tools to filter out points based on the software's confidence in the accuracy of their position. First, gradual selection was used to eliminate points with a reconstruction uncertainty < 10; this filtered out points whose location in 3D space was estimated with high uncertainty, for example when a point's location was estimated only from photos taken at parallel angles. Camera (i.e., the location of the photograph) alignment was then optimized using the "Optimize Cameras" tool by referencing the improved point cloud and refitting the relative position of the camera's location when each photograph was taken. Next, gradual selection was used to eliminate points with a reprojection error > 1 pixel; this filtered points whose 3D location deviated more than one pixel from the actual location on the photographs they were projected from. Then, gradual selection was used to eliminate points with a projection accuracy < 10; this removes a lot of the noise in sparse clouds by filtering out points that were matched from photographs with different scales (or distances to the target object) (Supplementary Figure 3). The final step in processing the sparse point cloud was to manually inspect and remove points that created "noise" in the model. Final sparse point clouds had an average of 60,000 points.

The software used the refined sparse point cloud as a guide to generate a high quality dense point cloud (Supplementary Figure 2b). This step was the most time-consuming, but performance was improved when GPU acceleration was enabled. Once created, the dense point cloud was inspected manually to remove extraneous points. Often, light blue "floating points" were observed in the dense cloud. Because of their color, it is suspected these were an artifact of the software's recognition and alignment of similarly colored swaths of blue water around the colonies. Such points were easily removed with the "select points by color" functionality in the dense cloud tools. Final dense point clouds had an average of five million points.

The model was then referenced by placing markers at each end of the 3D representation of the metal washer, creating a virtual scale bar from these markers in Photoscan. The scale error was calculated by repeating the process for another object in the 3D model for which the size was known, for example the length of the metal tag marking the colony or another dimension of the metal washer. After being referenced, a mesh was built using source data from the dense cloud and an average of one million faces (Supplementary Figure 2c). Next, a texture was generated (Mapping mode generic, Blending mode

average, texture size 4096 x 1-4). The texture is the photographic data superimposed onto the raw mesh, and this improves model appearance and makes it easier to visually distinguish between coral, sponge, and macroalgae (Supplementary Figure 2d). The average time to process each model (per coral colony) from beginning to end was about two hours, depending on the number of photographs taken and available machine memory at time of processing.

The textured model (mesh plus photographic data) was exported out of Agisoft Photoscan, and into Autodesk® Meshmixer™ (Autodesk, Inc. 2017). In Meshmixer, the selection tool was used to manually separate coral and sponge from the rest of the model. These were saved as independent objects, but reference information and relative location from the original 3D model was preserved in these new objects.

For a single colony, the component pieces for the models generated at both time points were then uploaded into CloudCompare (CloudCompare 2.8.1, 2017). The model from the first time point (made of its component coral and sponge pieces) was inspected in relation to the model from the second time point to see if there were any obvious issues with scale. These were roughly aligned using the transform tool and then more finely registered using the alignment tool built into CloudCompare.

The split tool in CloudCompare was then used to uniformly slice the models into the four treatment quadrants. The split was applied simultaneously to models from both time points and their component coral and sponge 3D objects, resulting in uniform separation of treatment quadrants across time points and individual competitors. The surface area of each competitor in each treatment quadrant at each time point was recorded using the “measure mesh” tool in CloudCompare (Figure 4).

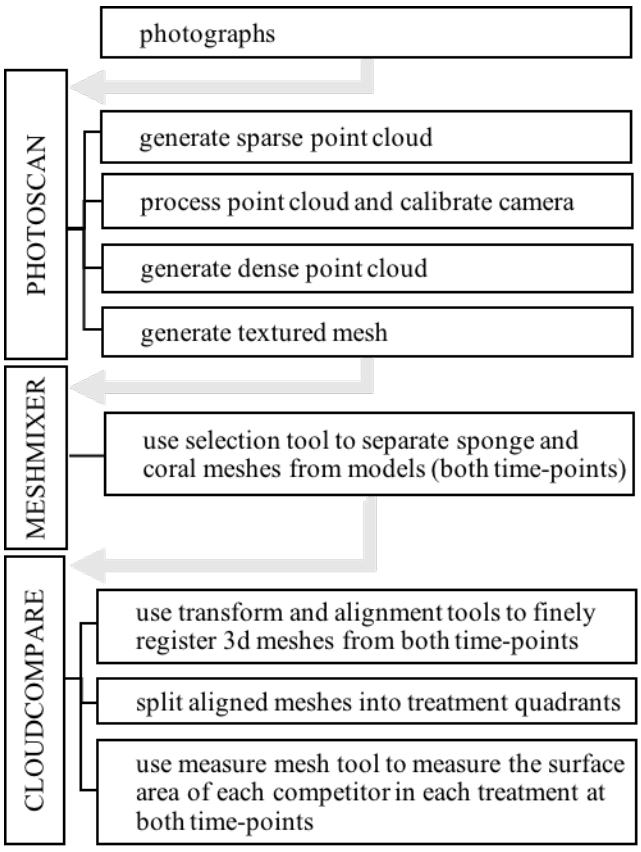

Figure 4: Photogrammetry workflow

Validation of Photogrammetric Methods

One limitation of *in situ* photogrammetry is the sensitivity of the reconstruction process to poor lighting. Inadequate lighting can cause poor image alignment and increase uncertainty in point clouds and meshes (Scott-Murray et al. 2016). This uncertainty was investigated by generating ten replicate meshes from a single set of photographs taken of an experimental colony (tag # 305) at Perseverance Bay, following the same workflow used to make 3D models of experimental and control colonies. The replicate meshes were contained in a single Photoscan file in ten separate chunks, and they were aligned with one another according to estimated camera locations. Mesh object files for each chunk were then exported from Photoscan into CloudCompare for fine-scale alignment. In CloudCompare, the split tool was used to uniformly crop the ten models to a rough outline of the coral colony, and then the areas of these ten cropped segments were measured. The standard error of the mean (SEM) of the ten segments' average surface area was investigated and compared to the change in surface area of coral and sponge segments; this verified whether change in surface area was due to ecologically relevant growth or a byproduct of 3D reconstruction variability.

No hole-filling operations were applied to the 3D meshes prior to surface area measurements because the raw meshes did not appear to contain many holes. To justify collecting surface area measurements from raw, un-processed meshes, a hole filling tool was applied to a subset of ten meshes representing individuals of *D. anchorata,* and the surface area of processed meshes was compared to that of the original meshes. *D. anchorata* was chosen because these were the most structurally complex meshes; structural complexity often leads photographic blindspots and thus large holes in reconstructed meshes. The hole filling tool in Meshlab was used to process the meshes, and the threshold was adjusted until every hole except for the large segment at the base of each mesh was filled. The average change in surface area due to hole filling was compared to the change in sponge surface area over time. The purpose of this was to confirm that the observed changes were in fact due to sponge growth and not a result of poor mesh architecture.

Analysis of Percent Change in 3D Surface Area of Sponges and Corals

Analyses were conducted on the segment of coral and sponge individual in each treatment quadrant. At Flat Key, one colony competing with *D. anchorata* (# 342) was not included in the analysis because of a poor photogrammetric scan. The analysis was conducted on the remaining 16 colonies (n = 8 with *A. cauliformis* and n = 8 with *D. anchorata*). At Perseverance Bay, one colony competing with *D. anchorata* (# 404) was not included in the analysis because of a poor photogrammetric reconstruction. The remaining 15 colonies were included in the analysis (n = 7 colonies with *A. cauliformis* and n = 8 with *D. anchorata*).

For each segment, the percent change in surface area was calculated by dividing the change in surface area (t_2-t_1) by the initial surface area. Three-factor ANOVAs were used to compare percent change in sponge surface area across treatments (sponge-algae, sponge), sponge species (*A. cauliformis, D. anchorata*), and site (Perseverance Bay, Flat Key). Data were Box-Cox transformed (lambda = -0.13, gamma = 36.53) in order to meet ANOVA assumptions (Bartlett's Test of homogeneity p = 0.47, Shapiro-Wilk Test of normality p = 0.6). Three-factor ANOVAs were also used to compare percent change in coral surface area across treatments, sponge species, and site. Data were Box-Cox transformed (lambda = -0.25, gamma = 33.25) in order to meet ANOVA assumptions (Bartlett's Test of homogeneity p = 0.37, Shapiro-Wilk Test of normality p = 0.98). When ANOVAs were significant, a Tukey HSD was conducted to test for pairwise differences among groups. Statistical analyses were performed in R (R core team, 2017).

Coral Size Class Transition Model

A size class transition model was developed to forecast how populations shrink due to competition. Surface area measurements were used to calculate the probability of coral transitioning to

smaller size classes during competition with sponge and algae, sponge only, algae only, or neither. Corals were separated into three size classes, and size class cutoffs were chosen to encompass the range of surface areas measured during the experiment (Hughes 1984). For each initial size class in each treatment, the transition probability was given by the fraction of the initial population that shrank or grew to another size class by the second time point. A matrix of these probabilities, with columns representing size class at t_1 and rows representing size class at t_2, was populated for each treatment combination and sponge species (Table 1).

Table 1: General layout of transition matrix. Values below the diagonal represent probabilities of growth to larger size classes (i.e. "Grow"). Values on the diagonal represent probability of remaining in the same size class (i.e. "Loop"). Values above the diagonal represent probability of shrinking to smaller size classes (i.e. "Shrink"). Adapted from Hughes (1984).

		Size at t1		
		Small	Medium	Large
Size at t2	Small	Loop	Shrink	Shrink
	Medium	Grow	Loop	Shrink
	Large	Grow	Grow	Loop

Static probabilities of transition, denoting the change in population size structure over ~91 d, were used to forecast future states. Transition probabilities were iteratively applied over 10 intervals of 91 d (total time = 910 d). The initial condition used in these forecasts was 1000 individuals in the largest size class, and this was different than previous studies that began forecasts with known population structure (e.g., Hughes 1984). Known populations were not used as the starting condition in this study because size classes reflected colony segments, not whole individuals. Also, the initial population comprised only the largest size class because the goal was to forecast how populations will shrink due to competition. Forecasted changes in coral size-structure were repeated four times to compare population response to i) multispecies competition with sponges and algae, ii) competition with sponges, iii) competition with algae, and iv) no competitors.

Photographic Analysis of Linear Growth

Linear growth and overgrowth rates were measured from photographs taken at two timepoints. The photographs of a single colony at two timepoints were imported into ImageJ (Abràmoff et al. 2004) and scaled according to scale bars photographed along with the colony. The distance between two features (e.g. two distinct coral polyps) was compared between time points to ensure that the scales were similar (< 3 mm difference) between images. Once the scales were confirmed to be similar, five measurements were taken in each photograph to get five rates of growth and overgrowth (Table 2). For the photo taken at the starting timepoint (t_1), a line was drawn from a distinct feature in the center of the

coral colony to the focal competitor in the corresponding treatment quadrant. For the ending time point (t_2), the same origin point used for t_1 was located, and a line was drawn from the origin point to the focal competitor in the treatment quadrant. To get the best estimate of linear growth, the lines visually inspected and compared to each other to ensure that they were drawn from the same origins and at the same angle with respect to the coral colony. The length of lines in t_1 and t_2 images were measured. Sponges and macroalgae grew inward, towards the center of the colony, thus their growth rate was given by the difference between t_1 and t_2 distances divided by elapsed time. Coral colonies extended outward, away from its center, thus coral growth rate was given by the difference between t_2 and t_1 distances divided by elapsed time.

Table 2: Growth and overgrowth rates variables that were measured during photographic analysis, and their definitions.

Variable	Definition
S_{c1}	Sponge rate of coral overgrowth in sponge-only treatment quadrant
S_{c2}	Sponge rate of coral overgrowth in sponge-algae treatment quadrant
M_s	Macroalgae rate of sponge overgrowth in sponge-algae treatment quadrant
M_c	Macroalgae rate of coral overgrowth in algae-only treatment quadrant
C_0	Coral rate of growth in any of the four treatment quadrants where colony perimeter was visible

In some cases, competitors were not visible in photographs; for example, some coral margins were completely obscured by sponge and macroalgae. If this was the case in any t_1 or t_2 photograph, the value of that variable for that colony and corresponding time interval was assigned as 'na' and omitted from analyses. In some cases, *L. variegata* was visible in t_1, but it appeared to recede or disappear in t_2. This could have been due to actual shrinkage of the algae, but this negative growth was often a result of loss of fronds. A loss of *L. variegata* fronds implied that the algae had failed to establish a holdfast on the colony. When this was the case, the value of the variable (M_s or M_c) for that colony and time interval was 0 and remained in the analyses. No negative values were assigned to *L. variegata* overgrowth variables (M_s or M_c) because of poor confidence in attributing negative growth to either shrinkage or loss of algae.

Two independent photographic analyses were conducted to compare across sites and seasons. The effect of site and season could not be analysed in a single analysis, though this would have been preferred, because photographs from each site were often taken at inconsistent time intervals. The dates of the photographic analysis also did not correspond to the dates that photogrammetric image sets were collected, because of the month-long delay between collection of 3D images. If photographic analysis was

conducted on these same dates, a delay between sites may have resulted in a confounded effect of site and time interval.

Photographic Analysis Including Site as Factor

The response of growth and overgrowth of each competitor to treatments, competing species, and sites over 62 d was analysed using photographs taken on November 19, 2016 and January 20, 2017. At Flat Key, one colony competing with *A. cauliformis* (#423) and two colonies competing with *D. anchorata* (#421, #424) were not included in the analysis due to poor or missing photos at either time-point. The analysis was conducted on the remaining 14 colonies (n = 7 with *A. cauliformis* and n = 7 with *D. anchorata*). At Perseverance Bay, two colonies competing with *D. anchorata* (#419, 497) were not included in the analysis due to poor or missing photos at either time-point. The analysis was conducted on the remaining 14 colonies (n = 7 with *A. cauliformis* and n = 7 with *D. anchorata*).

Two-factor ANOVAs were used to compare coral growth rates across overgrowing sponge species (*A. cauliformis* and *D. anchorata*) and sites (Perseverance Bay, Flat Key). Data were square-root transformed to meet assumptions of homoscedasticity (Bartlett Test p = 0.06) and normality (Shapiro-Wilk Test p = 0.46). Three-factor ANOVAs were used to compare sponge overgrowth rates of coral across treatments (sponge-algae, sponge only), sponge species, and sites. Untransformed data were leptokurtic and did not adhere to ANOVA assumptions. Parameters were fit to a heavy tail Lambert W & F distribution, and a bijective inverse transformation was used to back-transform the data according to the defined parameters (mu = 0.0332, sigma = 0.3944, alpha = 1, gamma = 0, delta =0.3136) and approximate a normal distribution. This transformed data adhered to assumptions of homoscedasticity (Bartlett Test p = 0.94) and normality (Shapiro-Wilk Test p = 0.57). Two-factor ANOVAs were used to compare algae overgrowth rates across competitors (*A. cauliformis, D. anchorata, and P. astreoides)* and sites (Perseverance Bay, Flat Key). Data were cube-root transformed to meet assumptions of homoscedasticity (Bartlett Test p = 0.09) and normality (Shapiro-Wilk Test p = 0.21).

Photographic Analysis Including Season as Factor

The response of growth and overgrowth to treatments, competitors, and seasons were analysed using photographs of Flat Key colonies comprising two intervals of 27-31 d. autumn photographs were taken on November 19, 2016 and December 16, 2016 and winter photographs were taken on February 11, 2017 and March 14, 2017. One colony competing with *D. anchorata* (#421) was not included in the analysis due to poor or missing photos at any time point. The analysis was conducted on the remaining 16 colonies (n = 8 with *A. cauliformis* and n = 8 with *D. anchorata*).

Coral growth rates were compared across seasons using a Welch's two-sample t-test. Untransformed data were adequate to meet assumptions of homoscedasticity (Bartlett Test p = 0.27) and

normality (Shapiro-Wilk Test $p = 0.064$). Three-factor ANOVAs were used to compare sponge overgrowth rates of coral across treatment (sponge-algae, sponge-only), sponge species (*A. cauliformis*, *D. anchorata*), and season (autumn, winter). Untransformed data adhered to ANOVA assumptions of homoscedasticity (Bartlett Test $p = 0.591$) and normality (Shapiro-Wilk Test $p = 0.059$). Data on macroalgae overgrowth rates across seasons were zero-inflated, and transformations (square root, cube root, logarithmic, inverse, and box-cox) were insufficient in making the data adhere to ANOVA assumptions. Alternatively, a binomial regression with a logit link function was used to investigate the binary response of algae overgrowth to season and competitors. Model fit was assessed incrementally by adding a predictor (sequence: null model, time int., time int. + competitor, and time int. + competitor + interaction) and conducting a X^2 goodness of fit test to compare the residual deviance between models with and without the added predictor. The best model was determined when, compared to a model with fewer predictors, the null hypothesis that the smaller model is adequate was rejected at the $p < 0.05$ level. The predictor from the best-fit model was determined to have a significant effect on the magnitude of the response at $p < 0.05$, and estimates were used to assess the direction of the response (algae overgrowth vs. no algae overgrowth) across levels of the predictor. Next, presence-only algae overgrowth rates were analyzed with non-parametric Kruskall-Wallis and Dunn's test of multiple comparisons using rank sums. A comprehensive summary of the experimental data that was collected from each of the techniques (photogrammetric and image analysis) can be found in Supplementary Table 1.

Analysis of Controls

Photographic analysis of control colonies from both sites was conducted to test whether there was any bias due to multiple types of competitive interactions (pairwise and multispecies) on a single coral colony. Photographs taken on November 19, 2016 and January 20, 2017 were analyzed. Growth rates measured on control colonies (pooled across site) were compared to growth rates in the sponge-only and algae-only treatment quadrants of experimental colonies measured over the same time interval. Even when pooled across sites, data on growth and overgrowth rates of competitors in control colonies still contained few replicates. A Wilcoxon Signed-Rank test was used to compare the sample means of growth and overgrowth rates of each competitor between control and treatment colonies. Sponge-coral overgrowth rates (*D. anchorata, A. cauliformis*) were compared between controls and sponge-only treatment quadrants on experimental colonies with matching sponge species. Macroalgae-coral overgrowth rates were compared between controls and algae-only treatments of all experimental colonies. Coral growth measurements on experimental colonies were conducted wherever the coral growth margin was visible, irrespective of treatment quadrant. Therefore, coral growth rates were compared between

sponge controls (either *D. anchorata* or *A. cauliformis*) and treatment colonies with the same sponge species, and coral growth rates were compared between macroalgae controls and all treatment colonies.

Benthic Surveys: Community-Scale Multispecies Competition

To examine frequency of competitive interactions between corals, sponges and algae, benthic surveys were conducted at both reef sites in October 2016. Five 5 x 2 m plots, comprised of aggregate or patch reef and at least 5 m apart from one another, were haphazardly chosen at each site (Figure 5). Surveys were conducted on target coral species *O. annularis, S. siderea,* and *P. astreoides*, sponge species *D. anchorata*, *A. cauliformis,* and *A. compressa,* and macroalgae species *Dictyota spp*. and *L. variegata.* Every pairwise coral-sponge, coral-macroalgae, and sponge-macroalgae interaction between target species in all plots was recorded, and individuals in each interaction were assigned as competitive "winners" or "losers" according to pre-defined criteria (Supplementary Table 2).

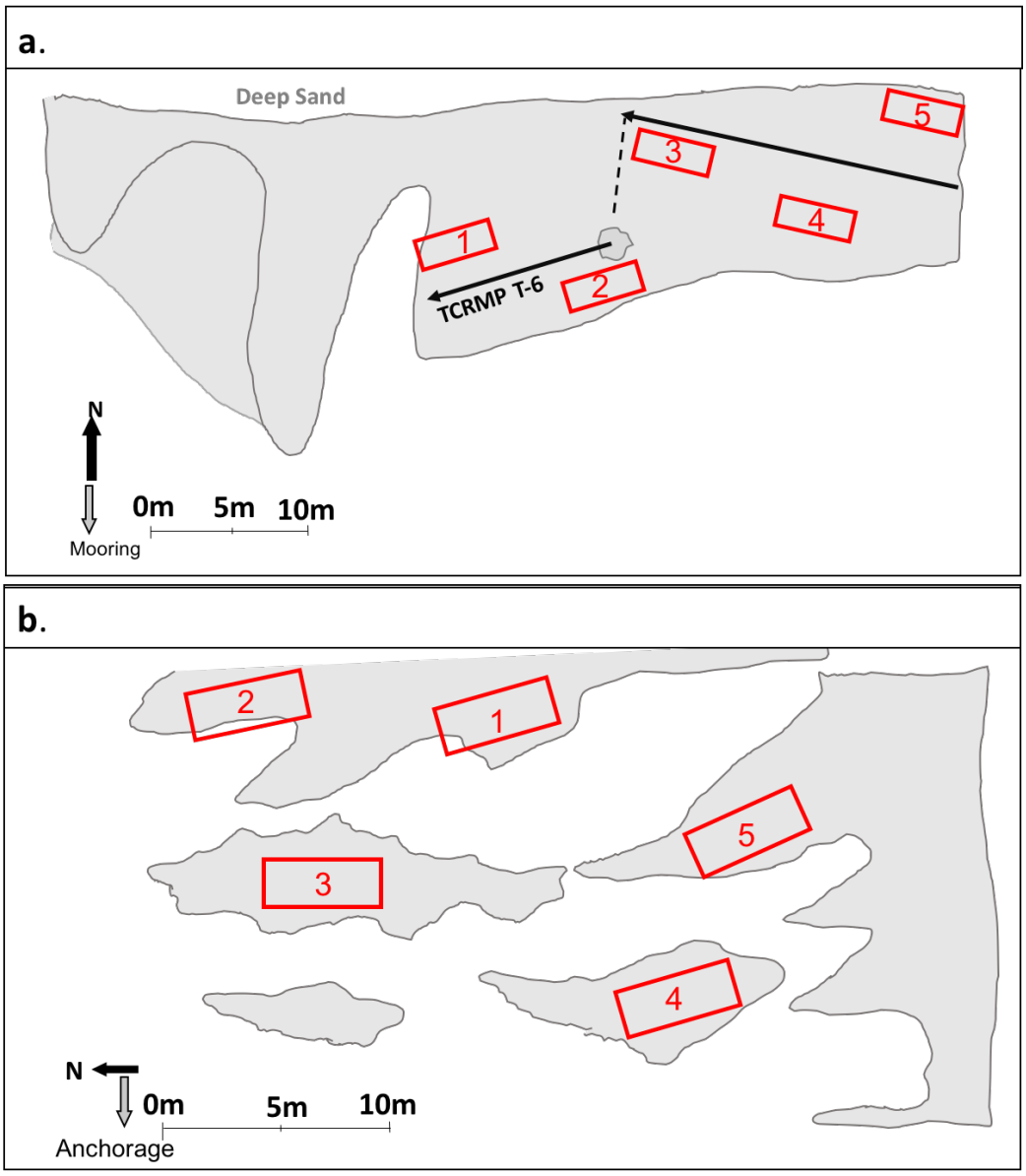

Figure 5: Map of plots at a) Flat Key and b) Perseverance Bay.

If the dominant competitor could not be determined, the interaction was marked as a standoff. Standoffs were defined in this work as margins of direct contact between individuals, with no visible overgrowth or tissue discoloration (Chadwick and Morrow 2011). The location of standoff interactions were mapped in each plot. Nails were attached to nearby substrate, taking care to not interfere with the competitive interaction and affect the competitive outcome (Aerts 2000). The standoff interactions, nearby reference nail, and ruler were photographed. Photographs were used to examine for visible overgrowth and tissue discoloration of each competitor, to confirm that the interaction was a standoff. For confirmed standoffs, ImageJ was used to measure the initial distance from standoff margin to reference

nail. In February 2017, four months after the initial survey, all confirmed standoffs were revisited and the distance from competitor margin to reference nail was re-measured. If the margin moved more than four millimeters, the interaction was characterized as an overgrowth, and the individual that grew more over its competitor was classified as the dominant competitor. If the distance from nail to margin moved less than four millimeters, the interaction remained classified as a standoff.

Analysis of Benthic Survey data

Frequencies of wins, losses, and standoffs were used to calculate an index of intransitivity for each of the 36 three-species combinations of the target species, according to the index system described by Tanaka and Nandakumar (1994). This technique is a precise way to characterize systems as having multiple types of hierarchies and networks, including networks that are based on symmetrical standoff interactions across species (Tanaka and Nandakumar 1994). Frequencies of wins, losses, and standoffs were tabulated for each unique species pair (Supplementary Table 3), and probabilities of wins, losses, and standoffs were calculated by dividing the number of each outcome (wins, losses, and standoffs) by the total number of encounters of those two species. For each three species combination, the following equations were used to transform these probabilities and numbers of interactions into win (WI), loss (LI) and standoff (SI) indices.

$$\boldsymbol{WI} = \sqrt{\frac{\sum_{i=1}^{n}\sum_{j=1}^{n} P_{ij}\,[W]^2}{\frac{n(n-1)}{2}}}$$

$$\boldsymbol{LI} = \sqrt{\frac{\sum_{i=1}^{n}\sum_{j=1}^{n} P_{ij}\,[L]^2}{\frac{n(n-1)}{2}}}$$

$$\boldsymbol{SI} = \sqrt{\frac{\sum_{i=1}^{n}\sum_{j=i+1}^{n} P_{ij}\,[S]^2}{\frac{n(n-1)}{2}}}$$

Where WI is the win index, P_{ij}[W] is the probability that species i wins over species j, n is the number of species, LI is the loss index, P_{ij}[L] is the probability that species i loses to species j, SI is the standoff index, and P_{ij}[S] is the probability that species i exists in a standoff with species j (Supplementary Table 4).

A boundary value (BV) was used as a reference to compare the WI from the observed outcomes to a competitively neutral system (neither hierarchical nor intransitive). To calculate the BV, the probabilities of wins and losses were rearranged (leaving the probability of standoffs the same) so that they reflect a maximum competitive hierarchy (macroalgae ←sponge ←coral) (Supplementary Table 5).

Next, probabilities were rearranged to reflect a maximum network (macroalgae ←sponge ←coral and coral ← macroalgae) by subtracting standoff probabilities from 1 and dividing the remaining probabilities equally across wins and losses in each pairwise interaction (Supplementary Table 6). WIs from both scenarios were averaged together to calculate the WI of a completely neutral system, and this average value was the BV. If SI = WI, the system was neutral (neither hierarchical or network), and if SI > WI, the system was a network due to stand-offs. If SI < WI, the WI from that system was compared to the BV. If WI > BV, the system was classified as hierarchical, and If WI < BV, the system was classified as a network due to wins and losses.

Results

Manipulative Experiment: Local Multispecies Competition

Validation of Photogrammetric Methods

The surface area of the coral segments generated from replicate reconstructions of Perseverance colony #305 demonstrated minimal variability. The average area of the measured segments was 147.96 cm^2 and the standard error of the mean (SEM) was 0.13 cm^2. The SEM was consistently less than the change in surface area recorded for sponge and coral competitors in all 3D reconstructions of experimental colonies. These results validate the use of photogrammetry for the analyses of percent change in 3D surface area. Additionally, the meshes that were processed with the hole filling tool exhibited, on average, a 1.202 ± 0.43 cm^2 increase in surface area, compared to original meshes. This increase was consistently less than the growth of sponges over the experimental duration (11.4 ± 1.88 cm^2). These results validate the use of raw meshes for the measurement of 3D surface area of these species over a three-month period.

Analysis of Percent Change in 3D Surface Area of Sponges and Corals

Over the 91 d experimental duration, the greatest average gain (± SEM) in coral surface area (7.06 ± 19.87%) occurred in coral-only treatment quadrants on colonies competing with *A. cauliformis* at Flat Key. The greatest loss in coral surface area (-35.06 ± 22.69%) occurred in sponge-algae treatment quadrants at Flat Key on colonies competing with *D. anchorata*. Coral percent change in surface area differed significantly across treatments ($p = 0.00$) and sponge species ($p = 0.02$), and there was no interaction ($p = 0.30$) (Table 3). A Tukey HSD test indicated that corals lost a greater percentage of surface area in sponge-algae treatment quadrants than in coral-only treatment quadrants for colonies competing with *D. anchorata* ($p = 0.02$). The percent change in coral surface area was also significantly lower in sponge-algae treatment quadrants of corals competing with *D. anchorata*, compared to the sponge, algae, and coral-only treatment quadrants of corals competing with *A. cauliformis* ($p = 0.05$, 0.02, 0.00, respectively) (Figure 6).

Table 3: ANOVA of percent change in coral surface area across treatment and sponge species.

	Df	Sum.Sq	Mean.Sq	F.value	p
Treatment	3	1.35	0.45	4.85	0.00
Sponge Spp.	1	0.52	0.52	5.63	0.02
Treatment: Sponge spp.	3	0.34	0.11	1.23	0.30
Residuals	109	10.15	0.09		

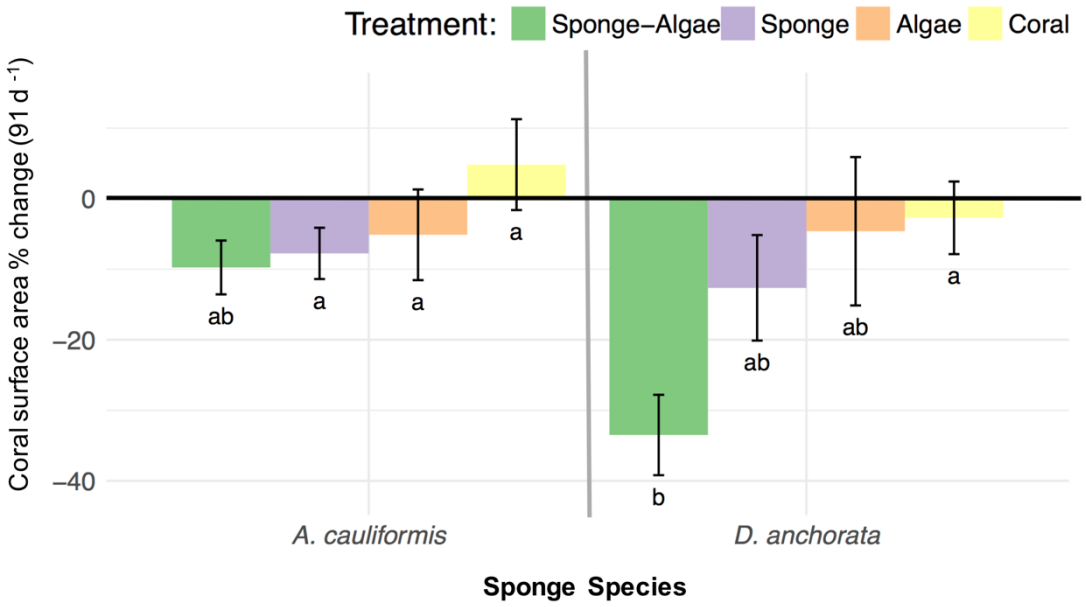

Figure 6: Average percent change in coral surface area (± SEM) over 91 d, separated by treatment and sponge species. Letters indicate significant differences across factor levels.

The greatest average gain (± SEM) in sponge surface area (20 ± 37.27%) was measured on *D. anchorata* in sponge-algae treatment quadrants at Flat Key. *A. cauliformis* demonstrated the greatest loss in surface area (-11.85 ± 27.3%), and this was also measured on sponge-algae treatment quadrants at Flat Key (Figure 7). Sponge percent change in surface area did not differ across treatments ($p = 0.75$), sponge species ($p = 0.97$), or sites ($p = 0.95$), and there were no interactions among any combination of factors (Table 4).

Table 4: ANOVA of percent change in sponge surface area across treatment, sponge species, and site.

	Df	Sum.Sq	Mean.Sq	F.value	p
Treatment	1	0.04	0.04	0.10	0.75
Sponge spp.	1	0.00	0.00	0.00	0.97
Site	1	0.00	0.00	0.00	0.95
Treatment:Sponge spp.	1	1.17	1.17	2.78	0.10
Treatment:Site	1	0.25	0.25	0.59	0.44
Sponge spp.:Site	1	0.70	0.70	1.67	0.20
Treatment:Sponge spp.:Site	1	0.01	0.01	0.03	0.87
Residuals	54	22.79	0.42		

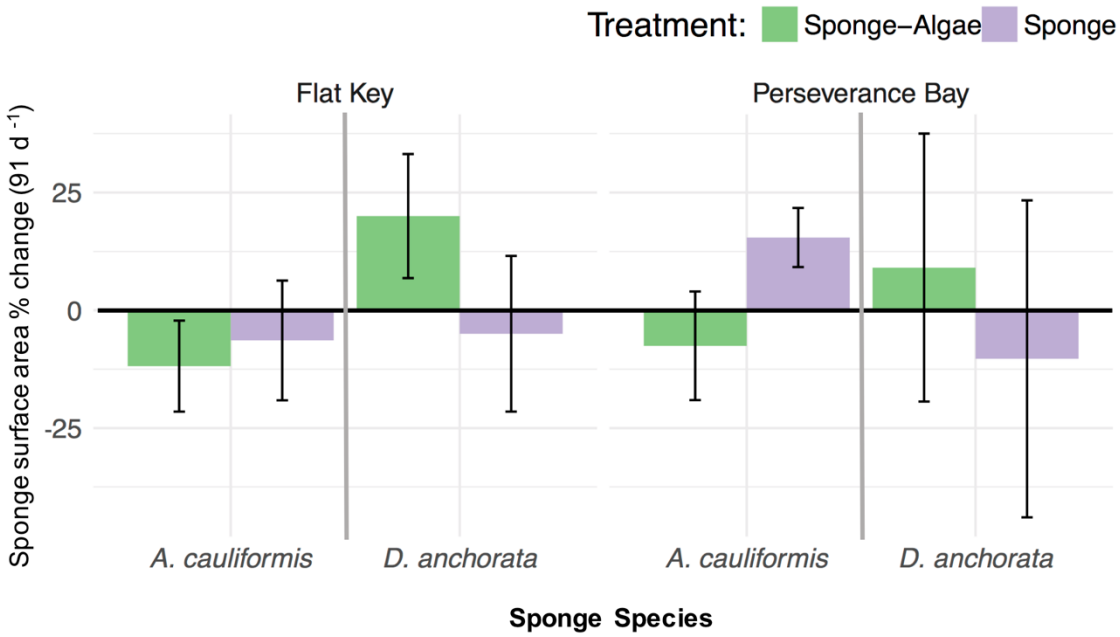

Figure 7: Average percent change in sponge surface area (± SEM) over 91 d, separated by treatment, sponge species, and site.

Coral Size Class Transition Model

The three size classes chosen to encompass the greatest variation were small (< 17cm^2), medium (17-33 cm^2) and large (33 cm^2). The probability of transition to a smaller size class was greatest for medium and large corals competing with sponges and algae, and large corals competing only with sponges. The only growth from a smaller to larger size class occurred in small corals competing only with algae. The probability of staying in the same size class was 100% for small corals competing with sponges and algae, small corals competing only with sponges, medium corals competing only with algae, and all size classes in the coral only treatments (Figure 8).

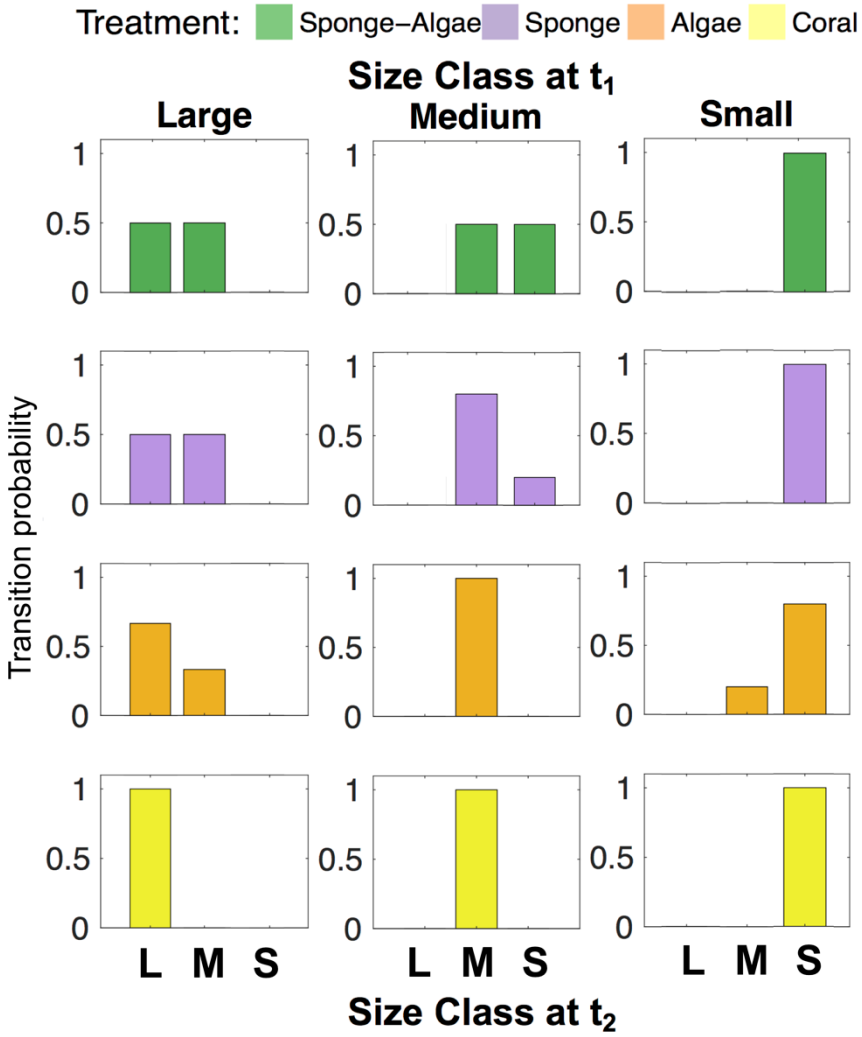

Figure 8: Proportion of individuals that transitioned to a smaller size class or stayed in the same size class.

When transition probabilities are forecasted over time, corals competing with sponge and algae shrink rapidly from the largest size class, followed by a small and brief peak in the medium size class, and a quick rise in the smallest size class to almost 100% of the population. When competing only with sponge, corals experience an equally rapid drop from the largest size class, but this is followed by a larger and more extended peak in the medium size class, and a slow rise of the smallest size class. When competing only with algae, there is a less severe drop from the largest size class that corresponds to an increase in the medium size class. With no competitors, the largest size class remains dominant throughout the simulated 800 d period. Forecasts of 800 d exceed the lifespan of sponges and macroalgae, but differences among competitive scenarios were evident prior to t = 270 d (~9 mo), the average lifespan of *D. anchorata* (Wulff 2008; van Duyl et al. 2011). At t = 270 d, the population in the sponge-algae

forecast was dominated by the small size class (60% of the cohort), while the populations in the sponge-only and algae-only forecasts were dominated by the medium size class (60% and 75% of the cohort, respectively) (Figure 9).

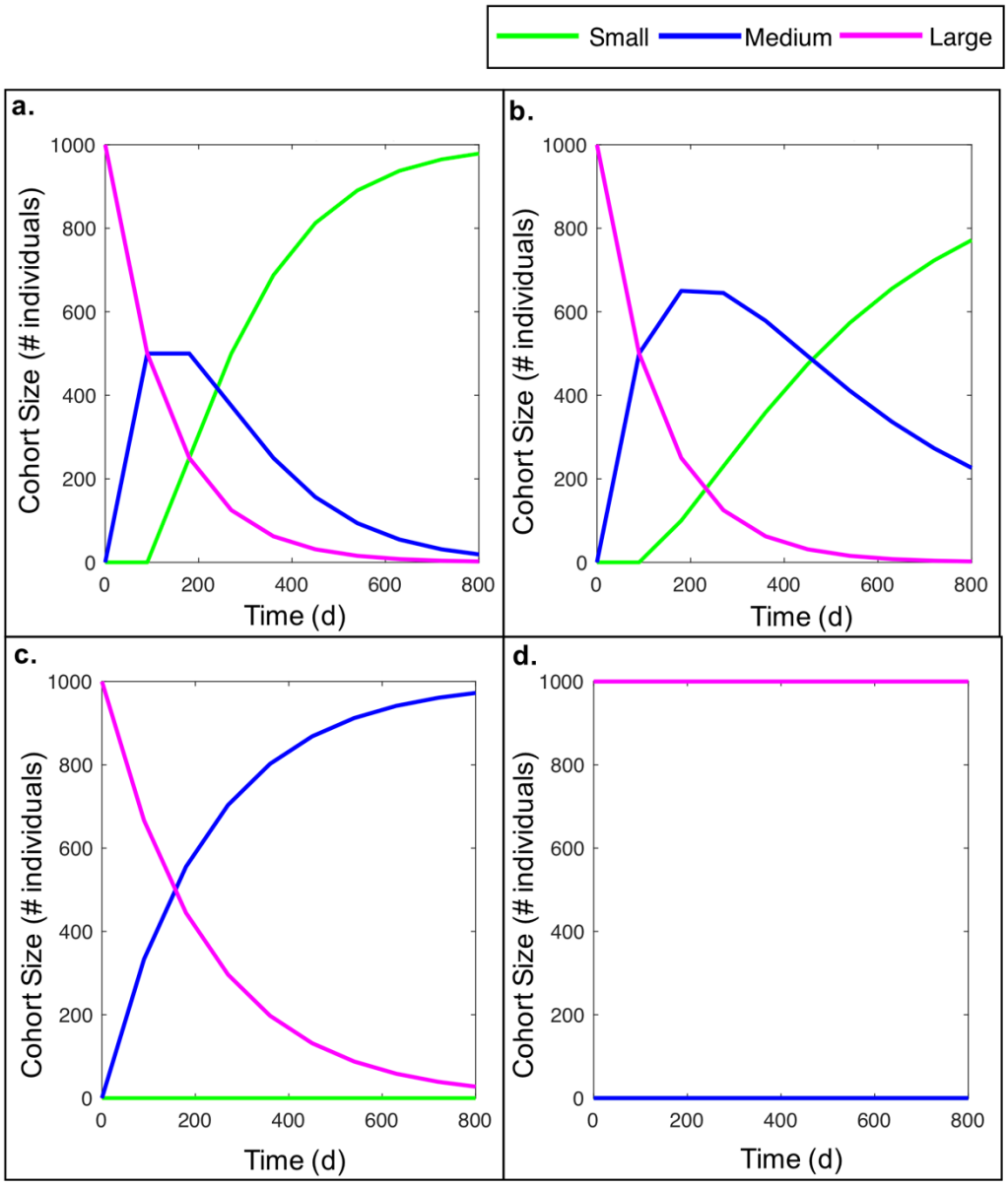

Figure 9: Forecasted population structure change over time for coral (*P. astreoides*) competing with (a) sponge (*D. anchorata*) and macroalgae (*L. variegata*), (b) sponge only, (c) algae only, (d) neither sponge or algae.

Photographic Analysis of Linear Growth

Photographic Analysis Including Site as Factor

At Flat Key, the average rate of coral growth (± SEM) was 0.52 ± 0.5 cm. At Perseverance Bay, the average rate of coral growth (± SEM) was 0.53 ± 0.43 cm. A Welch's two-sampled t-test indicated no significant differences in average coral growth rate across sites (t = -0.34, df = 16.67, p = 0.74) (Figure 10).

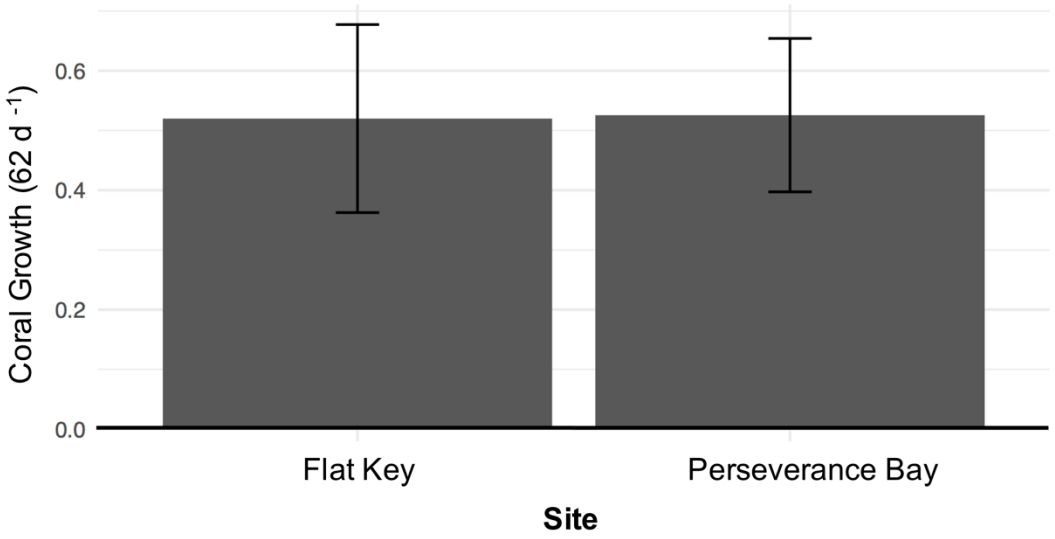

Figure 10: Average coral growth (± SEM) at each site over 62 d.

The greatest average linear growth of sponge over coral (± SEM) was 0.72 ± 0.79cm, and this occurred on *D. anchorata* in sponge-algae treatment quadrants at Perseverance Bay. The greatest negative growth (-0.32 ± 0.5cm) was measured on *A. cauliformis* in sponge-only treatment quadrants at Flat Key (Figure 11). Initially, the ANOVA design included treatment quadrants, sponge species, site, and all interactions as factors, but this design indicated no significant effect of site (p = 0.89). The ANOVA was rerun using only treatment, sponge species, and the interaction as factors. Sponge growth rates differed significantly across treatments (p = 0.02) and sponge species (p = 0), but there was no interaction (p = 0.11) (Table 5). A Tukey HSD test indicated that the growth rate of *D. anchorata* was significantly greater in sponge-algae treatment quadrants, compared to *D. anchorata* in sponge-only treatment quadrants (p = 0.0314), *A. cauliformis* in sponge-algae treatment quadrants (p = 0.003), or *A. cauliformis* in sponge-only treatment quadrants (p = 0.008) (Figure 11).

Table 5: ANOVA of sponge-coral overgrowth across treatment and sponge species.

	Df	Sum.Sq	Mean.Sq	F.value	p
Treatment	1	0.66	0.66	5.69	0.02
Sponge spp.	1	1.52	1.52	13.08	0.00
Treatment: Sponge spp.	1	0.30	0.30	2.62	0.11
Residuals	48	5.57	0.12		

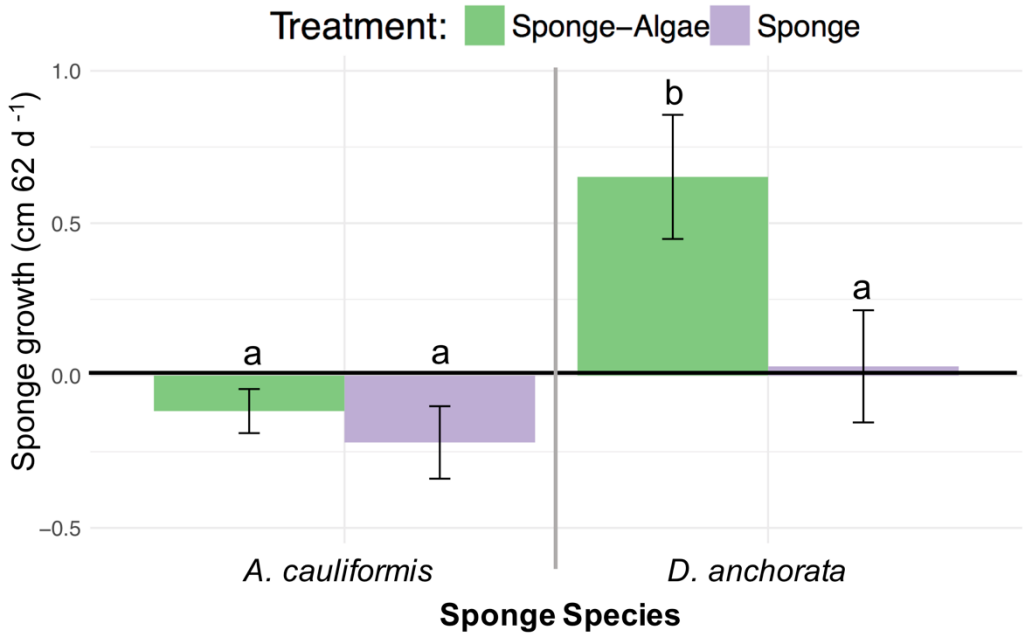

Figure 11: Average sponge-coral overgrowth (± SEM) over 62 d, separated by treatment and sponge species. Letters indicate significant differences across factor levels.

The average distance macroalgae overgrew coral (± SEM) was 0.36 ± 0.43 cm and 0.39 ± 0.29 cm at Flat Key and Perseverance Bay, respectively. Macroalgae-sponge overgrowth was the fastest (0.36 ± 0.62cm) on *A. cauliformis* at Flat Key. Conversely, no overgrowth of *D. anchorata* by *L. variegata* occurred at Perseverance Bay. Initially, the ANOVA design included competitor, site, and the interaction as factors, but this design indicated no significant effect of site ($p = 0.53$) or interaction ($p = 0.798$). The ANOVA was rerun using only competitor as a factor, and this test indicated significant differences in macroalgae overgrowth rates across competitors ($p = 0.001$) (Table 6). A Tukey HSD test indicated that macroalgae overgrowth rates were significantly greater on *P. astreoides* than on *D. anchorata* ($p = 0.0007$). (Figure 12).

Table 6: ANOVA of macroalgae overgrowth across competitors.

	Df	Sum.Sq	Mean.Sq	F.value	p
Competitor	2	1.992	0.996	8.01	0.001
Residuals	47	5.845	0.124		

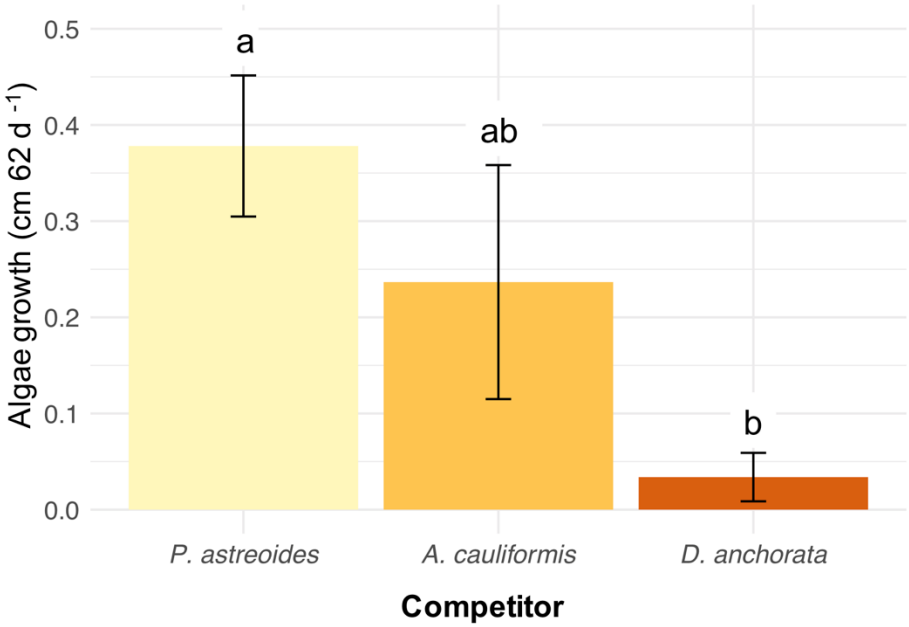

Figure 12: Average macroalgae overgrowth of each competitor over 62 d. Letters indicate significant differences among factors.

Photographic Analysis Including Season as Factor

In autumn, the average rate of coral growth (± SEM) was 0.09 ± 0.26 cm. In winter, the average rate of coral growth (± SEM) was 0.28 ± 0.51cm (Figure 13). A Welch's two-sampled t-test indicated no significant differences in coral growth rates across seasons ($t = 1.09$, $df = 14.9$, $p = 0.29$).

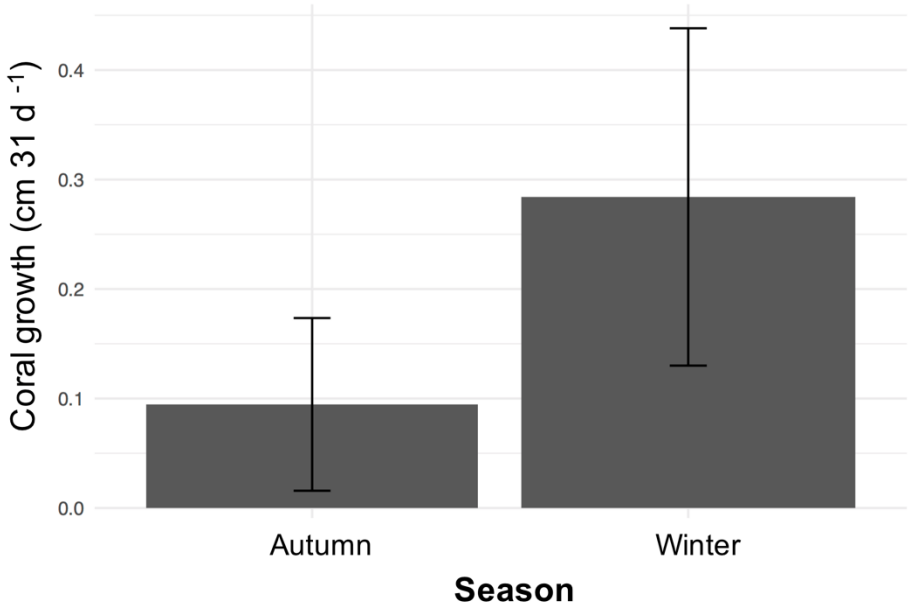

Figure 13: Average coral growth (± SEM) in each season over 31 d.

The greatest average sponge-coral overgrowth (± SEM) was 0.52 ± 0.37 cm in 30 d, and this was measured on *D. anchorata* in sponge-algae treatment quadrants in the winter. The greatest retreat of sponges (± SEM) was -0.19 ± 0.38 cm, and this was measured in sponge-only treatment quadrants also on *D. anchorata* in the winter. The ANOVA revealed no significant differences across season ($p = 0.6$), but there was a significant response of sponge growth to treatment ($p = 0.01$) and an interaction between treatment and sponge species ($p = 0.04$; Table 7). A Tukey HSD test indicated that *D. anchorata* overgrowth of coral was significantly greater in sponge-algae than in sponge treatment quadrants ($p = 0.007$; Figure 14).

Table 7: ANOVA of sponge-coral overgrowth across treatment, sponge species, and season.

	Df	Sum.Sq	Mean.Sq	F.value	p
Treatment	1	1.60	1.60	7.38	0.01
Sponge spp.	1	0.32	0.32	1.46	0.23
Season	1	0.06	0.06	0.28	0.60
Treatment: Sponge spp.	1	1.02	1.02	4.72	0.04
Treatment: Season	1	0.06	0.06	0.28	0.60
Sponge spp.: Season	1	0.00	0.00	0.01	0.94
Treatment: Sponge Spp.: Season	1	0.02	0.02	0.10	0.76
Residuals	44	9.56	0.22		

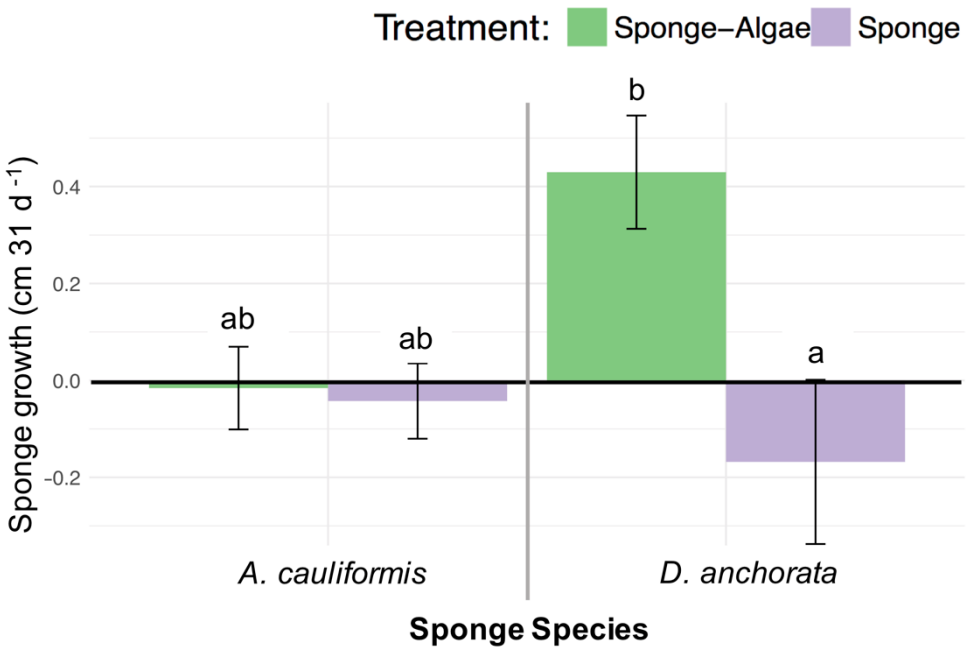

Figure 14: Average sponge-coral overgrowth (± SEM) over 31 d, separated by treatment and sponge species. Letters indicate significant differences across factors.

Macroalgae overgrew 64% of corals in the autumn and 100% of corals in the winter. Macroalgae overgrew 12.5% and 28.6% of sponges *D. anchorata* and *A. cauliformis* in the autumn, respectively, but macroalgae overgrew 100% of both species in the winter (Table 8). A chi-square test revealed that the best fit binary logistic regression model included competitor and season as predictors (model formula: presence ~ competitor + season); this was the smallest model that resulted in rejection of the null hypothesis of adequacy of the model with fewer predictors ($p = 0.00$). The GLM output indicated no significant differences in log odds of algae overgrowth between seasons ($p = 0.992$) even though the estimate was large (Est = 20.409). This was unexpected given the difference in proportion of overgrowth interactions between autumn and winter (Table 8). This appears to be due to an inflated standard error (SE = 2063.381) which may be a result of the small sample size. The only significant predictor in the model revealed that the log odds of macroalgae-*P. astreoides* overgrowth were 2.534 ± 1.206 higher than macroalgae-*D. anchorata* overgrowth ($p = 0.036$; Table 9).

Table 8: Summary of proportion of macroalgae overgrowths across season and competitor.

Season	Competitor	n	proportion
winter	*P. astreoides*	11	1.000
winter	*A. cauliformis*	6	1.000
winter	*D. anchorata*	6	1.000
autumn	*P. astreoides*	14	0.643
autumn	*A. cauliformis*	7	0.286
autumn	*D. anchorata*	8	0.125

Table 9: Results of the macroalgae overgrowth binomial logistic regression. AC = *A. cauliformis,* DA = *D. anchorata.* Res. Dev = Residual deviance, Null Dev. = Null deviance.

Coefficient	Est	SE	z	p
Intercept	-1.946	1.069	-1.82	0.069
Competitor (AC - DA)	1.03	1.358	0.758	0.448
Competitor (PA - DA)	2.534	1.206	2.101	0.036
Season (winter – autumn)	20.409	2063.381	0.01	0.992
Res. Dev (Null. Dev.)	32.653(65.726)			

Because macroalgae had a low proportion of overgrowths in the autumn, winter data were used in the analysis of presence-only macroalgae overgrowth rates. A Kruskall-Wallace test indicated significant differences across competitors (chi Sq = 8.102, df = 2, p = 0.017). Pairwise comparisons from a Dunn's test, a non-parametric analog of a Tukey HSD, revealed that macroalgae overgrowth of *A. cauliformis* was significantly greater than *P. astreoides* (p = 0.008) (Figure 15).

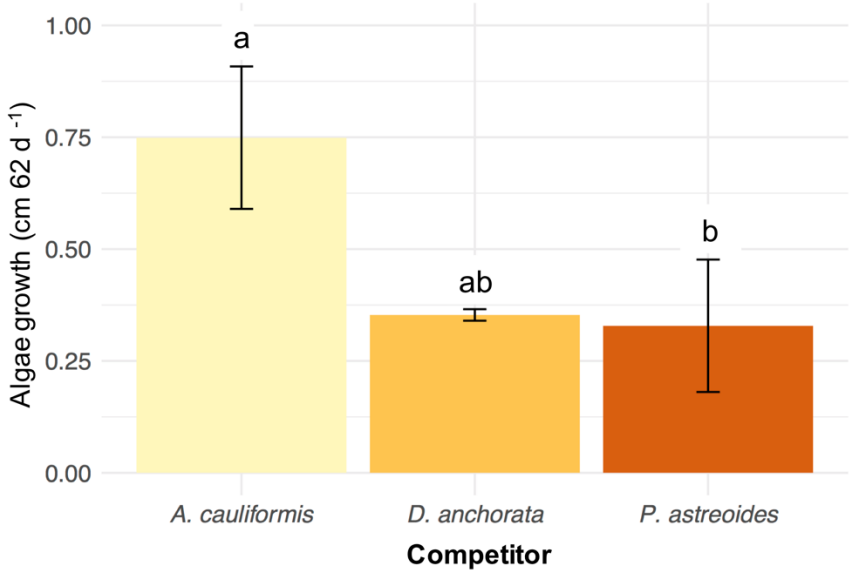

Figure 15: Presence-only macroalgae overgrowth (± SEM) over 31 d in the winter, separated by competitors. Letters from a Dunn's test indicate significant differences across levels.

Analysis of Controls

Even when pooled across sites, data on growth and overgrowth rates of competitors in control colonies contained few replicates (Table 10). This is why a Wilcoxon Signed-Rank test was used to compare the sample means of growth and overgrowth rates of each competitor in each control to the sample means of overgrowth rates in corresponding experimental treatments. All seven Wilcox tests

indicated that the growth rate of the competitor on the control did not differ significantly from the experimental treatment (Table 11).

Table 10: Summary of mean growth of each competitor on controls over 62 d.

Control	Competitor	Mean	SEM	n
A. cauliformis	Sponge	-0.038	0.245	4
A. cauliformis	Coral	0.178	0.127	4
D. anchorata	Sponge	0.588	0.126	3
D. anchorata	Coral	0.325	0.168	3
L. variegata	Macroalgae	0.427	0.260	2
L. variegata	Coral	0.170	0.016	2

Table 11: Summary of the Wilcox tests comparing the growth rates of each competitor in each control to corresponding competitor growth rates in experimental treatments.

Control	Competitor	W	p
A. cauliformis	Sponge	30	0.521
A. cauliformis	Coral	13	0.671
D. anchorata	Sponge	36	0.068
D. anchorata	Coral	12	0.364
L. variegata	Macroalgae	18	0.713
L. variegata	Coral	35	0.141

Benthic Surveys: Community-Scale Multispecies Competition

In total, 207 overgrowth interactions were recorded at Flat Key, and 144 overgrowth interactions were recorded at Perseverance Bay. *S. siderea* was the coral most frequently overgrown at Flat Key, followed by *P. astreoides* and *O. annularis* (Figure 16a). *P. astreoides* was the coral species most frequently overgrown at Perseverance bay, followed by *O. annularis* and *S. siderea* (Figure 16b). The sponge *A. cauliformis* overgrew corals more frequently than *A. compressa* at Flat Key (Figure 16a), but *A. compressa* and *A. cauliformis* overgrow corals with similar frequency at Perseverance Bay (Figure 16b). Of the sponge species surveyed, *A. cauliformis* was most commonly overgrown by both species of algae at both sites (Figure 17). The algae *Dictyota spp.* overgrew corals and sponges more frequently than *L. variegata* at both sites (Figure 16-17).

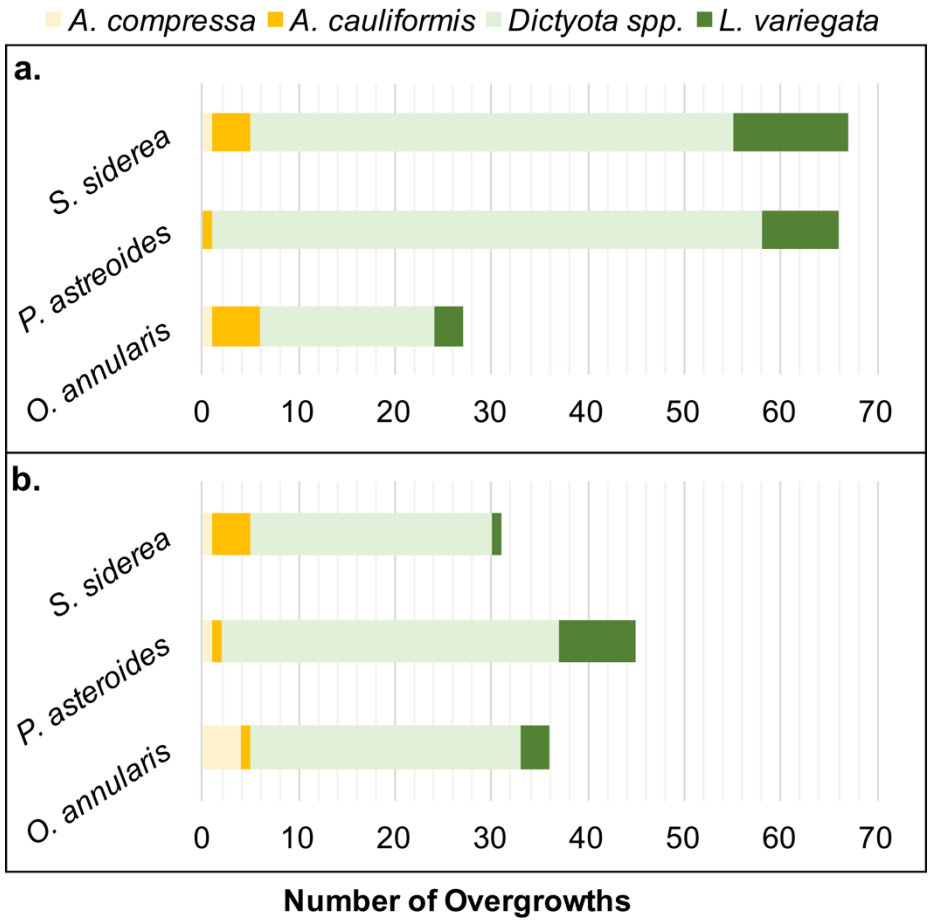

Figure 16: Frequency of coral overgrowths by sponge and macroalgae at a) Flat Key and b) Perseverance Bay.

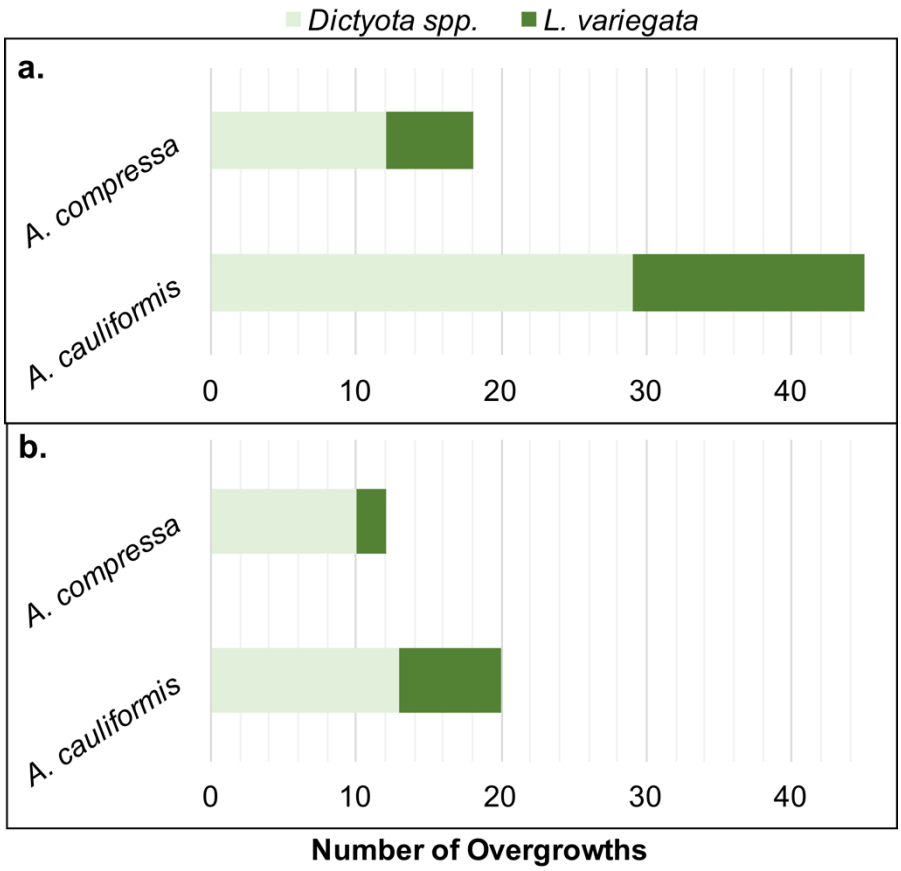

Figure 17: Frequency of sponge overgrowths by macroalgae at a) Flat Key and b) Perseverance Bay

Standoffs were less frequent than expected at both sites. Five standoffs in total were initially recorded at Flat Key, and four standoffs were initially recorded at Perseverance Bay (Table 12). Upon photographic examination, six standoffs were reclassified as overgrowth interactions because of the presence of a small degree of overgrowth. In total, two standoffs were confirmed at Flat Key and one standoff was confirmed at Perseverance Bay.

Table 12: Standoffs identified at Flat Key and Perseverance Bay. SO1 = Standoff competitor 1, SO2 = Standoff competitor 2, AC = *A. cauliformis*, AM = *A. compressa*, PA = *P. astreoides*, OA = *O. annularis*, SS = *S. siderea*, OG = Overgrowth. *standoff was not relocated in February.

Site	SO1	SO2	Confirmed standoff?	winner	Start Date	End Date
Flat Key	AC	SS	Yes	AC	10/28/16	2/11/17
Flat Key	AC	OA	no (OG).	AC	10/28/16	2/11/17
Flat Key	AC	OA	Yes	N/A*	10/28/16	2/11/17
Flat Key	AC	SS	no (OG).	AC	10/28/16	2/11/17
Flat Key	AM	OA	no (OG).	AM	10/28/16	2/11/17
Pers. Bay	PA	AM	no (OG).	AM	11/17/16	2/11/17
Pers. Bay	PA	AM	Yes	PA	11/17/16	2/11/17
Pers. Bay	PA	AC	no (OG).	AC	11/17/16	2/11/17
Pers. Bay	OA	AM	no (OG).	AM	11/17/16	2/11/17

None of the confirmed standoffs were persistent between October and February; all standoff margins moved and indicated competitive dominance of one species over another. At Flat Key, both standoffs were between *A. cauliformis* and either *S. siderea* or *O. annularis*. Repeated measurements in February confirmed that *A. cauliformis* overgrew *S. siderea,* but the second standoff (between *A. cauliformis* and *O. annularis*) could not be relocated. At Perseverance Bay, repeated measurements in February of the *P. astreoides-A. compressa* demonstrated competitive dominance of the coral. The sponge *A. compressa* appeared to retreat, while the coral managed to hold its ground and expand. This was the only interaction where coral appeared to be competitively dominant over any sponges or macroalgae in these surveys.

From intransitivity index calculations, 22 competitive hierarchies and zero competitive networks were identified for the 36 possible combinations of target coral, sponge, and macroalgae species across both sites. The remaining fourteen combinations could not be assessed due to the absence of pairwise interactions among *O. annularis*/*D. anchorata* (both sites), *P. astreoides*/*D. anchorata* (both sites), *P. astreoides*/*A. compressa* (Flat Key), and *S. siderea*/*D. anchorata* (both sites) (Table 13).

Table 13: Results of intransitivity index calculations for each combination of corals, sponges, and macroalgae. N/A indicates intransitivity index could not be calculated due to absence of pairwise interactions.

Site	Sponges	Corals			Macroalgae
		O. annularis	*P. astreoides*	*S. siderea*	
Flat Key	*A. cauliformis*	Hierarchy	Hierarchy	Hierarchy	*Dictyota spp*
		Hierarchy	Hierarchy	Hierarchy	*L. variegata*
	A. compressa	Hierarchy	N/A	Hierarchy	*Dictyota spp*
		Hierarchy	N/A	Hierarchy	*L. variegata*
	D. anchorata	N/A	N/A	N/A	*Dictyota spp*
		N/A	N/A	N/A	*L. variegata*
Pers. Bay	*A. cauliformis*	Hierarchy	Hierarchy	Hierarchy	*Dictyota spp*
		Hierarchy	Hierarchy	Hierarchy	*L. variegata*
	A. compressa	Hierarchy	Hierarchy	Hierarchy	*Dictyota spp*
		Hierarchy	Hierarchy	Hierarchy	*L. variegata*
	D. anchorata	N/A	N/A	N/A	*Dictyota spp*
		N/A	N/A	N/A	*L. variegata*

Discussion

Results from both the experiment and field surveys suggest that during multispecies competition with sponges and macroalgae, corals are the inferior competitor in a competitive hierarchy. In the experiment, outcomes of local competitive interactions suggested a greater risk of coral competitive exclusion during multispecies competition than during pairwise competition. Coral surface area was

significantly reduced in sponge-algae treatments compared to all other treatments, and size-structure forecasts indicated that corals competing with *D. anchorata* and *L. variegata* most rapidly shrank to the smallest size classes. When in contact with *L. variegata, D. anchorata* more rapidly overgrew *P. astreoides*. Sponge-algae contact seemed to confer a competitive advantage to *D. anchorata,* and this was directly contrary to the hypothesis that sponge-algae interactions would inhibit both competitors' ability and indirectly improve coral competitive success (i.e., "enemy's enemy indirect facilitation"; Laird and Schamp 2008). Similarly, benthic surveys revealed a unanimous pattern of competitive hierarchies (macroalgae ←sponges ←corals). A scarcity of standoffs prevented detection of coral competitive superiority, which was required to detect evidence of intransitivity in the surveys. As hypothesized, considerable species-specificity was detected in this work. In the experiment, contact between *L. variegata* and *A. cauliformis* did not accelerate sponge-coral overgrowth. Any facilitation resulting from contact between *L. variegata* and heterotrophic, encrusting *D. anchorata* may not apply to photosynthetic, rope-like *A. cauliformis* (McLean and Yoshioka 2008; Easson et al. 2014). In the benthic interaction surveys, some pairwise interactions were absent, notably between *D. anchorata* at both sites and *A. compressa* at Perseverance Bay. The choice of coral species may have affected the survey results, as these species do not possess competitive life-history strategies (Darling et al. 2012). Persistence of weedy corals (e.g., *P. astreoides*), which now comprise the most common reef-building corals on many Caribbean reefs (Green et al. 2008), may depend on whether these species' demographic processes (e.g., recruitment, mortality) can offset the competitive advantage of sponges and macroalgae.

Multispecies Competition is Hierarchical

Local Competition (Experiment)

It was theorized that sponge-macroalgae competition would impede the combative ability of either colonizing group and promote coral coexistence, a mechanism of intransitivity known as "enemy's enemy indirect facilitation" (Laird and Schamp 2008). The results of the experiment implied that the inverse of "enemy's enemy" facilitation occurs in interactions involving the sponge *Desmapsamma anchorata.* Coral surface area was significantly reduced in sponge-algae treatments compared to all other treatments, and size-structure forecasts indicated that corals competing with *D. anchorata* and *Lobophora variegata* most rapidly shrank to the smallest size classes. Loss of coral surface area coincided with increased lateral growth of *D. anchorata* in sponge-algae treatment quadrants, suggesting that contact with *L. variegata* confers a competitive advantage to the sponge. Mechanisms for macroalgae-mediated facilitation of sponge-overgrowth on coral, categorized by symbioses (mutualism, commensalism, and parasitism), are proposed here. Mutualistic or commensalistic interactions are proposed following many previously reported sponge-alga mutualistic associations (e.g., Easson et al. 2014, Davy et al. 2002), but a

sponge-alga parasitism is most likely because *L. variegata* did not appear to benefit from contact with the sponge.

A parasitic relationship between *L. variegata* and *D. anchorata* may exist if contact with both macroalgae and coral induces different antagonistic mechanisms in the sponge and makes it a more aggressive competitor. Similar to the competitive outcomes observed in this research, recent studies on wood-decay fungi demonstrated that some species procured more space on a wooden block when oriented between two competitors compared to when only faced with one competitor (Hiscox et al. 2017). It was proposed that the centrally located competitor developed a diverse arsenal of antagonistic mechanisms that made it more combatively aggressive overall (Hiscox et al. 2017). The antagonistic mechanisms evoked by wood decay fungi are allelochemicals, such as volatile organic compounds (VOC) (El Ariebi et al. 2016). Many sponges, including *D. anchorata,* utilize similar defenses during spatial competition; a number of secondary metabolites have been extracted from *D. anchorata* that possess anti-microbial, larvicidal, and anti-predator activities (McLean and Yoshioka 2008). Sponges produce different chemical defenses in response to different competitors (Wulff 2012). It is therefore conceivable that *D. anchorata* produces distinct chemicals to resist overgrowth by *L. variegata* and overgrow *P. astreoides,* and the macroalgae-specific metabolite may provide an incidental advantage to *D. anchorata* when overgrowing *P. astreoides.*

A mutualistic or commensalistic relationship between *L. variegata* and *D. anchorata* may exist if nutrients are transferred between competitors. Sponge-alga mutualisms are common, but little is known about how sponges benefit from these associations; most empirical evidence demonstrates nutrient transfer from sponges to macroalgae (Trautman et al. 2000). For example, the red alga *Ceratodictyon spongiosum* receives most of its required nitrogen (N) from waste ammonia produced by its sponge associate *Haliclona cymiforis* (Davy et al. 2002). Similarly, the sponge *A. cauliformis* transferred N and facilitated chlorophyll a production in the green macroalga *Microdictyon marinum* (Easson et al. 2014). Though not demonstrated for sponge-alga associations, sponges benefit from mutualisms with other autotrophs. The root-fouling sponges *Tedania ignis* and *Haliclona implexiformis* obtain important organic carbon resources from the red mangrove *Rhizopora mangle* (Ellison et al. 1996). Similar to *R. mangle,* macroalgae such as *L. variegata* produce vast amounts of carbon resources in the form of dissolved organic matter (DOM), a food source required by heterotrophic *D. anchorata* (van Duyl et al. 2011). Food availability is known to influence sponge morphology (Reiswig 1973), so access to abundant food resources could alter the morphology of *D. anchorata.* In particular, contact with *L. variegata* could diminish the sponges' need to grow upwards to obtain food and enable it instead to maximize basal stability by growing laterally. Additionally, the morphology of *L. variegata* may provide *D. anchorata*

structural support and enable the sponge to divert more energetic resources to competitive overgrowth of *P. astreoides*. It was previously proposed that the macroalgae *C. spongiosum* provides structural stability to its mutualistic associate sponge *H. cymiforis* (Davy et al. 2002). A gain of structural support by *D. anchorata* when in contact with *L. variegata* is plausible, given the flimsy skeletal morphology of *D. anchorata* and relatively rigid morphology of *L. variegata* (Wulff 2012; De Ruyter van Steveninck et al. 1988). While it was predicted that algae-sponge interactions would impair either species' ability to overgrow coral, it is conceivable that *D. anchorata* received some advantage – either in the form of nutrients or structural support – when in contact with *L. variegata.*

Competition Among Communities (Surveys)

Benthic surveys showed an abundance of hierarchies with corals as the inferior competitors. That corals have not yet become competitively excluded, despite their competitive inferiority, may be explained by top-down or bottom-up limiting controls on sponge and macroalgae populations. Indeterminate competitive success of corals can result from "top-down" grazing of sponges or macroalgae, or "bottom-up" limitation in nutrients that mitigates the proliferation of these groups on the reef (Sebens 1987; Lesser and Slattery 2013). Top-down and bottom-up factors can limit sponge and macroalgae abundance, but the importance of these factors relative to each other and to other structuring mechanisms is debated (Wulff 2012; Pawlik et al. 2013). Disturbances (e.g., hurricanes) can also promote coexistence among species in a competitive hierarchy (Hastings 1980; Sebens 1987).

Though ecological factors may play a role in mediating coral coexistence when competition is hierarchical, limitations in the survey method likely prevented detection of any competitive networks that may exist. Seven species of corals, sponges, and macroalgae were targeted on open-surface habitats in this study, while previous studies employing similar survey methods were not selective of species (Buss and Jackson 1979; Rinkevich et al. 1992). A broad survey, inclusive of more corals, sponges, or macroalgae species, may have changed results by reporting a greater number of overgrowth interactions. For comparison, Tanaka and Nandakumar (1994) reported over 500 overgrowth interactions, while only 351 overgrowths were reported in the present work. Only pairwise coral-sponge, coral-macroalgae, and sponge-macroalgae interactions were surveyed in this study, following the main objectives of this research; this narrow of a scope of pairwise interactions, however, precluded the detection of any four or five-species networks. Similar studies considered pairwise interactions among bryozoans, hyrdocorals, and ascidians, and identified competitive networks among diverse taxa, comprising four to seven species (Buss and Jackson 1979; Rinkevich et al. 1992).

It was hypothesized that competitive intransitivity would manifest itself as an abundance of coral-sponge standoffs that, when monitored, would demonstrate coral competitive dominance. The scarcity of

standoffs reported in this work thus played a large role in detection of competitive hierarchies. Only two standoffs (< 1% of total interactions) were reported in the present work. This is a very small number compared to similar studies (Tanaka and Nandakumar 1994) that reported 193 standoffs (> 25% of total interactions). Infrequent standoffs could imply that coral competitive ability is impaired by degrading environmental conditions. Competitive networks incorporating reef-building corals were conducted two to three decades ago (Buss and Jackson 1979; Rinkevich et al. 1992), when many Caribbean reefs were only beginning to show the combined impacts of overfishing, land-based sources of pollution, and hurricane damage (Hughes 1994). Competitive networks can fall apart on reefs that have degraded rapidly because environmental degradation can cause reversals in pairwise dominance orders (Benedetti-Cecchi and Cinelli 1996). Coral resistance to sponge overgrowth, for example, may be altered if corals are physically damaged or their microbial assemblages altered by environmental fluctuations (Aerts 2000; Morrow et al. 2013).

The absence of standoffs observed in this study may be explained by a limitation in the survey methods, particularly how a standoff was defined in the present work. The definition of a standoff applied in this study was visible direct contact but an absence of apparent overgrowth or tissue discoloration (Chadwick and Morrow 2011; Aerts 2000). The survey methods of the present study were adapted from Tanaka and Nandakumar (1994), and these authors defined standoffs as a cessation of growth after one species had overgrown another. The definition applied by Tanaka and Nandakumar was not used in this research because of logistic limitations. Confirming a "cessation of growth" would have required marking and monitoring many interactions among all target species, followed by advanced monitoring of suspected standoffs. However, implementing the definition used by Tanaka and Nandakumar may have led to detection of more standoffs. For example, *L. variegata* may only have a limited ability to overgrow some corals (Lirman 2001), and thus this algae may be a prime example of a competitor that overgrows but cannot competitively dominate. In general, applying the definition used by Tanaka and Nandakumar may have resulted in the reclassification of many overgrowths as standoffs.

The Effect of Sites and Seasons

The competitive ability of corals, sponges, and macroalgae can be influenced by site-specific differences in environmental stressors (Zea 1993; Littler et al. 2006), but the results of this study showed no differences in competitive outcomes between the two study sites. The sites are exposed to differential terrestrial impacts as a result of their relative location with respect to heavily populated St. Thomas. Nearshore Perseverance Bay was shown to have greater concentrations of total N and P, compared to mid-shelf Flat Key (Ennis 2014). Enhanced concentrations of N and P were previously shown to cause increased growth of *L. variegata* and corresponding mortality of *Porites cylindrica* (Jompa and McCook

2002). Similarly, reefs in closer proximity to runoff of terrestrial nutrients were shown to have greater loss of coral cover that is replaced by macroalgae when turbidity is low and sponges when turbidity is high (Zea 1993). Though the sites have different locations relative to shore that may drive differences in nutrient inputs, they display similar terrestrial, organic, and carbonate sediment accumulations (Sabine et al. 2015). These factors are also known to impact competitive outcomes between the three groups (Zea 1993; Chadwick and Morrow 2011). The results from this study suggest that Flat Key and Perseverance Bay were not distinct enough in environmental quality to influence competitive ability, or that competition was a more important structuring process than any differences in environmental quality that exist between these two sites.

Competitive outcomes were expected to vary with season because many benthic organisms are sensitive to seasonal variations in water temperatures, rainfall, and wind speed and direction (Duckworth and Battershill 2001; Chadwick and Morrow 2011). The only seasonal difference identified in the present work was reduced frequency of macroalgae-sponge overgrowths between the autumn (November 19-December 16, 2016) and winter (February 11-March 14, 2017). The seasonal ephemerality of macroalgae is well documented (Chadwick and Morrow 2011), although previous research has revealed no seasonality in *L. variegata* abundance (Mumby et al. 2005; Ferrari et al. 2012). Sponges also respond to seasonal fluctuations; the growth rate of *A. cauliformis* and other sponges can vary seasonally (Duckworth and Battershill 2001; Easson et al. 2014). *A. cauliformis* and *D. anchorata* may have had an impaired ability to resist macroalgae overgrowth in the winter, as a result of the seasonal fluctuations in temperature and rainfall. Alternatively, an effect of season may have been confounded by the duration of competitive interactions. Both sponges' resistance to macroalgae overgrowth may have degraded over time, and this is conceivable in light of the short life-span of *D. anchorata* and poor algal defenses of *A. cauliformis* (Wulff 2008; Easson et al. 2014).

Species-Specificity and Life-History Tradeoffs

In contrast to the facilitating interactions between *L. variegata* and *D. anchorata,* contact between *L. variegata* and *A. cauliformis* did not confer a competitive advantage to the sponge. Any advantage conferred to *D. anchorata* may not apply to *A. cauliformis* because each species has developed unique defenses and requirements to persist on the benthos (Wulff 2012). If the sponge-alga association between *L. variegata* and *D. anchorata* is parasitic (i.e., association increases the combative ability of *D. anchorata* over both groups), *A. cauliformis* likely does not have the same antagonistic response. Sponge morphology governs the degree of spatial competition it can accommodate, with encrusting *D. anchorata* likely experiencing more spatial competition than the upright, rope-like *A. cauliformis* (Engel and Pawlik 2000). In the experiment, the normally upright "ropes" of *A. cauliformis* were positioned level with the

surface of *P. astreoides.* This species can attach and grow horizontally, but its manipulated orientation likely exposed *A. cauliformis* to more spatial competition than it would normally encounter. The secondary metabolites produced by *A. cauliformis* are for anti-fouling and anti-predation purposes, and it does not have chemical defenses for aggressively colonizing benthic space or damaging neighboring macroalgae competitors (Easson et al. 2014). If contact with *L. variegata* provides a source of nutrients that increases *D. anchorata* overgrowth of coral, this DOM source likely does not provide the same advantage to *A. cauliformis. A. cauliformis* hosts an abundance of photosymbionts that provide the sponge with up to 75% of its energetic needs, thus it may not benefit from the DOM source released by neighboring *L. variegata*. (Easson et al. 2014).

It is hypothesized that tradeoffs in competitive ability, colonization ability and stress-tolerance promote diversity on the reef benthos (Darling et al. 2012). The target coral species examined in this work comprised weedy species and species tolerant to environmental stress. *P. astreoides,* which are small and reproduce by brooding, are better colonizers in harsh environments. *O. annularis* and *S. siderea,* which have domed morphologies, grow slowly, and reproduce by broadcast spawning, are more tolerant of environments with high sedimentation and turbidity. Weedy *P. astreoides* and stress-tolerant *O. annularis* and *S. siderea* do not have traits favorable to competition, which include rapid growth and efficient resource use (Darling et al. 2012). The inclusion of more competitive coral species in the surveys (e.g., *Dendrogyrus cylindrus* or *Montastrea cavernosa*) may have led to detection of more standoffs. Informal roving surveys conducted during this research led to identification of multiple standoffs between *Montastrea cavernosa* and *D. anchorata* that appeared to persist for at least three months (Supplementary Figure 4). *M. cavernosa* is a competitively aggressive species of coral that utilizes sweeper tentacles during intraspecific competition with *S. siderea* and interspecific competition with sponges *Niphates erecta* and *Scopalina rutzlieri* (Logan 1984; Aerts 2000; López-Victoria et al. 2006). The intricate competitive mechanisms evolved by *M. cavernosa,* at the cost of its growth-rate, may explain the continued coexistence of this slowly-growing species (Richardson et al. 1979). Inclusion of *M. cavernosa* in the surveys in the present work may have resulted in more standoffs and possibly evidence of a competitive network.

Anthropogenic Impacts and Alternative Stable States

In light of the shift towards weedy corals and proliferation of sponges and macroalgae on many Caribbean reefs (Green et al. 2008; Bell et al. 2013; Loh and Pawlik 2014), the inferiority of corals at both spatial scales is concerning. The coral species observed in this work are locally abundant (Smith et al. 2015), and environmental degradation in the Caribbean is inciting shifts from competitive (e.g., *Acropora spp.*) to weedy corals (e.g., *P. astreoides* and *Agaricia spp.*) (Green et al. 2008; Darling et al.

2012). Additionally, the exclusion of weedy corals could be more likely if a reciprocal feedback between sponges and macroalgae promotes the growth of both groups on Caribbean reefs. In this theorized "vicious circle", sponges provide inorganic nutrients to macroalgae, who in turn give sponges valuable DOC resources; this feedback may play a role in diminished resilience of Caribbean corals (Pawlik et al. 2016).

Multispecies competitive dynamics may reinforce or destabilize feedbacks leading to alternative stable states (González-Rivero et al. 2016), and the interactions between *L. variegata* and *D. anchorata* observed in this research demonstrate a potential mechanism favoring phase shifts to alternative organism. An initial increase of macroalgae could lead to increased sponge-alga direct contact, and this could drive accelerated sponge-coral overgrowth and loss of coral cover that could then be colonized by macroalgae (Figure 18). This potential feedback could have a considerable effect on loss of coral cover; macroalgae such as *L. variegata* are good colonizers but do not cause considerable mortality of many coral species (Lirman 2001; Nugues et al. 2004), while chemically defended sponges such as *D. anchorata* can cause substantial coral mortality in a short period and have short life spans (Wulff 2008). However, the potential magnitude of this feedback depends on the robustness of sponge-macroalgae facilitating interactions across species.

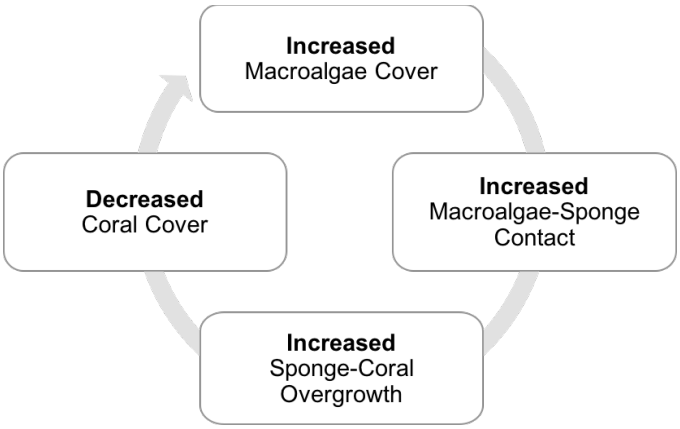

Figure 18: Proposed feedback mechanism favoring shifts to non-coral dominated systems.

The Benefits of Photogrammetry

This study represents the first known application of photogrammetry to measure sponge and coral morphological plasticity in situ. While image analysis allowed for the detection in differences in lateral growth rates, analysis of 3D models allowed for the detection of fine scale difference in coral surface area across treatments. Interestingly, unlike sponge lateral expanse (measured from photographs), sponge surface area did not differ significantly across treatments. Though not formally tested, visual inspection of

3D reconstructions revealed that *D. anchorata* growth was variable across treatments. In sponge-only treatments, reduced lateral growth of *D. anchorata* segments was often compensated by upwards growth and formation of branches. Branches of *D. anchorata,* attached to the substratum by a limited basal area, are especially vulnerable to fragmentation (Wulff 2008). In sponge-algae treatments, increased lateral growth of *D. anchorata* segments led to an increase in basal surface area. A larger basal area with lower center of gravity likely reduces the risk of fragmentation in high water motion and may bolster the long-term competitive advantage of *D. anchorata* over the coral that it is overgrowing.

Sponge morphological plasticity has been explored recently in a laboratory setting. Scott-Murray and Schläppy (2017) generated models of sponge individuals (*Pachymatissima johnsonii* and *Suberites domuncula*) at two time points and identified areas of localized growth and contraction using a modified Hausdorff sampling algorithm. Hausdorff sampling normally computes only the absolute values of mesh distances, but the authors adapted it to distinguish between positive and negative distances. Though this adapted algorithm is not yet available as an open-source tool, future uses of this sampling method will be particularly valuable in analyses of morphological plasticity (Scott-Murray and Schläppy 2017). Traditional Hausdorff sampling was explored in the present work, but the inability to distinguish between growth and shrinkage precluded its use for statistical analyses of morphological plasticity (Supplementary Figure 5).

Photogrammetry has gained popularity among coral scientists as a reliable means to measure structural complexity and, more recently, growth (Figueira et al. 2015; Burns et al. 2016; Scott-Murray and Schläppy 2017). In this work, such discrete changes in coral and sponge surface area would not have been detected without the use of photogrammetric techniques. Methods to validate this technology confirmed that the variability inherent the photogrammetric method was much smaller than changes in sponge morphology over the 91 d period. Minimizing variability requires proper choice of equipment and sites with proper environmental conditions, and Photogrammetric techniques are not recommended if equipment is limited to GoPros (which distort photos with a “fish-eye” effect) and sites are turbid, deep, or otherwise poorly lit. Fortunately, many reefs around St. Thomas have favorable environmental conditions (low turbidity, good lighting), and implementation of this technology in local coral reef monitoring projects (e.g. TCRMP; Supplementary Figure 6) may be advantageous.

Chapter 3: Spatial Model of Benthic Multispecies Competition

Introduction

Field observations of individual-based interactions among corals, sponges, and macroalgae described in the previous chapter suggest that some corals are the inferior members of a competitive hierarchy. As such, corals could become excluded on reefs where sponges and macroalgae proliferate (Grace et al. 1993), but coral coexistence may be possible if the competitive ability of sponges and macroalgae is gained at the cost of reproductive output (Edwards and Schreiber 2010). Such life-history tradeoffs add complexity in predicting competitive winners, but ecological models can be used to simulate these systems and determine the relative importance of intrinsic (e.g., competition and colonization ability) and extrinsic (e.g., disturbance, herbivory) factors in structuring benthic communities (González-Rivero et al. 2011, 2016).

The objective of this chapter was to develop a spatially-explicit individual-based model (IBM) that forecasts changes in benthic composition of corals (*P. astreoides*), sponges (*D. anchorata*), and macroalgae (*L. variegata*) as a function of empirical rules describing competitive ability and life-history characteristics. The model is written in MATLAB and was parameterized with a combination of experimentally derived growth and overgrowth rates and literature values for fragmentation and mortality rates. This model is unique from previous models (e.g., Kubicek et al. 2012; González-Rivero et al. 2016) because overgrowth rates vary not only with species but also with the number and identity of competitors. Specifically, the rate that sponge overgrows coral can differ, depending on whether or not the sponge is also in contact with macroalgae. The two specific questions that this model was built to address were (1) What effects do local multispecies competition, specifically macroalgae facilitation of sponge-coral overgrowth, have on emergent system behavior (i.e., percent cover of each competitor)? and (2) If corals are inferior competitors in a multispecies competitive hierarchy, do their longer life-spans and higher resistance to fragmentation, compared to sponges and macroalgae, promote long-term coexistence?

Methods

Model Description

The following model description follows the ODD (Overview, Design concepts, Details) protocol (Grimm et al. 2006, 2010).

Entities, State Variables, and Scales

Model entities comprise three collectives of corals, sponges, and macroalgae individuals. Individuals in a collective are depicted as polygons in the simulated model space, a 3 x 3 m reef patch. Each individual in a collective is defined by its polygonal centroid and vertex x and y coordinates. These fundamental state variables are given for each individual in their corresponding entity attribute list (i.e.,

poly_cor, poly_spo, poly_maca); further information derived from these state variables, including the distance (in cm) and angle (in degrees) from centroid to each vertex, are also given in the main attribute lists. A second set of lists, hereafter referred to as "area lists", stores the area (in cm^2) of each individual (row) at each time point (column) during a simulation. The area list ultimately serves as the report generator to evaluate system behavior; the area list is used to evaluate changes in percent cover and population size-structure across one month intervals (the time-step) for the nine-month simulation time.

Process Overview and Scheduling

In the body (or main "loop") of the simulation, each entity is first separated by each individual's status (competing with zero, one, or two other competitors), and index lists store the IDs of individuals with matching competitors. Each list corresponds to a single submodel that simulates growth or overgrowth of listed individuals; all individuals are therefore assigned to a list, and each is categorized in only one list. The simulation then sequentially runs each growth and overgrowth submodel for all three entities' index lists.

Within each submodel, the corresponding index list is first referenced to isolate the proper individuals from the main attribute list. The vertices of each focal individual are then moved away or towards the centroid, growing or shrinking the polygon according to the assigned growth rate. Different growth rates are applied to vertices of a single individual, depending on what competitor, if any, that vertex overlaps. The output of each submodel is a temporary attribute list of the updated individual polygons.

Once all growth and overgrowth submodels functions have been called and all temporary attribute lists are stored in memory, each main attribute list is synchronously updated. The polyClean() function is then called to remove any consecutive rows of NaNs in the attribute list and test for self-intersecting polygons. If self-intersecting polygons exist, the polygon removes one of the split segments by testing if either is < 0.05 cm^2 or has counterclockwise vertices. If neither criteria are met, the function removes the smaller polygon. The issue of self-intersecting polygons is largely exclusive to macroalgae polygons; these are relatively small, thus the occasional removal of a self-intersecting polygon has a minimal effect on system behavior. The cleaned polygons are then trimmed to the $9m^2$ simulation space, using trim2grid(), and all area lists are updated.

The next part of the loop body simulates death of individuals in each entity, and the submodels that are called depend on the entity. For coral and sponges, a deathOvergrowth() function is called to remove individuals from the attribute list when more than one third of the initial area of the focal individual has been overgrown (given by variable main_cor_frac). Individuals also experience random mortality via deathHalflife(), deathPercent(), and/or deathPercentFrag(), and these submodels and the

entities to which each submodel is applied are explained in greater detail in the stochasticity and submodel section. Next, fragmentation of sponges and macroalgae is simulated with fragHlSize(). In this function, parent individuals with the largest surface area are chosen to be fragmented and their areas are divided equally among the number of fragments they will eventually comprise. Macroalgae individuals are fragmented into two pieces, and sponge individuals are fragmented into two to four pieces, depending on their size. One fragment inherits the parents' centroid x and y coordinates, while the remaining fragment(s) is/are randomly assigned an x and y centroid within a 17 cm radius of the parent. The fragment radius is calculated from the area of a circle equation using the divided area of the parent fragment (r = sqrt(A)/pi), and used to produce new polygon vertices representing the new fragmented individual. All fragments, including the fragment that inherited the parents center coordinate, are assigned new IDs. The main attribute list is updated to include the polygonal information of newly fragmented individuals, and area lists are updated to include their new IDs and area at t = time-step. The original parent fragment is removed from the main attribute list, and the value for the parents' area in the area list is assigned a value of 'NaN' for the remainder of the simulation.

The final step in the main loop body is to remake the index lists that were referenced in the beginning of the loop. A binary region of interest (ROI), representing the collective areal coverage of all individuals in an entity, is generated on a grid with a resolution of 1000 x 1000 pixels. For a given focal entity, a point in polygon function is called to determine which focal individuals are in direct contact with one, two, or no other competitors. The IDs of focal individuals are stored in index lists that will be referenced in growth and overgrowth submodels in the next iteration of the loop body (Figure 19).

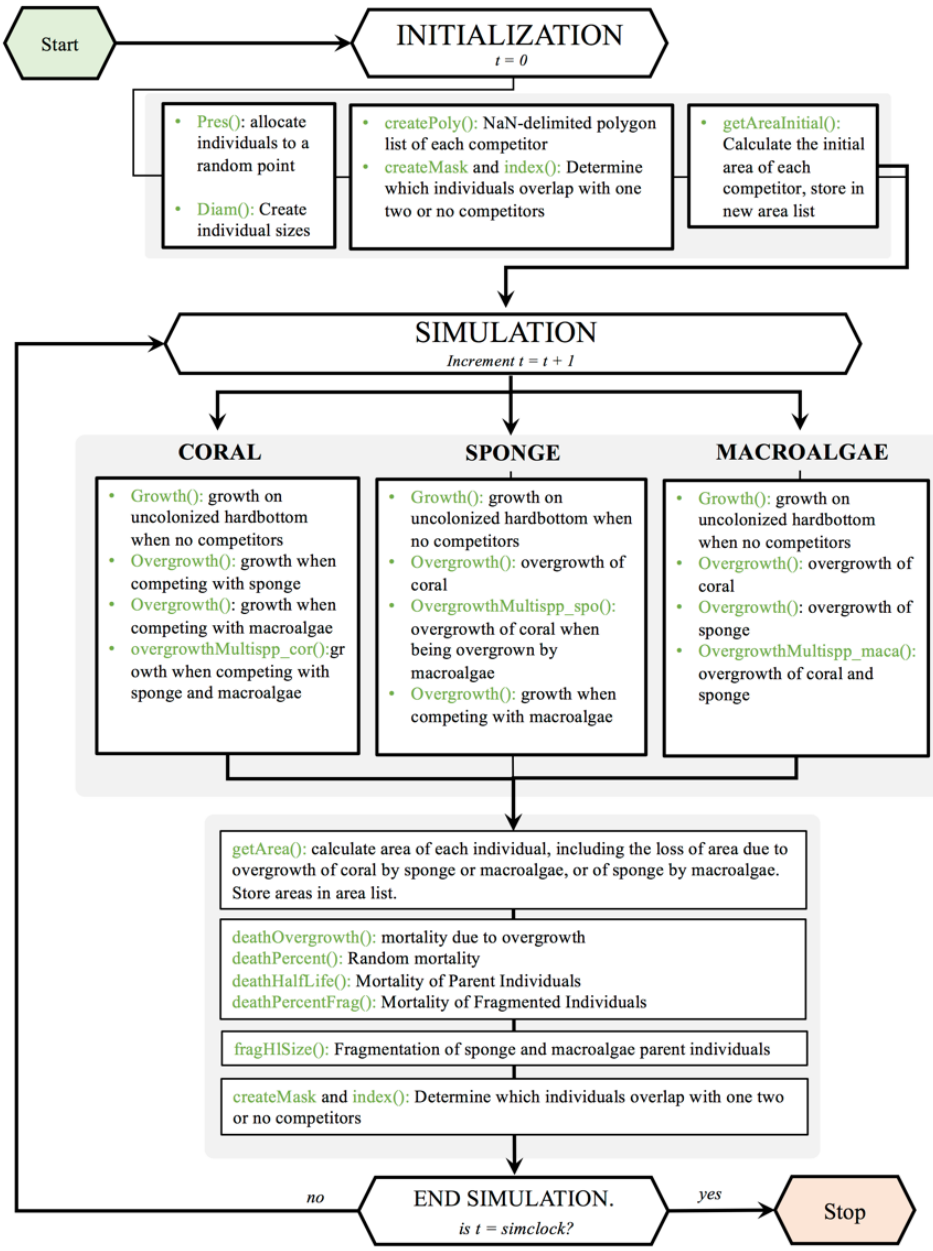

Figure 19: Model initialization and simulation flow chart.

Design Concepts

Basic Principles

The general hypothesis underlying this model is that species-specific competitive interactions influence ecosystem (referred to here as system behavior), and system behavior is evaluated using the

change in percent cover and population size-structure of the three entities over simulated time. Species-specificity is simulated at the submodel level by applying growth and overgrowth rates specific to the identity of the focal individual and the number, identities, and extent of interaction with its competitors. These are emergent traits because they depend on the properties of the system (i.e. surrounding organisms); individual behavior cannot be predicted when it is independent of the system.

This model is similar to previous simulations of percent cover as a response to spatial competition (Kubicek et al. 2012; González-Rivero et al. 2016). It is unique because it does not explicitly consider benthic community response to external conditions (i.e. grazing, physical disturbance, or bleaching). In lieu of simulating particular disturbances, individuals are subjected to probabilistic mortality and fragmentation at each time-step. These imposed traits also affect system behavior, but they are not affected by the individuals' simulated environment.

Emergence

System behavior is affected by individual properties at initialization, probability of mortality and fragmentation, and relative ability to overgrow and resist overgrowth by hetero- and conspecifics. As time progresses, individuals come into direct contact with others, eliciting a change of growth rate to reflect overgrowth in the presence of an inferior competitor or halted growth in the presence of a superior competitor. Individuals also lose contact with competitors, either by inflicting mortality (by overgrowing its neighbor) or having a neighbor that fragments or experiences random mortality. A loss of neighboring competitors elicits a change of growth rate to vacate the newly cleared space.

Sensing and Interaction

Sensing is constrained locally in this model; individuals only detect competitors in direct contact with themselves. Competitive interactions are mediated by space availability, a limiting resource on the reef benthos (Dayton 1971). All competitive interactions adversely affect both interacting entities by decelerating their growth in the direction of the opposing party. The exception to this is sponge-macroalgae interactions when the same sponge individual is overgrowing coral. In this case, the direct contact between sponge and macroalgae indirectly facilitates sponge overgrowth of coral, driving the sponge to overgrow the coral more rapidly than the macroalgae is overgrowing the sponge.

Stochasticity

The causes of varying mortality, whether due to disturbance, grazing, or disease, were deemed unimportant given the overall model objectives and therefore are not explicitly modeled. The variability caused by these processes, as well as individual life-span, was reproduced using submodels that randomly assign individuals to die. The life span of *P. astreoides* exceeds the simulated time, so mortality of corals is modeled using one function that assigns a percent chance of mortality at each time-step. This random

probability of mortality reflects the underlying chance of death due to factors other than longevity (e.g. disease, bleaching). Mortality is also simulated randomly for sponge and macroalgae. In addition, both species are shorter lived than the 9 mo simulated time. A number of submodels are therefore employed to emulate extrinsic and intrinsic mortality of both parents (existed at t = 0) and fragments (did not exist at t = 0).

The lifespan of *D. anchorata* is highly variable but recent studies have found that 50% of a population of *D. anchorata* can experience mortality in 9 mo (Wulff 2008). The number of sponge parent individuals that are randomly assigned to die at time t is thus modeled using an exponential decay function with a half-life of 9 months. Similarly, the number of sponge parent individuals that are chosen to fragment is also modeled using an exponential decay function with a half-life of 21 months, and this was derived from the findings of Wulff (2008) that 25% of a population had fragmented (75% had not fragmented) by 9 mo. The number of sponge fragments that are randomly assigned to die at time t follows an unrelated exponential decay function. At each time-step, each fragment is assigned a probability of mortality similar to that assigned to corals. This probability changes at each time-step and is based on a reverse exponential decay function with a half-life equal to the fragmentation half-life of 21 months.

The lifespan of *L. variegata* can be between one and five months, and they are also good dispersers (De Ruyter van Steveninck et al. 1988; Van Der Zande et al. 2013). Instead of employing a mortality half-life function on parent individuals, macroalgae are simulated to rapidly fragment, and half of all parent individuals are fragmented in three months. The number of macroalgae fragments that are randomly assigned to die at time t follows the same exponential decay function used on sponge fragments. Each fragment is assigned a probability of mortality that changes at each time-step and is based on a reverse exponential decay function with a half-life equal to the fragmentation half-life of 3 months. The purpose of this time-dependent probability of random mortality of fragments is to create an inverse relationship between number of fragments and probability of mortality and stabilize the percent cover of macroalgae and sponge fragments, so probability of mortality decreases with increasing number of fragments.

Initialization

Each entity (i.e. corals, sponges, or macroalgae) is represented by a matrix of center points of each individual, with the initial number of points being dictated by the percent cover input parameter. Points are generated with a spatially random distribution and separated by a minimum distance across a 10 x 10 grid. Next, the diameter of each individual is randomly assigned according to a normal distribution centered about the mean diameter, and polygons representing each individual are generated from the center points and corresponding diameters. A NaN-delimited list is generated for each entity,

and these three matrices contain the state variables: the xy coordinates of the polygon vertices, xy coordinates of center points of each individual, and an individual's unique identifier.

After these initial state variable lists are made, a function is used to determine if any polygons of the same species overlap; if overlap occurs, the larger individual overtops the smaller one and the state variables are updated accordingly. Next, a binary region of interest (ROI), representing the collective areal coverage of all individuals in an entity, is generated on a grid with a resolution of 1000 x 1000 pixels. For a given focal entity, a point in polygon function is called to determine which focal individuals are in direct contact with one, two, or no other competitors; this is done using polygons representing the individuals in the focal entity and ROIs of the non-focal species. The output is a list with unique focal polygon identifiers and what they overlap (e.g. 'index_cor_spo' is a list of coral individual polygon ids that overlap *only* sponges); this list is used to determine which sub-model will be called to simulate growth or overgrowth of the focal individual. Finally, the initial area of each individual is calculated and stored in a matrix corresponding to its entity. A column is sequentially added at each time point (number of columns = number of time points, number of rows = number of polygons at t_0), and is used in the analysis of how percent cover and size structure of each entity changes over time.

Input Data and Submodels

Input parameters required to run the model and their descriptions are listed in Table 14. Submodels and their descriptions are listed in Table 15.

Table 14: Model input parameters.

Focal Competitor	Variable	Description	Default Value	Reference
Coral	main_cor	Percent cover of coral (%)	10	(Smith et al. 2015)
	main_cor_ave_diam	Coral average diameter (cm)	25	Will change to 18 cm in future runs, following image analysis of colonies and Holstein et al. (2016)
	main_cor_sd_diam	St. Dev. Of coral diameter	6	Experiment data and Holstein et al. (2016)
	main_cor_frac	Threshold t0/t1 area ratio to use to eliminate overgrown coral	1.3	(Kubicek et al. 2012)
	main_cor_death_percent	Percent chance of individual coral death	0.17	(González-Rivero et al. 2016)
	grow_c	Coral growth rate over hardbottom (cm/time-step)	0.17	(González-Rivero et al. 2016)
	grow_cs	Coral growth rate over hardbottom when competing with sponge (cm/time-step)	0.1625	Control colonies, Table 10, row 4 (divided value by 2 for 1-month time-step)
	grow_cm	Coral growth rate over hardbottom when competing with macroalgae (cm/time-step)	0.085	Control colonies, Table 10, row 6 (divided value by 2 for 1month time-step)
	grow_csm	Coral growth rate over hardbottom when competing with sponge and macroalgae (cm/time-step)	0.09	Experimental colonies, Figure 13, autumn growth rate
Sponge	main_spo	Percent cover of sponge (%)	15	(Smith et al. 2015)
	main_spo_ave_diam	Sponge average diameter (cm)	12	The approximate length of sponge fragments applied in experiment
	main_spo_sd_diam	St. Dev. Of sponge diameter	3	Approximate sd of sponge fragments applied in experiment
	main_spo_death_hl	The time-step at which half of all original Sponge individuals will have died. The number of individuals that die at each time-step is determined by an exponential decay function with this half-life.	8	58% mortality by 9 mo (Wulff 2008) solved for half-life
	main_frag_hl_spo	The time-step at which half of all original Sponge individuals will have fragmented. The number of individuals that fragment at each time-step is determined by an exponential decay function with this half-life.	21	~25% fragged/75% not fragged by 9 mo (Wulff 2008) solved for half-life

	grow_s	Sponge growth rate over hardbottom (cm/time-step)	0.33	Converted from change in area (mclean and Yoshioka 2008) to change in radius. This value is highly variable in lit
	grow_sc	Sponge rate of Coral overgrowth (cm/time-step)	-0.15	Experimental colonies, *D. anchorata* growth in sponge only treatments in the autumn (Figure 14)
	grow_scm	Sponge rate of Coral overgrowth when Sponge is also in contact with macroalgae (cm/time-step)	0.35	Experimental colonies, *D. anchorata* growth in sponge-algae treatments in the autumn (Figure 14)
	grow_sm	Sponge growth rate over hardbottom when competing with macroalgae (cm/time-step)	0	(Mclean and Yoshioka 2008)
Macroalgae	main_maca	Percent cover of macroalgae	20	(Smith et al. 2015)
	main_maca_ave_diam	Maca average diameter (cm)	5	Approximate size of *L. variegata* blades applied to colonies
	main_maca_sd_diam	St. dev of maca diameter	1	Approximate st. Dev of *L. variegata* blades applied to colonies
	main_area_threshold_maca_cor	The threshold area that maca can overgrow Coral.	0.67	(González-Rivero et al. 2016)
	main_maca_death_percent	Percent chance of individual maca death	3	Calibrated value to stabilize macroalgae cover
	main_frag_hl_maca	The time-step at which half of all original macroalgae individuals will have fragmented/dispersed. The number of individuals that fragment at each time-step is determined by an exponential decay function with this half-life.	5	About half of macroalgae remained on colonies after 4 months, and changed value to 5 months to stabilize macroalgae cover.
	main_maca_death_percent_frag	Percent chance of individual mortality of macroalgae fragments. This is a vector with length = number of time-steps calculated by flipping the fragmentation/ dispersal half-life exponential decay function. The purpose is to stabilize macroalgae cover, so probability of mortality increases with increasing number of fragments. (%)	time: t1 t2 t3 t4 t5 t6 t7 %: 0 2.5 5 7.5 10 12.5 15	Derived from main_frag_hl_maca

			t8 17.5 t9 20	
	grow_m	Macroalgae growth rate over hardbottom (cm/time-step)	0.18	(Van Der Zande et al. 2013)
	grow_ms	Macroalgae rate of sponge overgrowth (cm/time-step)	0.08	Experimental colonies, macroalgae rate of overgrowth of *D. anchorata.* value differs from presence-only overgrowths given in Figure 15 because it includes zeros from ~12.5% frequency of overgrowths (Table 8).
	grow_mc	Macroalgae rate of coral overgrowth (cm/time-step)	0.12	Experimental colonies, macroalgae rate of overgrowth of coral. Value differs from presence-only overgrowths given in Figure 15 because it includes zeros from ~60% frequency of overgrowths (Table 8).

Table 15: Submodel description.

Focal Competitor	Submodel	Description
Coral	Growth on uncolonized hardbottom (no competitors)	Applies to coral that are not in contact with any sponge or macroalgae. Growth occurs equally across all vertices at a rate of ***grow_c*** cm/time-step.
	Growth when being overgrown by Sponge	Applies to coral that is being overgrown by only sponge. No growth occurs from vertices that overlap sponge (growth rate = 0 cm/ time-step). Vertices that do not overlap sponge are grown at a rate of ***grow_c*** cm/time-step.
	Growth when being overgrown by macroalgae	Applies to coral that is being overgrown by only macroalgae. No growth occurs from vertices that overlap macroalgae (growth rate = 0 cm/ time-step). Vertices that do not overlap macroalgae are grown at a rate of ***grow_c*** cm/time-step.
	Growth when being overgrown by sponge and macroalgae	Applies to coral that is being overgrown by both sponge and macroalgae. No growth occurs from vertices that overlap sponge or macroalgae (growth rate = 0 cm/ time-step). Vertices that do not overlap sponge or macroalgae are grown at a rate of ***grow_c*** cm/time-step.
	Mortality due to overgrowth	When a competitor (either sponge, macroalgae, or both) overgrows more than ***main_cor_frac*** % of coral's original surface area, that polygon "dies" and is eliminated from the main attribute list.
	Random mortality	Each individual coral polygon has a ***main_cor_death_percent*** % chance of dying.

Sponge	Growth on uncolonized hardbottom (no competitors)	Applies to sponge that is not in contact with any coral or macroalgae. Growth occurs equally across all vertices at a rate of ***grow_s*** cm/time-step.
	Overgrowth of Coral	Applies to sponge that is overgrowing coral (but not in contact with macroalgae). Vertices that overlap coral grow at a rate of ***grow_sc*** cm/time-step. Vertices that do not overlap coral grow at a rate of ***grow_s*** cm/time-step.
	Overgrowth of Coral when being overgrown by macroalgae	Applies to sponges that are overgrowing coral and are also being overgrown by macroalgae. Vertices that overlap coral are grown at a rate of ***grow_scm*** cm/time-step, and vertices that do not overlap coral are grown at a rate of ***grow_s*** cm/time-step.
	Growth when being overgrown by macroalgae	Applies to sponges that are being overgrown by macroalgae. No growth occurs from vertices that overlap macroalgae, and vertices that do not overlap macroalgae are grown at a rate of ***grow_s*** cm/time-step.
	Mortality due to overgrowth	When a macroalgae overgrows more than three quarters of sponge original surface area, that polygon "dies" and is eliminated from the main attribute list.
	Random mortality of parents	Applies only to parent individuals (those that existed at t = 0). The number of individuals that die at each time-step is determined by an exponential decay function with half-life = ***main_spo_death_hl***. Individuals that die are chosen randomly.
	Random mortality of fragments	Applies only to fragments (those that did not exist at t = 0). The percent chance of individual death at each time-step is determined by ***main_spo_death_percent_frag***. Each individual fragment has the same percent chance of dying, regardless of the time they were fragmented off their parent.
	Fragmentation	Applies to parent individuals (those that existed at t = 0). The number of individuals to be fragmented depends on the number of individuals at time t = 0, and the half-life ***main_frag_hl_spo*** of an exponential decay function that is the number of time steps at which half of the parent individuals should be fragmented. Parent individuals to be fragmented are chosen randomly and are randomly fragmented into 2-4 pieces, with one piece remaining in the original location. The remaining piece(s) is/are randomly assigned to a location within a 17 cm radius of the parent, following dispersal distances given by Wulff (2008).
Macroalgae	Growth on uncolonized hardbottom (no competitors)	Applies to macroalgae that are not in contact with any sponge or coral. Growth occurs equally across all vertices at a rate of ***grow_m*** cm/time-step.
	Overgrowth of coral	Applies to macroalgae that are overgrowing coral. Growth of vertices that overlap coral is given by a random normal distribution (mean = ***grow_mc*** and sd = 0.13 cm following experimental standard deviations), with the vertices closest to corals center growing the least, and the vertices farthest from corals center growing the most. This is to reflect the limited capability of macroalgae to overgrow coral and favor growth around the coral perimeter (González-Rivero et al. 2016). Vertices that do not overlap Coral are grown at a rate of ***grow_m*** cm/time-step.
	Overgrowth of sponge	Applies to macroalgae that are overgrowing sponges. Vertices that overlap sponge are grown at a rate of ***grow_ms*** cm/time-step. Vertices that do not overlap dponge are grown at a rate of ***grow_m*** cm/time-step.
	Overgrowth of coral and Sponge	Applies to macroalgae that are overgrowing coral and sponge. Vertices that overlap sponge are grown at a rate of ***grow_ms*** cm/time-step, vertices that overlap coral are grown at a rate of ***grow_mc*** cm/time-step, and vertices that overlap neither are grown at a rate of ***grow_m*** cm/time-step.

	Zero growth when individuals exceed maximum surface area	Applies to macroalgae that exceed a maximum surface area ***main_max_maca_area***. Stores the individuals that are too large (polygon vertices remain the same as last time point) and adds this list back to main poly_maca prior to running the death and fragmentation submodels.
	Random mortality	Applies to both parent and fragment individuals. Each individual macroalgae polygon has a ***main_maca_death_percent*** % chance of dying.
	Random mortality of fragments	Applies only to fragments (those that did not exist at t = 0). The percent chance of individual death at each time-step is determined by ***main_maca_death_percent_frag***. Each individual fragment has the same percent chance of dying, regardless of the time they were fragmented off their parent.
	Fragmentation	Applies to parent individuals (those that existed at t = 0). The number of individuals to be fragmented depends on the number of individuals at time t = 0 and the half-life of an exponential decay function (variable ***main_frag_hl_maca***) that is the number of time steps at which half of the parent individuals should be fragmented. Parent individuals to be fragmented are chosen randomly and are randomly fragmented into 2 pieces, with one piece remaining in the original location and the remaining piece being randomly assigned to a location within a 17 cm radius of the parent.

Sensitivity Analysis

Model sensitivity was evaluated against 18 parameters representing initial percent cover, mortality, growth, and overgrowth rate of each competing entity. The default values of parameters were varied by 20% while holding the other input parameters at default values. The sensitivity analysis comprised 370 simulations: one set of ten replicate simulations with all default values and 36 sets of ten replicate simulations with one varied parameter at a time (20% above or below default value). The change in percent cover of coral, sponge, and macroalgae from start to end of the simulation was used as a model output in the sensitivity analysis. Linear regression was used to investigate whether a there was a functional relationship between the response and scaled parameter values (0, 0.5, 1). The slope of the regression line indicates the effect that the scaled parameter has on change in percent cover, and this was used as the sensitivity index (Yñiguez et al. 2008).

Preliminary Model Analysis

A preliminary analysis was conducted to determine system behavior in response to altered sponge-coral overgrowth rates (grow_sc, grow_scm). This preliminary analysis comprised three sets of ten simulations, for a total of 30 simulations. The first (sim#1) used all default values as inputs; this provided a baseline for comparison to sim#2 and sim#3. In the second simulation (sim #2), grow_scm was set equal to the default value of sponge-coral overgrowth (grow_sc = -0.15). The second simulation represented the absence of macroalgae facilitation of sponge-coral overgrowth. In the third simulation (sim #3), grow_sc was set equal to 0.35 cm/month, the default value of grow_scm. This third simulation represented a scenario in which macroalgae facilitation of sponge-coral overgrowth applied also to sponges not in contact with macroalgae. Simulation #3 agrees with the results of the controls analysis.

Results and Discussion

The sensitivity analysis indicated that percent cover of each entity is highly sensitive to fragmentation and mortality of alternative organisms and less sensitive to overgrowth rates and initial percent cover. All of the most sensitive parameters (scaled SI > 2) only affected the cover of species directly affected by that parameter; the most sensitive parameters included macroalgae growth (SI_{maca} = 4.8), macroalgae fragmentation (SI_{maca} = 4.15), macroalgae mortality (SI_{maca} = -2.72), sponge mortality (SI_{spo} = 2.96), and sponge growth (SI_{spo} = 2.37) (Table 16). Model output was less sensitive to initial conditions (main_cor, main_spo, main_maca) than to fragmentation, mortality, and growth, but some unexpected patterns were revealed. Variation in initial cover of macroalgae and corals had the greatest effect on sponge percent cover, while initial cover of sponges had the least effect on sponge percent cover. The response of sponges to initial percent cover of its competitors could imply emergent patterns resulting from individual interactions, specifically macroalgae facilitation of sponge coral overgrowth.

However, considerable sensitivity to fragmentation and mortality parameters suggests that the model in its current state may be a poor representation of benthic interactions.

Table 16: Scaled sensitivity indices (SI) for each species at each parameter.

Category	Variable	Default Value	Species	Scaled SI
Initial percent cover	main_cor	10	coral	0.28
			sponge	1
			macroalgae	-0.31
	main_spo	15	coral	-0.15
			sponge	-0.35
			macroalgae	-0.32
	main_maca	20	coral	-0.52
			sponge	-1.18
			macroalgae	0.16
Fragmentation	frag_hl_spo	21	coral	-0.11
			sponge	0.13
			macroalgae	-0.01
	frag_hl_maca	5	coral	1.62
			sponge	-0.54
			macroalgae	4.15
Mortality	cor_death_percent	0.17	coral	-0.84
			sponge	-0.57
			macroalgae	0.27
	maca_death_percent	3	coral	-0.26
			sponge	0.16
			macroalgae	-2.72
	spo_death_hl	8	coral	0.07
			sponge	2.96
			macroalgae	0.09
Growth/Overgrowth	grow_c	0.17	coral	-0.44
			sponge	-0.04
			macroalgae	-0.08
	grow_cm	0.085	coral	0.86
			sponge	-0.34
			macroalgae	0.23
	grow_cs	0.1625	coral	-0.77
			sponge	0.13
			macroalgae	-0.03
	grow_csm	0.09	coral	0.17
			sponge	-0.46
			macroalgae	-0.2
	grow_s	0.33	coral	-1.37
			sponge	2.37
			macroalgae	0.02
	grow_sc	-0.15	coral	1.25
			sponge	0.64
			macroalgae	-0.43
	grow_scm	0.35	coral	-0.39
			sponge	0.29
			macroalgae	0.15
	grow_m	0.18	coral	-0.56
			sponge	-1.4

			macroalgae	4.8
	grow_mc	0.12	coral	0.52
			sponge	0.01
			macroalgae	0.74
	grow_ms	0.08	coral	-0.1
			sponge	-0.51
			macroalgae	0.47

Because the sensitivity analysis exposed some flaws in the models' depiction of multispecies benthic competition, only a qualitative, informal analysis of the preliminary model analysis was conducted. The preliminary model analysis did not demonstrate many notable outcomes from varying the input values of sponge growth, with the exception of coral cover in simulation 3. In simulation 1 and 2, coral sustained at least 8% cover over the simulated time, but there was a considerable loss of coral cover in simulation 3 to < 8% by t1 and sustained loss of coral cover to < 6% through t9 (Figure 20). In simulation 3, the macroalgae-facilitated sponge overgrowth rate (grow_scm) was applied to sponges not in contact with macroalgae (grow_sm). It is reasonable that coral cover may have declined as a result of increased sponge-coral overgrowth, but it was expected that this would correspond to an increase in sponge or macroalgae cover. Poorly modeled fragmentation of sponges and macroalgae may have prevented this increase in sponge or macroalgae cover.

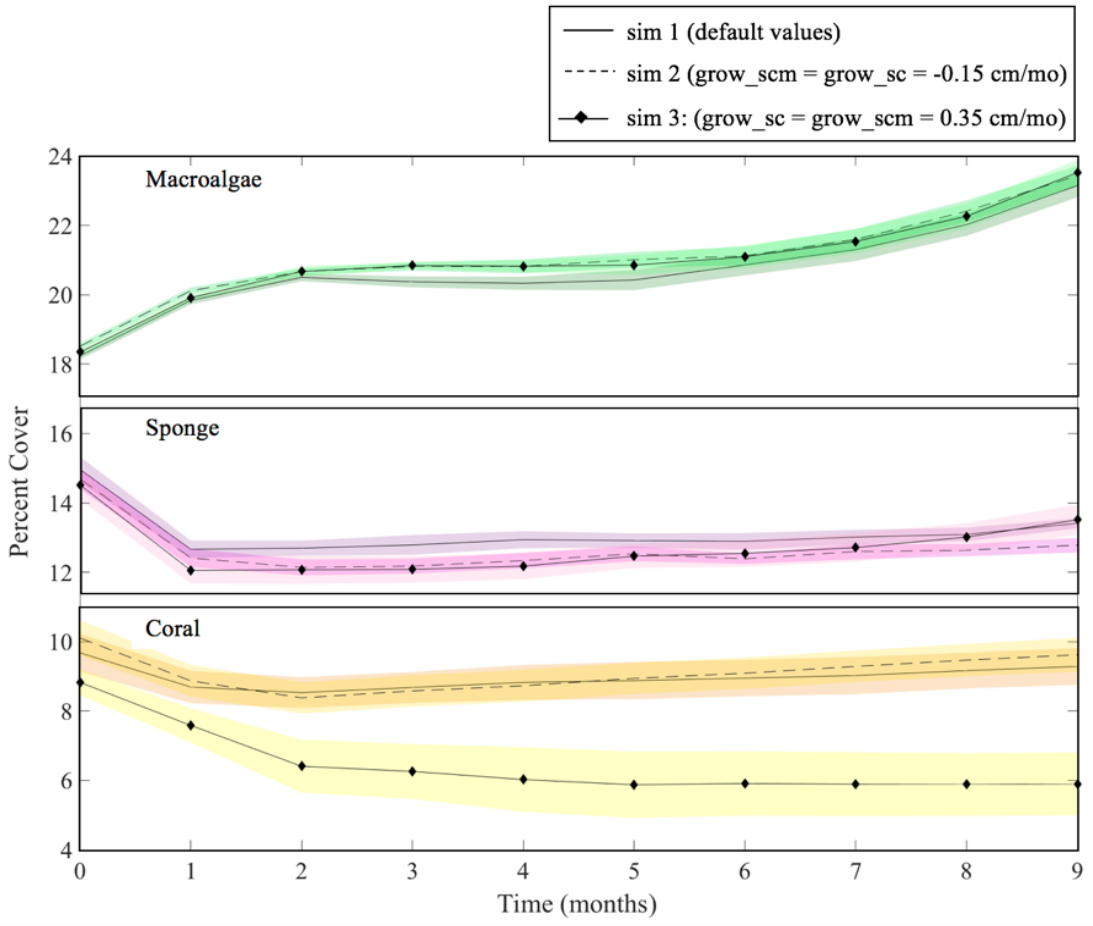

Figure 20: Modeled trajectories of total percent cover of each competitor (coral, sponge, macroalgae) in each of the three simulations. Black lines give the mean for each simulation and colored regions represent the standard error of the mean (SEM).

Creation of the IBM in the present work is an ongoing process. The software underlying the simulation model has been verified; it matches the conceptual model and has been largely debugged (Supplementary Figure 7). However, the model is not yet considered valid because it is not a close enough representation of the benthic interactions that it was built to simulate (Law 2007). One flaw that inhibits model validity is the use of fragmentation as a substitution for macroalgae dispersal/recruitment. The application of fragmentation to simulate macroalgae dispersal has been used in previous studies, but these previous works simulated fragmentation in conjunction with recruitment submodels (Kubicek et al. 2012). *L. variegata* can cycle through more than one generation over a single simulation because its average lifespan, though highly variable, is shorter than the nine-month simulation time (Van Der Zande et al. 2013); model validity therefore depends on accurate representation of the complete life history of *L. variegata.* Modeling *L. variegata* fragmentation to increase as a function of time elapsed (with 50%

fragmented by 5 mo) led to rapid increases of macroalgae percent cover, and this is contrary to previous observations that *L. variegata* percent cover is generally stable over time (Van Der Zande et al. 2013). To mitigate exponential growth and coerce stable macroalgae cover, the mortality submodel was adapted to increase the probability of macroalgae mortality with number of fragments being generated. This attempt to calibrate – or coerce model inputs (mortality rate) to suit known model outputs (stable macroalgae cover) – may have deviated too far from the ecological reality and therefore diminished model validity.

The next step in model formation will be creation of a recruitment sub-model. Inclusion of this demographic process will provide a more realistic depiction of the net expansion of a population (birth-death) than the fragmentation submodel (Crowley et al. 2005). A way to track the age of fragments or parents in the current model will also be incorporated; in the model's current state, it is only possible to discern fragments from parents. To keep track of individuals that were recruited or fragmented, the model will be changed to store the "age" (in time steps) of all fragments and individuals as a fundamental state variable in area lists. Inclusion of an individuals' age as a state variable will allow mortality probability to be modeled as a function of age. The mortality submodel will be changed to assign increasing probability of mortality to older individuals, and this will be an improvement over the current way that mortality is modeled (as a half-life function that increases with time).

Other ways the model will be improved will include better estimates of variables. For example, the default value for coral average diameter will be changed to 18 cm to reflect the findings from the present research as well as previous studies (Holstein et al. 2016). Moreover, macroalgae overgrowth submodels may be adapted to reflect the frequency of macroalgae overgrowths. Macroalgae overgrew *D. anchorata* in only ~13% of experimental colonies in the autumn (Table 8). A section may be added to the macroalgae overgrowth submodel that applies this presence-absence ratio and picks a subset of macroalgae-sponge interactions to apply overgrowth rates to. For interactions that overgrowths are determined to be present, the overgrowth rates (grow_mc, grow_ms) will reflect the presence-only data (Figure 15). This will result in a smaller fraction of macroalgae sponge interactions, but more rapid sponge overgrowth for the individuals randomly chosen to overgrow sponges. Separation of presence-absence and presence-only overgrowth rates may improve the models' representation of actual interactions.

After model improvements are made, the sensitivity analysis will be repeated. Next, the degree of interactions between parameters will be assessed; such interactions occur when the model's sensitivity to one parameter is a function of another parameter (Railsback et al. 2006). For example, the current model may be highly sensitive to mortality of fragments when fragmentation rate is highest. For the parameters that were estimated with high uncertainty, an uncertainty analysis will be used to evaluate model

robustness to variation in suspect parameters (Railsback et al. 2006). A next step will also be to compare the model outcomes to previously observed time-series data on percent cover and population structure of corals, sponges, and macroalgae on coral reefs (Law 2007). These quality controls will help determine whether further improvements are needed, or if the simulation is an adequate proxy for benthic interactions. If the model is adequate following these next improvements, formal statistical methods will be used. Analyses will address how localized macroalgae facilitation of sponge-coral overgrowth affects system behavior, and whether demographic processes of weedy coral species are able to offset the competitive ability of sponges and macroalgae.

Chapter 4: Conclusions and Future Guidelines

Conclusions

This research highlights the importance of multispecies competition among corals, sponges, and macroalgae – the three most abundant benthic taxa – in structuring benthic communities. Field observations demonstrated that some reef-building corals are the inferior members of a competitive hierarchy. These species may deteriorate rapidly and are at risk of becoming excluded as a result of increased competition with sponges and macroalgae. Much uncertainty remains, however, regarding the robustness of these competitive outcomes across species. A simulation modeling framework is being built to explore these interactions. Once validated, the model will be used to assess emergent patterns resulting from individual-based behaviors (e.g., macroalgae facilitation of sponge-coral overgrowth). Simulations may also clarify whether tradeoffs in competitive ability and life-history dynamics may promote coral coexistence despite proliferation of sponges and macroalgae.

Future Guidelines

Yesterday's tools will not be sufficient to solve tomorrow's problems, and the continued degradation of Caribbean reefs will necessitate a better understanding of processes structuring benthic communities. Such understanding may be gained by implementing novel technologies such as photogrammetry in research. Recent studies have demonstrated the validity of this technology in marine environments. The models generated in this study exhibited consistent millimeter-scale accuracy, providing further evidence of legitimate and ecologically-relevant measurements from photogrammetric models. Extensive processing time was needed to generate high-resolution 3D models. However, the computing time demands were offset by the time saved in the field, making this a cost effective technique that required less manpower, less equipment and smaller boats. Applications of this technology in future research can lead to more accurate data, lower costs, and preservation of a digital 3D records of coral reefs.

Future studies are needed to better understand whether corals may persist on reefs subjected to expanding populations of competitive macroalgae and sponges. The mechanisms of macroalgae-sponge facilitation proposed here were not tested and should be confirmed. Further research should also be conducted on a broader range of coral, sponge and macroalgae species to evaluate the robustness of facilitating interactions among sponge and macroalgae species. This will help clarify the magnitude of the impact such facilitating interactions could have on benthic composition and whether there is a potential for these interactions to reinforce feedbacks leading to non-coral dominated states. Multispecies competition among these groups should also be evaluated in the context of anthropogenic stressors.

Factorial experiments (e.g., Zaneveld et al. 2016) can be used to test how herbivory and nutrients could affect competitive dynamics. Simulation modeling frameworks, like the one described in this study, can be expanded to simulated competition among multiple species of corals, sponges, and macroalgae (González-Rivero et al. 2016). Better understanding of these complex competitive dynamics can help clarify the processes structuring benthic communities, the factors impairing coral resilience, and the most effective means to mitigate loss of corals on Caribbean reefs.

The US Virgin Islands comprises the most threatened coral reef ecosystems in the world (Pittman et al. 2017), and the cumulative effect of sustained environmental degradation and recent severe hurricanes – particularly Hurricane Irma – could have drastic implications on reef resilience (Smith et al. 2008; Anthony et al. 2015). Hurricane Irma likely decimated branching corals, while massive corals may have been subjected to overwhelming inputs of sediment and nutrients due to torrential rainwater runoff (Heron et al. 2008). These conditions favor widespread coral mortality, and vacated space that can be easily exploited by colonizing sponges and macroalgae (Chadwick and Morrow 2011). The ability of hurricane impacted reefs to recover has likely been undermined by their exposure to years of terrestrial pollutants and sedimentation, particularly reefs in close proximity to populated St. Thomas (Smith et al. 2008; Anthony et al. 2015). Reefs that have been subjected to extensive impacts prior to the storm should be prioritized for monitoring and management, and the recovery of these reefs should be tracked following the storms. Reefs that sustained little damage or recovered quickly after the storm should also be identified, as these 'reefs of hope' may help managers find what key assets are necessary for a coral reef ecosystem to remain stable in the face of intense disturbances (Pittman et al. 2017).

Local recovery planning and direct intervention following a disturbance can assist in helping reefs to recover to pre-disturbance condition, but preemptive measures are also necessary. Mitigation of chronic stressors can improve coral resilience and increase the likelihood of recovery after future disturbances (Anthony et al. 2015). The bottom up factors promoting macroalgae and sponge growth should be mitigated by regulating terrestrial sedimentation and nutrient inputs to coral reefs that result from agriculture or development (Pawlik et al. 2016). The top down controls limiting macroalgae and sponge growth should be promoted by regulating and enforcing fishing activities of important herbivore and spongivore species (Loh et al. 2015). Multifaceted and adaptive management of both chronic and acute stressors will be necessary to prevent community shifts to algae and sponge dominated states and strengthen the resilience of Caribbean coral reefs (Anthony et al. 2015).

References

Abràmoff MD, Magalhães PJ, Ram SJ (2004) Image processing with imageJ. Biophotonics Int 11:36–41

Aerts LAM (2000) Dynamics behind standoff interactions in three reef sponge species and the coral *Montastraea cavernosa*. Mar Ecol 21:191–204

Aerts LAM, Van Soest RWM (1997) Quantification of sponge/coral interactions in a physically stressed reef community, NE Colombia. Mar Ecol Prog Ser 148:125–134

Allesina S, Levine JM (2011) A competitive network theory of species diversity. Proc Natl Acad Sci 108:5638–5642

Anthony KRN, Marshall PA, Abdulla A, Beeden R, Bergh C, Black R, Eakin CM, Game ET, Gooch M, Graham NAJ, Green A, Heron SF, van Hooidonk R, Knowland C, Mangubhai S, Marshall N, Maynard JA, Mcginnity P, Mcleod E, Mumby PJ, Nyström M, Obura D, Oliver J, Possingham HP, Pressey RL, Rowlands GP, Tamelander J, Wachenfeld D, Wear S (2015) Operationalizing resilience for adaptive coral reef management under global environmental change. Glob Chang Biol 21:48–61

El Ariebi N, Hiscox J, Scriven SA, Müller CT, Boddy L (2016) Production and effects of volatile organic compounds during interspecific interactions. Fungal Ecol 20:144–154

Aronson RB, Precht WF, Toscano MA, Koltes KH (2002) The 1998 bleaching event and its aftermath on a coral reef in Belize. Mar Biol 141:435–447

Baker AC, Glynn PW, Riegl B (2008) Climate change and coral reef bleaching: An ecological assessment of long-term impacts, recovery trends and future outlook. Estuar Coast Shelf Sci 80:435–471

Bell JJ, Barnes DKA (2003) The importance of competitor identity, morphology and ranking methodology to outcomes in interference competition between sponges. Mar Biol 143:415–426

Bell JJ, Davy SK, Jones T, Taylor MW, Webster NS (2013) Could some coral reefs become sponge reefs as our climate changes? Glob Chang Biol 19:2613–2624

Benedetti-Cecchi L, Cinelli F (1996) Patterns of disturbance and recovery in littoral rock pools: Nonhierarchical competition and spatial variability in secondary succession. Mar Ecol Prog Ser 135:145–161

Burns JHR, Delparte D, Kapono L, Belt M, Gates RD, Takabayashi M (2016) Assessing the impact of acute disturbances on the structure and composition of a coral community using innovative 3D reconstruction techniques. Methods Oceanogr 15–16:49–59

Buss LW, Jackson JBC (1979) Competitive networks: nontransitive competitive relationships in cryptic coral reef environments. Am Nat 113:223–234

Chadwick NE, Morrow KM (2011) Competition among sessile organisms on coral reefs. Coral Reefs: An Ecosystem in Transition. pp 347–371

Connell JH (1983) On the prevalence and relative importance of interspecific competition: evidence from field experiments. Am Nat 122:661–696

Crowley PH, Davis HM, Ensminger AL, Fuselier LC, Jackson JK, McLetchie DN (2005) A general model of local competition for space. Ecol Lett 8:176–188

Darling ES, Alvarez-Filip L, Oliver TA, McClanahan TR, Côté IM (2012) Evaluating life-history strategies of reef corals from species traits. Ecol Lett 15:1378–1386

Davy SK, Trautman D a, Borowitzka M a, Hinde R (2002) Ammonium excretion by a symbiotic sponge supplies the nitrogen requirements of its rhodophyte partner. J Exp Biol 205:3505–11

Dayton PK (1971) Competition, disturbance, and community organization: the provision and subsequent utilization of space in a rocky intertidal community. Ecol Monogr 41:351–389

Dizon RT, Yap HT (2006) Understanding coral reefs as complex systems : degradation and prospects for recovery. Science (80-) 70:219–226

Duckworth AR, Battershill CN (2001) Population dynamics and chemical ecology of New Zealand Demospongiae *Latrunculia sp.* nov. and *Polymastia croceus* (Poecilosclerida: Latrunculiidae: Polymastiidae). New Zeal J Mar Freshw Res 35:935–949

van Duyl FC, Moodley L, Nieuwland G, van Ijzerloo L, van Soest RWM, Houtekamer M, Meesters EH, Middelburg JJ (2011) Coral cavity sponges depend on reef-derived food resources: stable isotope and fatty acid constraints. Mar Biol 158:1653–1666
Easson CG, Slattery M, Baker DM, Gochfeld DJ (2014) Complex ecological associations: competition and facilitation in a sponge-algal interaction. Mar Ecol Prog Ser 507:153–167
Edwards KF, Schreiber SJ (2010) Preemption of space can lead to intransitive coexistence of competitors. Oikos 119:1201–1209
Ellison AM, Farnsworth EJ, Twilley RR (1996) Facultative mutualism between red mangroves and root-fouling sponges in belizean mangal. Ecology 77:2431–2444
Engel S, Pawlik JR (2000) Allelopathic activities of sponge extracts. Mar Ecol Prog Ser 207:273–281
Ennis R (2014) Coral reef health responses to chronic and acute changes along water quality gradients in St. Thomas, US Virgin Islands. University of the Virgin Islands
Fenner D (2001) Mass bleaching threatens two coral species with extinction. Reef Encount 29:9–10
Ferrari R, Gonzalez-Rivero M, Ortiz JC, Mumby PJ (2012) Interaction of herbivory and seasonality on the dynamics of Caribbean macroalgae. Coral Reefs 31:683–692
Ferrari R, McKinnon D, He H, Smith RN, Corke P, González-Rivero M, Mumby PJ, Upcroft B (2016) Quantifying multiscale habitat structural complexity: A cost-effective framework for underwater 3D modelling. Remote Sens 8:113
Figueira W, Ferrari R, Weatherby E, Porter A, Hawes S, Byrne M, Phinn S, Roelfsema C, Li X, Thenkabail PS (2015) Accuracy and precision of habitat structural complexity metrics derived from underwater photogrammetry. Remote Sens 7:16883–16900
Ginsburg RN (ed. . (1994) Proceedings of the colloquium on global aspects of coral reefs: health, hazards and history. 420 pp.
González-Rivero M, Bozec YM, Chollett I, Ferrari R, Schönberg CHL, Mumby PJ (2016) Asymmetric competition prevents the outbreak of an opportunistic species after coral reef degradation. Oecologia 181:161–173
González-Rivero M, Yakob L, Mumby PJ (2011) The role of sponge competition on coral reef alternative steady states. Ecol Modell 222:1847–1853
Grace JB, Guntenspergen GR, Keough J (1993) The examination of a competition matrix for transitivity and intransitive loops. Oikos 68:91–98
Green DH, Edmunds PJ, Carpenter RC (2008) Increasing relative abundance of *Porites astreoides* on Caribbean reefs mediated by an overall decline in coral cover. Mar Ecol Prog Ser 359:1–10
Grimm V, Berger U, Bastiansen F, Eliassen S, Ginot V, Giske J, Goss-Custard J, Grand T, Heinz SK, Huse G, Huth A, Jepsen JU, Jørgensen C, Mooij WM, Müller B, Pe'er G, Piou C, Railsback SF, Robbins AM, Robbins MM, Rossmanith E, Rüger N, Strand E, Souissi S, Stillman RA, Vabø R, Visser U, DeAngelis DL (2006) A standard protocol for describing individual-based and agent-based models. Ecol Modell 198:115–126
Grimm V, Berger U, DeAngelis DL, Polhill JG, Giske J, Railsback SF (2010) The ODD protocol: A review and first update. Ecol Modell 221:2760–2768
Hastings A (1980) Disturbance, coexistence, history, and competition for space. Theor Popul Biol 18:363–373
Henderson L (2012) The relative importance of nutrients and herbivory on benthic community structure: nearshore vs. offshore reefs. University of the Virgin Islands
Heron S, Morgan J, Eakin M, Skirving W (2008) Hurricanes and their effects on Coral Reefs. In: Wilkinson C., Souter D. (eds) Status of Caribbean coral reefs after bleaching and hurricanes in 2005. Global Coral Reef Monitoring Network, Townsville,
Hiscox J, Savoury M, Toledo S, Kingscott-Edmunds J, Bettridge A, Waili N Al, Boddy L (2017) Threesomes destabilise certain relationships: multispecies interactions between wood decay fungi in natural resources. FEMS Microbiol Ecol 93:

Holstein DM, Smith TB, Paris CB (2016) Depth-Independent reproduction in the reef coral *Porites astreoides* from shallow to mesophotic zones. PLoS One 11:
Hughes TP (1984) Population dynamics based on individual size rather than age : a general model with a reef coral example. Am Nat 123:778–795
Hughes TP (1994) Catastrophes, phase shifts, and large-scale degradation of a caribbean coral reef. Science (80-) 265:1547–1551
Jompa J, McCook LJ (2002) The effects of nutrients and herbivory on competition between a hard coral (*Porites cylindrica*) and a brown alga (*Lobophora variegata)*. Limnol Oceanogr 47:527–534
Karlson RH, Jackson JBC (1981) Competitive networks and community structure: a simulation study. Ecology
Kubicek A, Muhando C, Reuter H (2012) Simulations of long-term community dynamics in coral reefs - how perturbations shape trajectories. PLoS Comput Biol 8:
Laird RA, Schamp BS (2008) Does local competition increase the coexistence of species in intransitive networks? Ecology 89:237–247
Law AM (2007) Simulation modeling and analysis.
Lesser MP, Slattery M (2013) Ecology of caribbean sponges: Are top-down or bottom-up processes more important? PLoS One
Lirman D (2001) Competition between macroalgae and corals: effects of herbivore exclusion and increased algal biomass on coral survivorship and growth. Coral Reefs 19:392–399
Littler MM, Littler DS, Brooks BL (2006) Harmful algae on tropical coral reefs: bottom-up eutrophication and top-down herbivory. Harmful Algae 5:565–585
Logan A (1984) Interspecific aggression in hermatypic corals from Bermuda. Coral Reefs 3:131–138
Loh T-L, McMurray SE, Henkel TP, Vicente J, Pawlik JR (2015) Indirect effects of overfishing on Caribbean reefs: sponges overgrow reef-building corals. PeerJ 3:e901
Loh T-L, Pawlik JR (2014) Chemical defenses and resource trade-offs structure sponge communities on Caribbean coral reefs. Proc Natl Acad Sci 111:4151–4156
López-Victoria M, Zea S, Weil E (2006) Competition for space between encrusting excavating Caribbean sponges and other coral reef organisms. Mar Ecol Prog Ser 312:113–121
Luter HM, Duckworth AR (2010) Influence of size and spatial competition on the bioactivity of coral reef sponges. Biochem Syst Ecol 38:146–153
Mallison H, Wings O (2014) Photogrammetry in paleontology - A practical guide. J Paleontol Tech 12:1–31
McLean EL, Yoshioka PM (2008) Substratum effects on the growth and survivorship of the sponge *Desmapsamma anchorata*. Caribb J Sci 44:83–89
Morrow KM, Liles MR, Paul VJ, Moss AG, Chadwick NE (2013) Bacterial shifts associated with coral-macroalgal competition in the Caribbean Sea. Mar Ecol Prog Ser 488:103–117
Morrow KM, Paul VJ, Liles MR, Chadwick NE (2011) Allelochemicals produced by Caribbean macroalgae and cyanobacteria have species-specific effects on reef coral microorganisms. Coral Reefs 30:309–320
Mumby PJ, Foster NL, Fahy EAG (2005) Patch dynamics of coral reef macroalgae under chronic and acute disturbance. Coral Reefs 24:681–692
Mumby PJ, Hastings A, Edwards HJ (2007) Thresholds and the resilience of Caribbean coral reefs. Nature 450:98–101
Norström A V., Nyström M, Lokrantz J, Folke C (2009) Alternative states on coral reefs: beyond coral-macroalgal phase shifts. Mar Ecol Prog Ser 376:293–306
Nugues MM, Delvoye L, Bak RPM (2004) Coral defence against macroalgae: Differential effects of mesenterial filaments on the green alga *Halimeda opuntia*. Mar Ecol Prog Ser 278:103–114
Olinger LK, Heidmann SL, Durdall AN, Howe C, Ramseyer T, Thomas SG, Lasseigne DN, Brown EJ, Cassell JS, Donihe MM, Romero MDD, Duke MA, Green D, Hillbrand P, Grimes KRW, Nemeth

RS, Smith TB, Brandt M (2017) Altered juvenile fish communities associated with invasive *Halophila stipulacea* seagrass habitats in the U.S. Virgin Islands. PLoS One

Pawlik JR, Burkepile DE, Thurber RV (2016) A vicious circle? altered carbon and nutrient cycling may explain the low resilience of Caribbean coral reefs. Bioscience 66:470–476

Pawlik JR, Loh TL, McMurray SE, Finelli CM (2013) Sponge communities on Caribbean coral reefs are structured by factors that are top-down, not bottom-up. PLoS One 8:

Pawlik JR, Steindler L, Henkel TP, Beer S, Ilan M (2007) Chemical warfare on coral reefs: sponge metabolites differentially affect coral symbiosis in situ. Limnol Oceanogr 52:907–911

Pittman SJ, Poti M, Jeffrey CFG, Kracker LM, Mabrouk A (2017) Decision support framework for the prioritization of coral reefs in the U.S. Virgin Islands. Ecol Inform

Railsback SF, Cunningham PC, Lamberson RH (2006) A strategy for parameter sensitivity and uncertainty analysis of individual-based models. Ecol Modell 111:207–222

Reiswig HM (1973) Population dynamics of three Jamaican demospongiae. Bull Mar Sci 23:191–226

Richardson CA, Dustan P, Lang JC (1979) Maintenance of living space by sweeper tentacles of *Montastrea cavernosa*, a Caribbean reef coral. Mar Biol 55:181–186

Rinkevich B, Shashar N, Liberman T (1992) Nontransitive xenogeneic interactions between four common Red Sea sessile invertebrates. Proc Seventh Int Coral Reef Symp

De Ruyter van Steveninck ED, Van Mulekom LL, Breeman AM (1988) Growth inhibition of *Lobophora variegata* (Lamouroux) Womersley by scleractinian corals. J Exp Mar Bio Ecol 115:169–178

Sabine AM, Smith TB, Williams DE, Brandt ME (2015) Environmental conditions influence tissue regeneration rates in scleractinian corals. Mar Pollut Bull 95:253–264

Scott-Murray A, Linley TD, Singh H, Jamieson A, Mayor DJ (2016) 3D photogrammetry for marine biologists enables improved archiving and reference materials, and will lead to new methods for in situ data collection.

Scott-Murray A, Schläppy M-L (2017) Using 3D photogrammetry to model sponge morphological plasticity. World Sponge Conf

Sebens KP (1987) Competition for space: effects of disturbance and indeterminate competitive success. Theor Popul Biol

Smith TB, Nemeth RS, Blondeau J, Calnan JM, Kadison E, Herzlieb S (2008) Assessing coral reef health across onshore to offshore stress gradients in the US Virgin Islands. Mar Pollut Bull 56:1983–1991

Smith TT, Ennis RSR, Kadison E, Weinstein DDW, Jossart J, Gyory J, Henderson L (2015) The United States Virgin Islands Territorial Coral Reef Monitoring Program. 2015 Annual Report.

Tanaka M, Nandakumar K (1994) Measurement of the degree of intransitivity in a community of sessile organisms. J Exp Mar Bio Ecol 182:85–95

Tanner JE (1997) Interspecific competition reduces fitness in scleractinian corals. J Exp Mar Bio Ecol 214:19–34

Trautman DA, Hinde R, Borowitzka MA (2000) Population dynamics of an association between a coral reef sponge and a red macroalga. J Exp Mar Bio Ecol 244:87–105

Veal CJ, Holmes G, Nunez M, Hoegh-Guldberg O, Osborn J (2010) A comparative study of methods for surface area and three-dimensional shape measurement of coral skeletons. Limnol Oceanogr Methods 8:241–253

Wulff J (2012) Ecological interactions and the distribution, abundance, and diversity of sponges. Elsevier Ltd.

Wulff JL (2008) Life-history differences among coral reef sponges promote mutualism or exploitation of mutualism by influencing partner fidelity feedback. Am Nat 171:597–609

Yñiguez AT, McManus JW, DeAngelis DL (2008) Allowing macroalgae growth forms to emerge: use of an agent-based model to understand the growth and spread of macroalgae in Florida coral reefs, with emphasis on *Halimeda tuna*. Ecol Modell 216:60–74

Van Der Zande R, Leon R de, Sluijs A (2013) Growth, mortality and recruitment rates of the brown alga *Lobophora variegata* in relation to herbivory and nutrients on Bonaire.

Zaneveld JR, Burkepile DE, Shantz AA, Pritchard CE, McMinds R, Payet JP, Welsh R, Correa AMS, Lemoine NP, Rosales S, Fuchs C, Maynard JA, Thurber RV (2016) Overfishing and nutrient pollution interact with temperature to disrupt coral reefs down to microbial scales. Nat Commun 7:11833

Zea S (1993) Cover of sponges and other sessile organisms in rocky and coral reef habitats of Santa Marta, Colombian Caribbean Sea. Caribb J Sci 29:75–88

Appendix: Supplementary Material

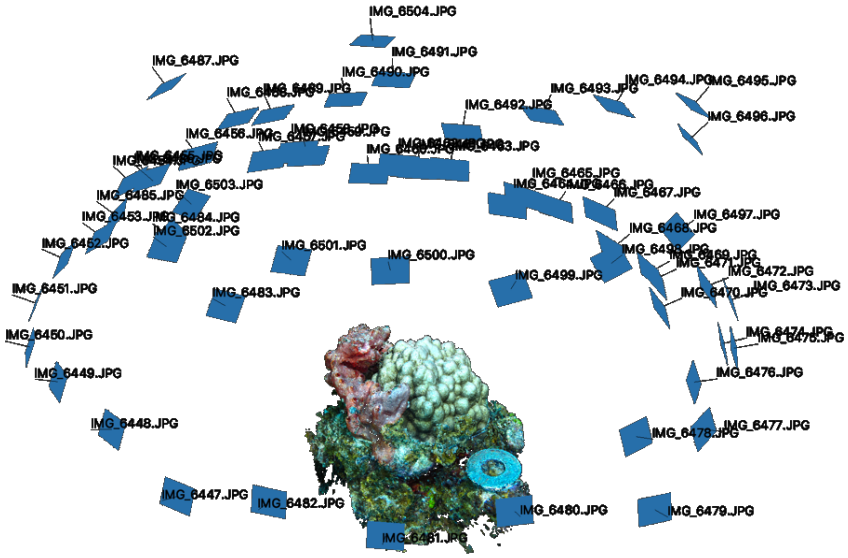

Supplementary Figure 1: 3D reconstruction showing the location of the camera when each photograph was taken

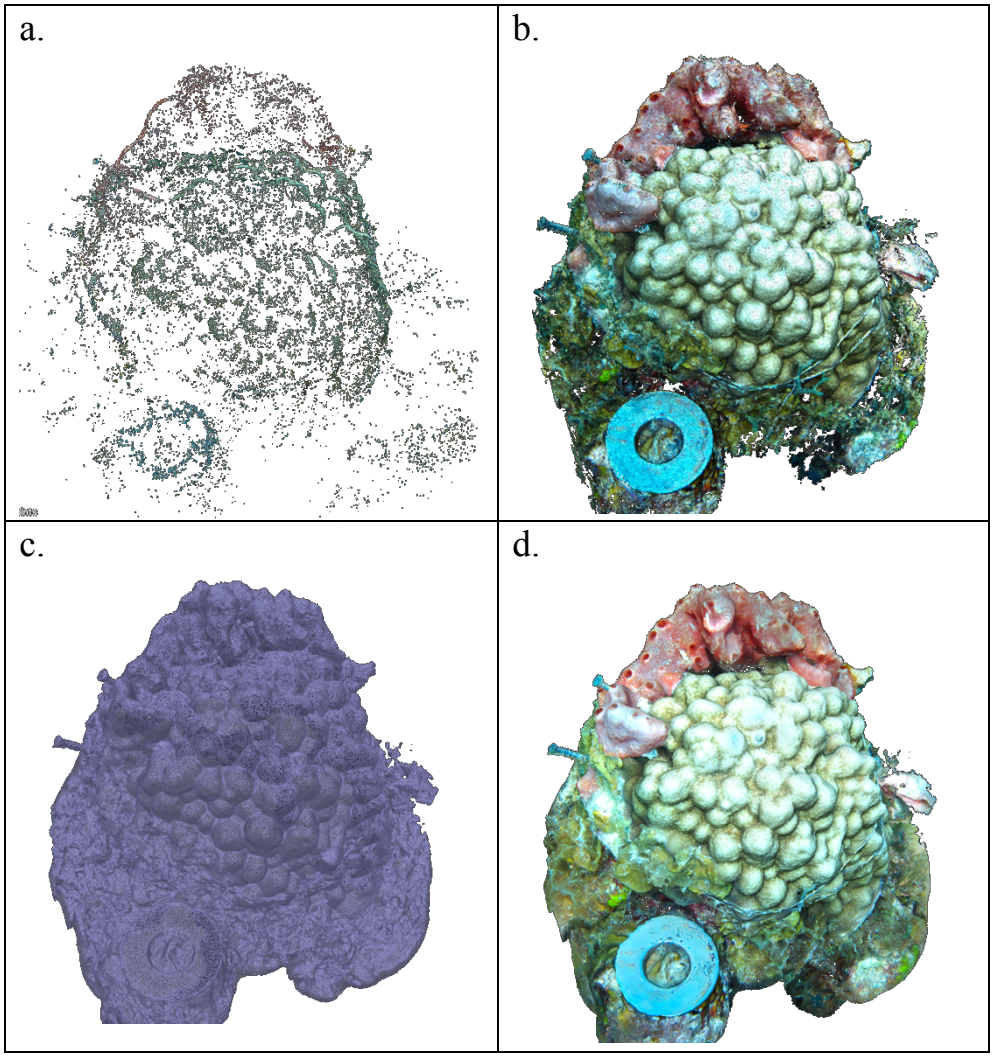

Supplementary Figure 2: Screenshots of 3D model of experimental colonies during photogrammetric processing. a) sparse point cloud, b) dense point cloud, c) mesh, d) textured mesh. 3D model can be viewed at https://skfb.ly/ZRqI.

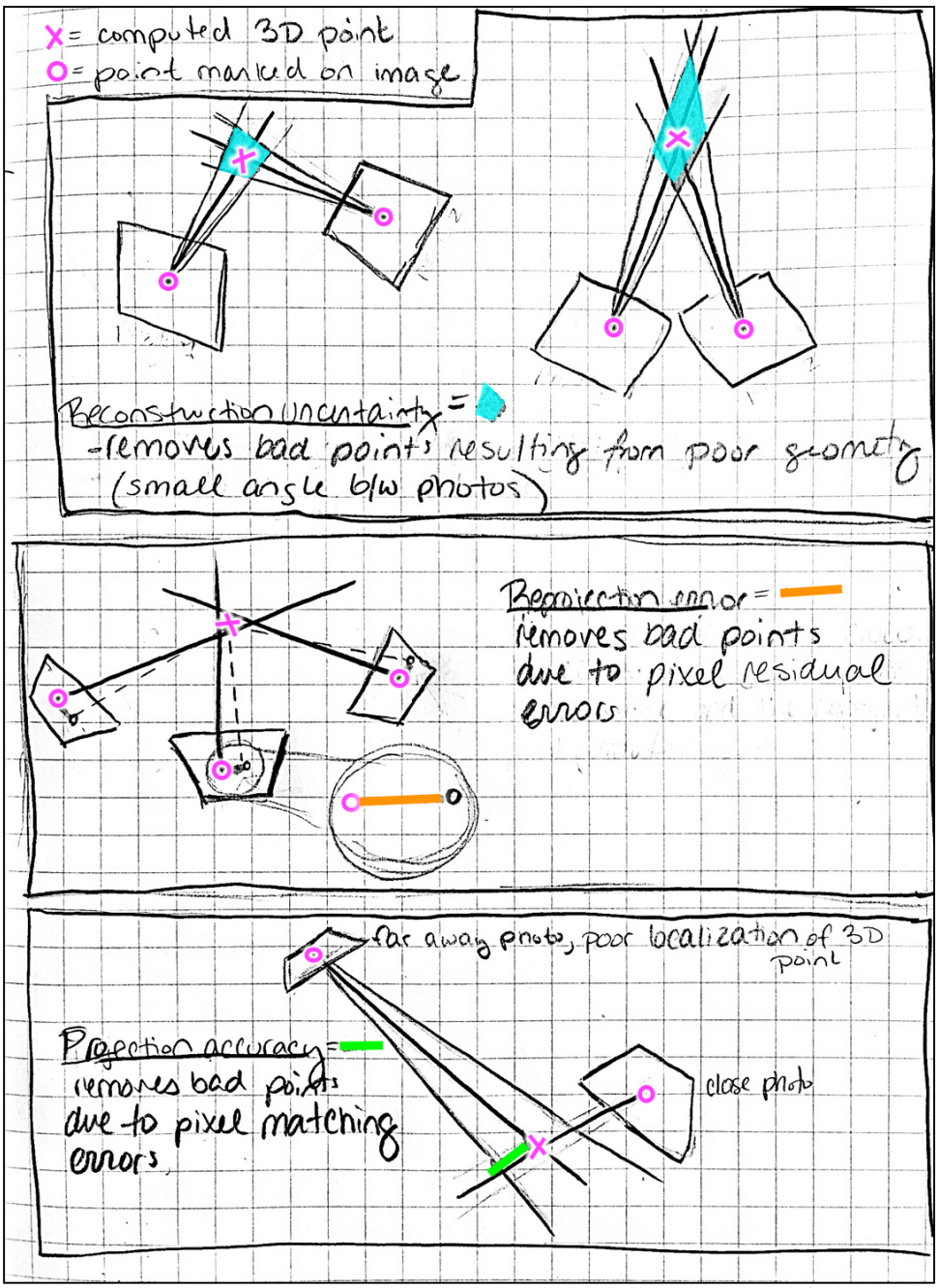

Supplementary Figure 3: Drawn representation of different filters applied to sparse point cloud. The area of the teal box represents the reconstruction uncertainty, the length of the orange line represents the reprojection error, and the length of the green line represents the projection accuracy.

Supplementary Table 1: Summary of experimental data collected from each technique (photogrammetry and image analysis). Comprises three sub-tables. The far left sub-table gives the technique and variable measured, the middle sub-table gives the dates that photographs were captured from each site, and the far right sub-table gives the factors, statistical tests, and data transformations used to analyze each competitor. Tech. = technique, Comp. = competitor.

Tech.	Variable	Site	Season	Dates (# days)	Comp.	Factors	Analysis (transformation)
Photogrammetry	Surface Area Percent Change	Flat Key	autumn-spring	Dec 16, 2016-Mar 14, 2017 (91 d)	Coral	Treatment, sponge spp., site	ANOVA (Box-Cox)
		Pers. Bay	winter-spring	Jan 20, 2017-Apr 25, 2017 (91 d)	Sponge		ANOVA (Box-Cox)
Image Analysis	Linear Growth	Flat Key & Pers. Bay	autumn-winter	Nov 19, 2016-Jan 20, 2017 (62 d)	Coral	Sponge spp., site	ANOVA (square root)
					Sponge	Treatment, sponge spp., site	ANOVA (Lambert W x F heavy-tail)
					Algae	Competitor, site	ANOVA (cube-root)
		Flat Key	autumn	Nov 19, 2016-Dec 16, 2016 (27 d)	Coral	Sponge spp., season	Welch's two-sample t-test
					Sponge	Treatment, sponge spp., season	ANOVA
			winter	Feb 11, 2017-Mar 14, 2017 (31 d)	Algae	Treatment, sponge spp., season	Binomial regression on presence/absence of algae overgrowth

Supplementary Table 2: Criteria to characterize a win, loss and standoff for coral -sponge, coral-macroalgae, and sponge-macroalgae interactions. Coral = "C", sponge = "S", macroalgae = "M", t1 = first observation, t2 = second observation (standoffs only) after 4 months.

	C			S			M		
	win	loss	standoff	win	loss	standoff	win	loss	standoff
C	-	-	-	B	A	C	E	D	C
S	A	B	C	-	-	-	G	F	C
M	D	E	C	F	G	C	-	-	-

A. Coral < Sponge:
   - T_1: Upward growth of coral over sponge (Lopez-Victoria 2006), discoloration of sponge (Rinkevich et al. 1992)
   - T_2: change in standoff margin distance (Chornesky 1989) that indicates sponge lost to coral.

B. Sponge < Coral:
   - t_1: Sponge overgrows coral (Buss and Jackson 1979)
   - t_2: change in standoff margin distance (Chornesky 1989) that indicates coral lost to sponge.

C. Coral-Sponge/ Coral-Macroalgae/ Sponge-Macroalgae Standoff:
   - Distance from reference nail to standoff margin does not change between t_1 and t_2.

D. Coral < Macroalgae:
   - t_1: inhibited algal growth around coral margin, with sign of damage (notches and frayed edges) on algal fronds (Nugues et al. 2004).
   - t_2: Change in standoff margin distance (Chornesky 1989) that indicates macroalgae lost to coral

E. Macroalgae < Coral:
   - t_1: macroalgae overgrows coral (Buss and Jackson 1979)
   - t_2: change in standoff margin distance (Chornesky 1989) that indicates coral lost to macroalgae.

F. Sponge < Macroalgae:
   - t_1: inhibited algal growth around sponge margin, with sign of damage (notches and frayed edges) on algal fronds (Nugues et al. 2004). Visible upward growth margin of sponge over macroalgae (Rinkevich et al. 1992).
   - t_2: change in standoff margin distance (Chornesky 1989) that indicates macroalgae lost to sponge.

G. Macroalgae < Sponge:
   - t_1: macroalgae overgrows sponge (Buss and Jackson 1979)
   - t_2: change in standoff margin distance (Chornesky 1989) that indicates sponge lost to macroalgae.

Supplementary Table 3: Sample data for coral species C, Sponge species S, Macroalgae species M. Frequency of wins, losses and standoffs for C vs. S, C vs. M, and S vs. M;

C vs. S	#C wins	14
	#S wins	12
	# standoffs	30
C vs. M	#C wins	0
	#M wins	25
	#standoffs	20
S vs. M	#S wins	40
	#M wins	12
	#standoffs	20

Supplementary Table 4: Proportion of observed wins, losses and standoffs for C vs. S, C vs. M, and S vs. M. SS = sum of squares. WI = Win Index, LI = Loss Index, SI = Standoff Index

	C			S			M		
	win	loss	standoff	win	loss	standoff	win	loss	standoff
C	-	-	-	0.21	0.25	0.54	0.56	0.00	0.44
S	0.25	0.21	0.54	-	-	-	0.17	0.56	0.28
M	0.00	0.56	0.44	0.56	0.17	0.28	-	-	-
SS column values	Pij[W]^2	Pij[L]^2	Pij[S]^2	Pij[W]^2	Pij[L]^2	Pij[S]^2	Pij[W]^2	Pij[L]^2	Pij[S]^2
	0.06	0.35	0.48	0.35	0.09	0.08	0.34	0.31	0.00
Σ probs	Pij[W]^2	Pij[L]^2	Pij[S]^2						
	0.75	0.75	0.56						
Indices	WI	LI	SI						
	0.50	0.50	0.43						

Supplementary Table 5: Proportion of wins, losses and standoffs for C vs. S, C vs. M, and S vs. M that reflect maximum hierarchy (M > S > C). SS = sum of squares. WI = Win Index, LI = Loss Index, SI = Standoff Index

	C			S			M		
	win	loss	standoff	win	loss	standoff	win	loss	standoff
C	-	-	-	0.46	0.00	0.54	0.56	0.00	0.44
S	0.00	0.46	0.54	-	-	-	0.72	0.00	0.28
M	0.00	0.56	0.44	0.00	0.72	0.28	-	-	-
SS column values	Pij[W]^2	Pij[L]^2	Pij[S]^2	Pij[W]^2	Pij[L]^2	Pij[S]^2	Pij[W]^2	Pij[L]^2	Pij[S]^2
	0.00	0.52	0.48	0.22	0.52	0.08	0.83	0.00	0.00
Σ probs	Pij[W]^2	Pij[L]^2	Pij[S]^2						
	1.05	1.05	0.56						
Indices	WI	LI	SI						
	0.59	0.59	0.43						

Supplementary Table 6: Proportion of wins, losses and standoffs for C vs. S, C vs. M, and S vs. M that reflect Maximum Network (M > S > C and C > M). SS = sum of squares. WI = Win Index, LI = Loss Index, SI = Standoff Index.

	C			S			M		
	win	loss	standoff	win	loss	standoff	win	loss	standoff
C	-	-	-	0.23	0.23	0.54	0.28	0.28	0.44
S	0.23	0.23	0.54	-	-	-	0.36	0.36	0.28
M	0.28	0.28	0.44	0.36	0.36	0.28	-	-	-
SS column values	Pij[W]^2	Pij[L]^2	Pij[S]^2	Pij[W]^2	Pij[L]^2	Pij[S]^2	Pij[W]^2	Pij[L]^2	Pij[S]^2
	0.13	0.13	0.48	0.18	0.18	0.08	0.21	0.21	0.00
Σ probs	Pij[W]^2	Pij[L]^2	Pij[S]^2						
	0.52	0.52	0.56						
Indices	WI	LI	SI						
	0.42	0.42	0.43						

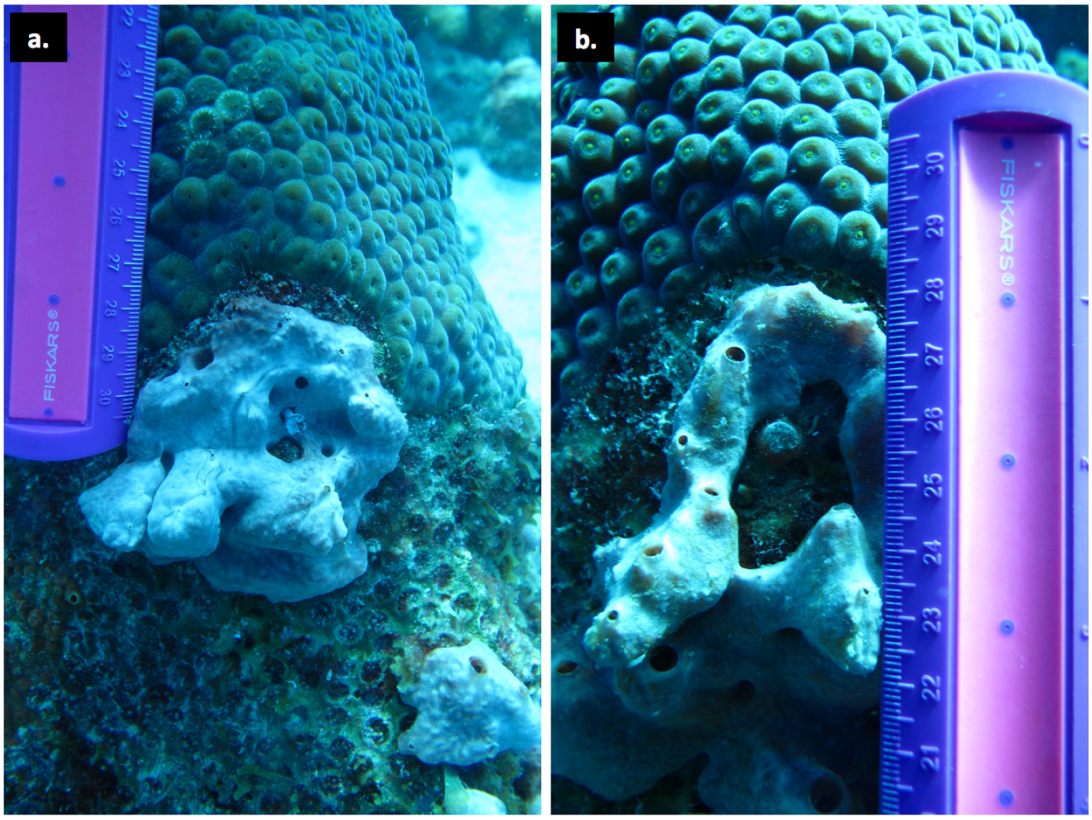

Supplementary Figure 4: Persistent standoff between *M. cavernosa* and *D. anchorata* at Flat Key over 3 mo. Photographs were taken on a) October 26, 2016 and b) January 20, 2017.

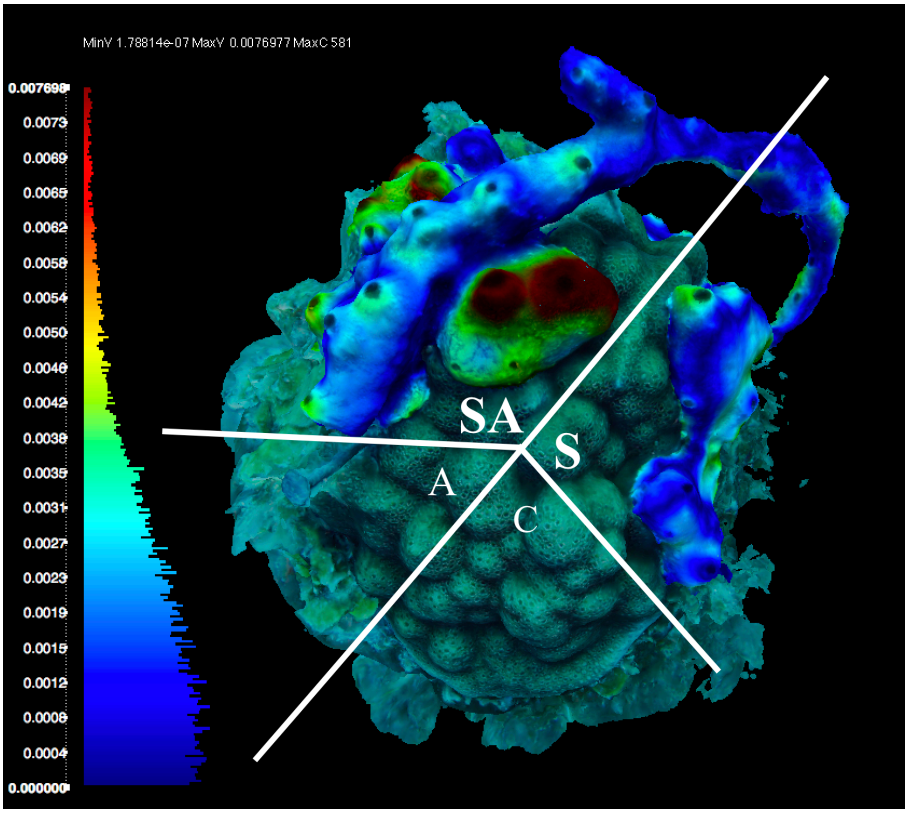

Supplementary Figure 5: Hausdorff sampling applied to the sponge competitor on Flat Key colony #314. The model shown was generated from photographs taken during the second timepoint, on March 14, 2017, and the sponge is colorized according to the absolute value of the distance to the mesh vertices at the first timepoint. The histogram gives the relative frequency of mesh distances in meters. The large red portion in the SA treatment represents new growth of the sponge.

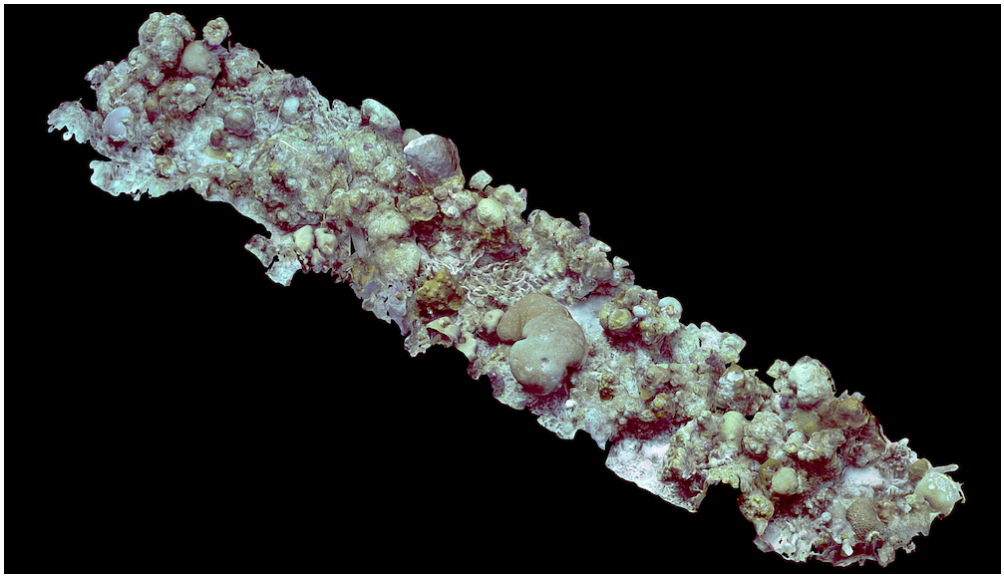

Supplementary Figure 6: 6x1 m area of TCRMP transect #6, Flat Key, St. Thomas, USVI. 292 photos captured at ~35 ft with Canon G1X in Ikelite housing, Model generated using Agisoft Photoscan Professional Edition (processing time: 6 hrs w/Intel HD graphics 530 GPU: 24 cores @ 1050 MHz, 1536 MB). Mesh = 2,000,000 faces. 3D model can be viewed at https://skfb.ly/67y8p.

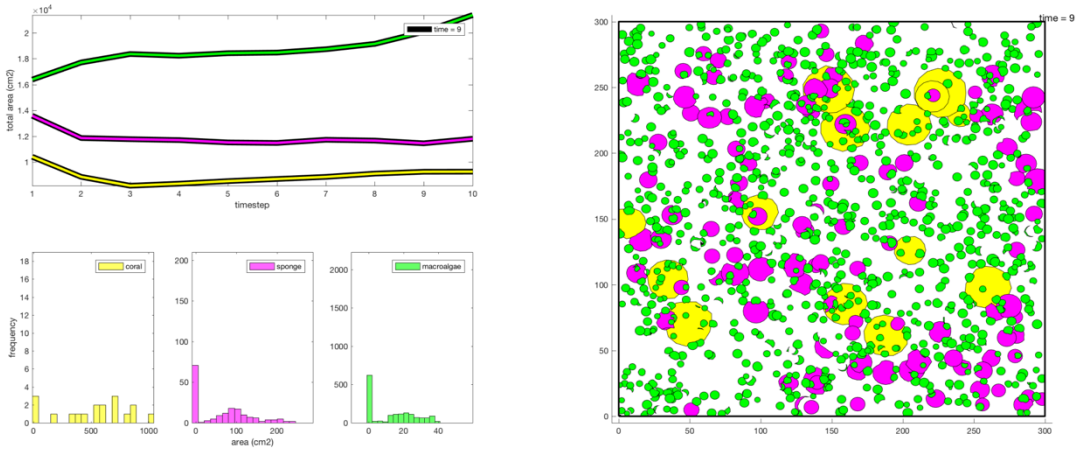

Supplementary Figure 7: Graphic output of the simulation, with percent cover in top left corner, size structure of each entity in bottom left corner, and simulation on right. Colored by entity with yellow = coral, pink = sponge, and green = macroalgae. Animation can be viewed here.